(12) INTERNATIONAL APPLICATION PUBLISHED UNDER THE PATENT COOPERATION TREATY (PCT)

(19) World Intellectual Property Organization
International Bureau

(43) International Publication Date
1 November 2012 (01.11.2012)

WIPO | PCT

(10) International Publication Number
WO 2012/149141 A1

(51) International Patent Classification:
B01D 71/06 (2006.01)

(21) International Application Number:
PCT/US2012/035188

(22) International Filing Date:
26 April 2012 (26.04.2012)

(25) Filing Language: English

(26) Publication Language: English

(30) Priority Data:
61/479,393 26 April 2011 (26.04.2011) US

(71) Applicant *(for all designated States except US)*: **THE REGENTS OF THE UNIVERSITY OF CALIFORNIA** [US/US]; 1111 Franklin Street, Oakland, CA 94607-5200 (US).

(72) Inventors; and

(75) Inventors/Applicants *(for US only)*: **HOEK, Eric, M., V.** [US/US]; 11606 Montana Ave., Unit 9, Los Angeles, CA 90049 (US). **LIND, Mary, L.** [US/US]; 1000 Cordova #308, Pasadena, CA 91106 (US). **GUILLEN, Greg, R.** [US/US]; 4000 Oakfield Dr., Sherman Oaks, CA 91423 (US). **WONG, Mavis, C.y.** [CA/US]; 3705 Westwood Blvd #17, Los Angeles, CA 90034 (US).

(74) Agents: **SHORTELL, D., Brian** et al.; Ballard Spahr LLP, 999 Peachtree Street, Suite 1000, Atlanta, GA 30309 (US).

(81) Designated States *(unless otherwise indicated, for every kind of national protection available)*: AE, AG, AL, AM, AO, AT, AU, AZ, BA, BB, BG, BH, BR, BW, BY, BZ, CA, CH, CL, CN, CO, CR, CU, CZ, DE, DK, DM, DO, DZ, EC, EE, EG, ES, FI, GB, GD, GE, GH, GM, GT, HN, HR, HU, ID, IL, IN, IS, JP, KE, KG, KM, KN, KP, KR, KZ, LA, LC, LK, LR, LS, LT, LU, LY, MA, MD, ME, MG, MK, MN, MW, MX, MY, MZ, NA, NG, NI, NO, NZ, OM, PE, PG, PH, PL, PT, QA, RO, RS, RU, RW, SC, SD, SE, SG, SK, SL, SM, ST, SV, SY, TH, TJ, TM, TN, TR, TT, TZ, UA, UG, US, UZ, VC, VN, ZA, ZM, ZW.

(84) Designated States *(unless otherwise indicated, for every kind of regional protection available)*: ARIPO (BW, GH, GM, KE, LR, LS, MW, MZ, NA, RW, SD, SL, SZ, TZ, UG, ZM, ZW), Eurasian (AM, AZ, BY, KG, KZ, RU, TJ, TM), European (AL, AT, BE, BG, CH, CY, CZ, DE, DK, EE, ES, FI, FR, GB, GR, HR, HU, IE, IS, IT, LT, LU, LV, MC, MK, MT, NL, NO, PL, PT, RO, RS, SE, SI, SK, SM, TR), OAPI (BF, BJ, CF, CG, CI, CM, GA, GN, GQ, GW, ML, MR, NE, SN, TD, TG).

Declarations under Rule 4.17:

— *as to applicant's entitlement to apply for and be granted a patent (Rule 4.17(ii))*

Published:

— *with international search report (Art. 21(3))*

WO 2012/149141 A1

(54) **Title**: FORWARD OSMOSIS MEMBRANE WITH BLENDED POLYMERIC SUPPORT

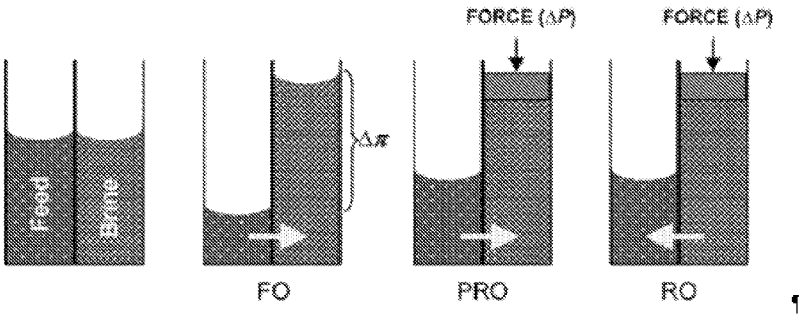


Figure 1

(57) **Abstract**: A semi-permeable forward osmosis membrane has exceptional permeability and stability and is designed for applications including: low energy desalination via forward osmosis, osmotic energy production, drug delivery, food and beverage dehydration, and osmotic water sampling devices. The membrane may comprise a polymeric support layer, and a film polymerized on the support layer. The polymeric support layer may comprise a blend of two or more polymers, including a polysulfone and/or a polyaniline. The film may comprise polyamide, a polyether, a polyether-urea, a polyester, or a polyimide, or their copolymers or mixtures.

FORWARD OSMOSIS MEMBRANE WITH BLENDED POLYMERIC SUPPORT

CROSS-REFERENCE TO RELATED APPLICATIONS

[0001] This application claims the benefit of United States Application No. 61/479,393, filed April 26, 2011, which is hereby incorporated by reference in its entirety.

BACKGROUND

[0001] Osmosis is a spontaneous process that occurs whenever two solutions of different chemical potentials are separated by a semi-permeable membrane (i.e., permeable to water but not the solutes). Engineered osmotic processes known as forward osmosis (FO) or direct osmosis, pressure-retarded osmosis (PRO) and reverse osmosis (RO) are depicted visually in Figure 1. Relatively dilute "feed" and concentrated "brine" (RO) or "draw" (FO/PRO) solutions are not in equilibrium. In FO processes, water spontaneously diffuses from the dilute feed through membrane into the concentrated brine at atmospheric pressure ($\Delta p = 0$; $\Delta\pi > 0$). In RO processes, water permeates from the brine solution through membrane into the dilute solution because the applied hydraulic pressure greatly exceeds the osmotic pressure difference ($\Delta p \gg \Delta\pi$). In PRO processes, a hydraulic pressure is applied, but sufficiently below the osmotic pressure such that water spontaneously diffuses from the feed into the brine ($\Delta p < \Delta\pi$).

[0002] While RO is a well-understood, relatively mature commercial technology – predominantly applied to desalination, wastewater purification, ultrapure water production and small molecule concentration – FO processes are just beginning to be explored at industrial scales. In small-scale applications, FO processes offer great potential for use in hydration bags for hiking, mountaineering and the military, osmotic pumps in microfluidic devices, small molecule dialysis and drug delivery, as well as biomolecule and fruit juice concentration. Large-scale processes like FO desalination and water purification and osmotic power production by PRO, however promising, are not yet commercially viable. In all FO applications – large and small – better performing osmotic membranes are needed to (1) enhance performance or (2) enable commercial viability.

[0003] High-performance RO membranes, modules, and systems have been a commercial reality for more than a decade. However, traditional RO membranes are highly inefficient when used in FO and PRO processes. Specifically, the porous support membranes (that have been engineered for over 40 years to provide the biological, chemical and mechanical stability needed in high-pressure RO desalination applications) hinder salt and water transport through RO membrane composite structures due to their low porosity and hydrophobicity. A new class of membrane materials are needed with structure and chemistry designed specifically for osmotic processes. Once viable osmotic membranes are available, they must be optimized for each specific FO or PRO application, and subsequently, new module and system designs will be required to optimally leverage high-performance osmotic membranes in a given application.

[0004] Commercial FO membrane technology is currently limited to the CTA membrane made by Hydration Technologies Innovations (Albany, Oregon, USA), comprising a woven polyester fabric encapsulated by a cellulose triacetate phase inverted membrane structure. As the CTA membrane is proprietary, the details of the membrane are limited, see Wong et al. (*Desalination,* 287, p.340-349 (2012)). Without wishing to be bound by theory, it is believed that the cellulose triacetate polymer is hydrophilic. It is unfortunate, however, that such structures can be incompatible with high pH conditions, found, for example, in membrane cleaning conditions and in the "ammonia - carbon dioxide" FO process conditions, see J. R. McCutcheon, et al. (*J. Membr. Sci.* 2006, 284, (1-2), 237-247). In contrast, traditional asymmetric composite RO membrane structures (e.g., polyamide, polysulfone, polyester) can typically tolerate high pH conditions, but can be subject to internal concentration polarization – excessive buildup of feed or draw solute in the support membrane structure, which lowers the effective osmotic driving force across the membrane – when used in FO processes.

[0005] Thus, despite advances in semi-permeable membrane research, there is still a scarcity of FO membrane structures that exhibit high water permeability, low salt passage, tolerate high pH conditions, and effectively resist internal concentration polarization. These needs and other needs are satisfied by the present invention.

SUMMARY

[0006] In accordance with the purpose(s) of the invention, as embodied and broadly described herein, the invention relates to semi-permeable forward osmosis (FO) membranes

having exceptional water permeability, salt selectivity, internal mass transfer and high pH (or chemical) stability.

[0007] In one aspect, the invention relates to a semi-permeable osmotic membrane having an osmosis-driven water permeability of from about 0.01 gfd/psi to about 0.10 gfd/psi (10^{-12} m/Pa-s to 10^{-11} m/Pa-s), for example about 0.05 gfd/psi to about 0.10 gfd/psi. The semi-permeable osmotic membrane can also have a sodium chloride permeability of less than 10^{-7} m/s , such as, for example, a sodium chloride permeability of 10^{-7} m/s to 10^{-8} m/s. The semi-permeable osmotic membrane can also have a support membrane with deionized water contact angle below 20 degrees. The semi-permeable osmotic membrane can also have up to 50% porosity through the volume of support membrane (flat sheet and hollow fiber) and support fabric (flat sheet only). The semi-permeable osmotic membrane can also have a stability for at least about 1 year under continuous exposure to pH of 10 to 13 (i.e., for the ammonia-carbon dioxide draw solution) and periodic exposure to pH $\leq$ 1 or pH $\geq$ 13 (chemical cleaning) and temperatures up to 50 degrees Celsius.

[0008] In a further aspect, the invention relates to a method for preparing a semi-permeable osmotic membrane, the method comprising polymerizing a semi-permeable film onto a hydrophilic or blended polymeric support layer.

[0009] In a further aspect, the invention relates to products produced by the disclosed methods.

[0010] In a further aspect, the invention relates to a method for osmosis-driven separation, the method comprising creating an osmotic pressure gradient across a semi-permeable osmotic membrane comprising a film polymerized on a blended support layer.

[0011] While aspects of the present invention can be described and claimed in a particular statutory class, such as the system statutory class, this is for convenience only and one of skill in the art will understand that each aspect of the present invention can be described and claimed in any statutory class. Unless otherwise expressly stated, it is in no way intended that any method or aspect set forth herein be construed as requiring that its steps be performed in a specific order. Accordingly, where a method claim does not specifically state in the claims or descriptions that the steps are to be limited to a specific order, it is no way intended that an order be inferred, in any respect. This holds for any possible non-express basis for

interpretation, including matters of logic with respect to arrangement of steps or operational flow, plain meaning derived from grammatical organization or punctuation, or the number or type of aspects described in the specification.

BRIEF DESCRIPTION OF THE FIGURES

[0012] The accompanying figures, which are incorporated in and constitute a part of this specification, illustrate several aspects and together with the description serve to explain the principles of the invention.

[0013] Figure 1 illustrates FO, PRO, and RO processes.

[0014] Figure 2 shows SEM images of standard TFC-RO membrane cross-section and skin layer. Polysulfone layer + fabric support is ~150 μm and the skin layer is ~0.05-0.25μm.

[0015] Figure 3 shows SEM images of cross-section and skin layer of the HTI-CTA membrane. Total thickness of the fabric-embedded polymer film is ~100 μm, while the skin layer is ~10 μm.

[0016] Figure 4 illustrates driving force profiles, expressed as water chemical potential, μ_w, for osmosis through (a) CTA membrane, (b) a TFC membrane operating in PRO-mode, and (c) a TFC membrane operating in FO-mode.

[0017] Figure 5 is a plot of commercial CTA and TFC membrane performance when tested in FO and RO operating modes.

[0018] Figure 6 shows the ratio of hindered-to-bulk diffusivity as a function of support membrane porosity.

[0019] Figure 7 is an illustration relating composite membrane permeability to support membrane skin layer pore size and porosity.

[0020] Figure 8 is a plot of permeability ratio changes resulting from changes in skin layer thickness and support membrane skin layer porosity assuming a fixed support membrane skin layer pore size of 50 nm.

[0021] Figure 9 is a plot of permeability ratio changes resulting from changes in support membrane skin layer pore size (r1) and porosity assuming a fixed coating film thickness of 100 nm.

[0022] Figure 10 illustrates (a) individual support membrane skin layer "unit cells" as well as multiple unit cells considering (b) large skin layer pores and (c) small skin layer pores.

[0023] Figure 11 is a plot of (a) specific water flux (observed flux per unit applied pressure) and (b) observed salt rejection as a function of support membrane skin layer pore size and porosity.

[0024] Figure 12 Illustrates internal and external mass transfer limitations for (a) ideal FO membranes, (b) the CTA FO membrane, and (c) a conventional TFC RO membrane (operated in FO-mode).

[0025] Figure 13 shows plots of water flux versus (a) support membrane macrovoid porosity, (b) support membrane thickness assuming 50% porosity, (c) thin film water permeability (Pw) with 50% porosity and 40 μm thick support, and (d) versus feed/draw (bulk) solution osmotic pressure difference.

[0026] Figure 14 shows SEM images of UF membranes containing blend ratios of PANi:PSf of (a) 1:0, (b), 3:1, (c) 2:2, (d) 1:3, and (e) 0:1. From left to right, images are of membrane surface (left), entire membrane cross-section (middle), and high magnification close-up of skin layer pores.

[0027] Figure 15 shows experimentally determined water (P_w) and salt (P_s) permeability coefficients for commercial CTA/TFC membranes and 3 generations of UCLA composite FO membranes tested in FO-mode. UCLA FO1, FO2, and FO3 membranes represent polyamide coated membranes with 0:1 (pure PSf), 2:2 and 1:3 PANi:PSf blend ratios, which correspond to images (e), (c), and (d) in Fig. 14, respectively.

[0028] Figure 16 shows grey-scale SEM surface image of PANi membrane (left) converted to black and white image (right) to determine membrane pore size and porosity. Figure 16 was originally published by R. Guillen, et al. (*J. Mater. Chem.* 2010, 20, 4621-4628).

[0029] Figure 17 shows PANi:PSf composite membranes.

[0030] Figure 18 shows FTIR spectra for polyaniline–polysulfone blend membranes.

[0031] Figure 19 shows plan view time sequence SEM images of PANi–PSf blend membranes exposed to a focused ion beam.

[0032] Figure 20 shows the water permeability and salt permeability for preliminary PSf and PANi-blended TFC membranes compared to CTA membrane.

[0033] Figure 21 shows the water permeability and salt permeability of PANi-blended TFC membranes using isopar and hexane as the organic solvent compared to the CTA membrane when tested in forward osmosis experiments.

[0034] Additional advantages of the invention will be set forth in part in the description which follows, and in part will be obvious from the description, or may be learned by practice of the invention. The advantages of the invention will be realized and attained by means of the elements and combinations particularly pointed out in the appended claims. It is to be understood that both the foregoing general description and the following detailed description are exemplary and explanatory only and are not restrictive of the invention, as claimed.

DETAILED DESCRIPTION

[0035] The present invention may be understood more readily by reference to the following detailed description of aspects of the invention and the Examples included therein and to the Figures and their previous and following description.

[0036] Before the present compounds, compositions, articles, devices, and/or methods are disclosed and described, it is to be understood that they are not limited to specific synthetic methods unless otherwise specified, or to particular reagents unless otherwise specified, as such may, of course, vary. It is also to be understood that the terminology used herein is for the purpose of describing particular aspects only and is not intended to be limiting.

A. DEFINITIONS

[0037] Although any methods and materials similar or equivalent to those described herein can be used in the practice or testing of the present invention, example methods and materials are now described.

[0038] All publications mentioned herein are incorporated herein by reference to disclose and describe the methods and/or materials in connection with which the publications are cited. The publications discussed herein are provided solely for their disclosure prior to the filing date of the present application. Nothing herein is to be construed as an admission that the present invention is not entitled to antedate such publication by virtue of prior invention. Further, the dates of publication provided herein may be different from the actual publication dates, which can require independent confirmation.

[0039] As used in the specification and the appended claims, the singular forms "a," "an" and "the" include plural referents unless the context clearly dictates otherwise. Thus, for example, reference to "a component," "a polymer," or "a particle" includes mixtures of two or more such components, polymers, or particles, and the like.

[0040] Ranges can be expressed herein as from "about" one particular value, and/or to "about" another particular value. When such a range is expressed, another aspect includes from the one particular value and/or to the other particular value. Similarly, when values are expressed as approximations, by use of the antecedent "about," it will be understood that the particular value forms another aspect. It will be further understood that the endpoints of each of the ranges are significant both in relation to the other endpoint, and independently of the other endpoint. It is also understood that there are a number of values disclosed herein, and that each value is also herein disclosed as "about" that particular value in addition to the value itself. For example, if the value "10" is disclosed, then "about 10" is also disclosed. It is also understood that when a value is disclosed that "less than or equal to" the value, "greater than or equal to the value" and possible ranges between values are also disclosed, as appropriately understood by the skilled artisan. For example, if the value "10" is disclosed the "less than or equal to 10" as well as "greater than or equal to 10" is also disclosed. It is also understood that throughout the application, data is provided in a number of different formats and that this data represents endpoints and starting points, and ranges for any combination of the data points. For example, if a particular data point "10" and a particular data point 15 are disclosed, it is understood that greater than, greater than or equal to, less than, less than or equal to, and equal to 10 and 15 are considered disclosed as well as between 10 and 15. It is also understood that each unit between two particular units are also disclosed. For example, if 10 and 15 are disclosed, then 11, 12, 13, and 14 are also disclosed.

[0041] A residue of a chemical species, as used in the specification and concluding claims, refers to the moiety that is the resulting product of the chemical species in a particular reaction scheme or subsequent formulation or chemical product, regardless of whether the moiety is actually obtained from the chemical species. Thus, an ethylene glycol residue in a polyester refers to one or more $-OCH_2CH_2O-$ units in the polyester, regardless of whether ethylene glycol was used to prepare the polyester. Similarly, a sebacic acid residue in a polyester refers to one or more $-CO(CH_2)_8CO-$ moieties in the polyester, regardless of whether the residue is obtained by reacting sebacic acid or an ester thereof to obtain the polyester.

[0042] As used herein, the terms "optional" or "optionally" means that the subsequently described event or circumstance may or may not occur, and that the description includes instances where said event or circumstance occurs and instances where it does not.

[0043] Disclosed are the components to be used to prepare the compositions of the invention as well as the compositions themselves to be used within the methods disclosed herein. These and other materials are disclosed herein, and it is understood that when combinations, subsets, interactions, groups, etc. of these materials are disclosed that while specific reference of each various individual and collective combinations and permutation of these compounds may not be explicitly disclosed, each is specifically contemplated and described herein. For example, if a particular compound is disclosed and discussed and a number of modifications that can be made to a number of molecules including the compounds are discussed, specifically contemplated is each and every combination and permutation of the compound and the modifications that are possible unless specifically indicated to the contrary. Thus, if a class of molecules A, B, and C are disclosed as well as a class of molecules D, E, and F and an example of a combination molecule, A-D is disclosed, then even if each is not individually recited each is individually and collectively contemplated meaning combinations, A-E, A-F, B-D, B-E, B-F, C-D, C-E, and C-F are considered disclosed. Likewise, any subset or combination of these is also disclosed. Thus, for example, the sub-group of A-E, B-F, and C-E would be considered disclosed. This concept applies to all aspects of this application including, but not limited to, steps in methods of making and using the compositions of the invention. Thus, if there are a variety of additional steps that can be performed it is understood that each of these additional steps can be performed with any specific aspect or combination of aspects of the methods of the invention.

[0044] It is understood that the compositions disclosed herein have certain functions. Disclosed herein are certain structural requirements for performing the disclosed functions, and it is understood that there are a variety of structures that can perform the same function that are related to the disclosed structures, and that these structures will typically achieve the same result.

B. COMMERCIAL RO AND FO MEMBRANE MATERIALS

[0045] Traditional "thin film composite" (TFC) reverse osmosis membranes comprise a ~100 μm thick non-woven polyester fabric supporting a ~50 μm thick porous polysulfone membrane (Figure 2a), which is then coated with a ~50-250 nm thick, very dense polyamide film. The nanoscale polyamide film provides a highly productive and selective skin layer, but the composite membrane suffers from extremely high "internal concentration polarization" thereby greatly reducing productivity when used in FO processes. The underlying porous support membrane and fabric hinders the diffusion of solutes due to their relatively low-porosity, which lowers the effective osmotic driving force across the membrane limiting water permeation. This is not a problem in RO applications because salt that enters the backside of the membrane is flushed out by water permeating the thin film in the same direction. In osmotic processes, water and salt move in opposite directions (more detail is provided below) so this hydraulic flushing of salt through the support membrane and fabric layers does not occur.

Modern reverse osmosis (RO) membranes are formed as flat sheets or hollow fibers comprising an ultra-thin polyamide film coated over a porous polysulfone support membrane (S.H. Chen, et al. *J. Appl. Polym. Sci.* 83 (2002) 1112; R.J. Petersen, *J. Membr. Sci.* 83 (1993) 81). The selective polyamide barrier layer is formed *in situ* by polycondensation reaction of polyfunctional amine and acid chloride monomers at the interface of two immiscible solvents. These elegantly engineered materials exhibit excellent performance in many desalination and water purification applications; however, significant interest remains in discovering more energy-efficient, contaminant-selective, and fouling-resistant versions of these membranes. Tailoring separation performance and interfacial properties of RO membranes requires understanding, at a fundamental level, the mechanisms governing thin film formation.

In forming a polyamide thin film, a polyfunctional amine is dissolved in water and a polyfunctional acid chloride is dissolved in apolar organic solvents like hexane, naptha, cyclohexane, freon, or isoparrafin (M.M. Chau, US Patent 5,271,843, 1993; H. Hachisuka, K. US Patent 6,413,425, 2002; S. Verissimo, et al., *J. Membr. Sci.* 264 (2005) 48). When the two monomer solutions are brought into contact, both monomers partition across the liquid-liquid interface and react to form a polymer; however, polymerization occurs predominantly in the organic phase due to the relatively low solubility of most acid chlorides in water (V. Freger, *Langmuir* 21 (2005) 1884; P.W. Morgan, Chapter 2: Interfacial polymerization without stirring. In *Condensation Polymers: By Interfacial and Solution Methods*, Interscience Publishers: New York, NY, 1965; pp 19-64; P.W. Morgan, et al., J. *Polym. Sci. Pt. A-Polym. Chem.* 34 (1996) 531). Therefore, it is common to use a large excess of amine over acid chloride (typically about 20:1), which drives partitioning and diffusion of the amine into the organic phase. Any factors that alter the solubility and diffusivity of the amine monomer in the organic phase affect the reaction rate, and thus, the morphology and structure of the resulting polyamide film, which ultimately define separation performance and interfacial properties (P.W. Morgan, et al., *J. Polym. Sci. Pt. A-Polym. Chem.* 34 (1996) 531; E.L. Wittbecker, et al., *J. Polym. Sci. Pt. A-Polym. Chem.* 34 (1996) 521).

[0046] Selecting the organic solvent is critical since it governs, at a minimum, the amine monomer solubility and diffusivity in the reaction zone. For example, one recent study demonstrated that hexane and isopar produced significantly different TFC membranes, where isopar produced RO membranes with smaller apparent pore size (I.C. Kim, et al., *J. Polym. Sci. Pt. B-Polym. Phys.* 40 (2002) 2151). Solvent properties and reaction conditions (particularly temperature) affect the density, viscosity, and surface tension of the organic solvent. Viscosity clearly influences diffusion; however, solvent surface tension controls the amine solubility and, as a consequence, the amine-to-acid chloride concentration ratio in the reaction zone and the degree of polymerization. Organic solvent surface tension also governs miscibility of the two liquid phases (particularly penetration of the organic phase by water), which might alter hydrolysis and protonation states of acid chloride and amine moities and the extent of cross-linking.

[0047] It is common in practice to use combinations of additives to influence monomer solubility, diffusivity, hydrolysis, or protonation or to scavenge inhibitory reaction

byproducts. For example, addition of small amounts of hydrophilic water-soluble polymers or a polyhydric alcohol to the amine solution can produce high-flux reverse osmosis membranes with good rejection (M. Hirose, et al., US Patent 5,576,057, 1996). In a patent issued to M.M Chau et al. (US Patent 5,271,843, 1993.), aprotic solvents like N, N-dimethylformamide (DMF) are added to the aqueous aromatic amine solution. Initially, DMF reacts with an acyl chloride to produce an amidinium chloride, which is relatively unreactive toward aromatic amines. Later the amidinium chloride hydrolyzes to a carboxylate group, which inhibits cross-linking and produces more negative charge and higher water flux. Such additives include, but are not limited to, IPA, DMSO, HMPA and acetone.

[0048] Adding dimethyl sulfoxide (DMSO) to the aqueous amine solution increases the miscibility of water and hexane and probably also enhances MPD diffusivity, ultimately, improving water flux by formation of a thinner polyamide film (S.H. Kim, et al., *Environ. Sci. Technol.* 39 (2005) 1764; S.Y. Kwak, et al., *Environ. Sci. Technol.* 35 (2001) 4334.). Increased water-organic miscibility may cause hydrolysis of acid chlorides or de-protonation of amines, thereby reducing their reactivity and the extent of cross-linking. These authors report that surface roughness and surface area of these membranes increase as the concentration of DMSO increases, which suggests a correlation between surface roughness and permeability.

[0049] Sodium hydroxide, sodium tertiary phosphate, dimethyl piperazine, triethyleamine (TEA), and other acylation catalysts accelerate the MPD-TMC reaction by removing hydrogen halides formed during amide bond formation (R.J. Petersen, *J. Membr. Sci.* 83 (1993) 81.). It is suggested that the strength of the acid acceptor affects the degree of concurrent hydrolysis, and hence, membrane structure and performance. The aqueous solution may further contain a surfactant or organic acids like camphor sulfonic acid (CSA) improve absorption of the amine solution in the support(M.A. Kuehne, et al., *Environ. Prog.* 20 (2001) 23; J.E. Tomaschke US Patent 4,872,984, 1989).

[0050] Most studies of the MPD-TMC system indicate that curing is a necessary step to stabilize polyamide thin films (A.P. Rao, et al. *J. Membr. Sci.* 124 (1997) 263; A.P. Rao, *J. Membr. Sci.* 211 (2003) 13). Heat curing is used after film formation to remove residual organic solvent from the film and to promote additional cross-linking through dehydration of amine and carboxylic acid residues. This tends to increase water flux and salt rejection. With

increase in curing time or temperature, the porosity of the polyamide film is reduced by cross-linking. This is accompanied by significant decrease in water flux, but increase in salt rejection. However, exposure to high curing temperatures or long curing times can damage the microporous skin layer of the support membrane, which tends to decrease both water flux and salt rejection. Generally, curing temperatures ranging from 40 to 120 °C are used (W.E. Mickols US Patent 6,562,266, 2003.).

[0051] In a recent study, Ghosh et al. (*J. Membr. Sci.* 311 (2008) 34–45) concluded the following. Generally, RO membrane water permeability and salt rejection increase with increasing MPD diffusivity and decreasing MPD solubility. If higher MPD diffusivity is accomplished by changing to an organic solvent also giving higher MPD solubility, films exhibit higher water flux, salt passage, thickness, and roughness, but less crosslinking. If higher MPD diffusivity is accomplished by heating an organic solvent with low MPD solubility, films exhibit higher water flux, salt passage, crosslinking, and roughness. Curing at higher temperatures is needed to fully remove high boiling point solvents. Adding the salt of TEA and CSA to the aqueous-MPD solution increases MPD-TMC performance by inhibiting amine protonation and acid chloride hydrolysis, and possibly by protecting the support membrane during high temperature curing. Also, MPD-TMC film thickness and morphology are not intrinsically related to water permeability. The lack of correlation between film thickness and water permeability suggest the entire film thickness does not determine the pressure drop across composite RO membranes. Rather, permeation may occur at a "dense inner barrier layer" and the visible surface morphology is an unfortunate byproduct of the polymerization reaction. Interestingly film thickness and surface area strongly correlate with salt permeability, which suggests mass transfer (and external concentration polarization) may be influenced by RO membrane surface morphology. Finally, reaction and curing conditions that produce optimal separation performance tend to produce relatively rough, hydrophobic membrane surfaces.

[0052] Polyamide interfacial composite membranes are the most popular commercial form of reverse osmosis (RO) and nanofiltration (NF) membranes. The ability to independently tailo r support layer and thin film characteristics permitted optimization of the overall composite m embrane structure, permeability, selectivity, and stability. As a result, composite RO and NF membranes are now commonly employed in water purification applications such as desalinati on of brackish and ocean water, fresh water softening and organic removal, ultrapure water pr

oduction, and advanced wastewater purification (L. Raghuraman, *Desalin.* 91 (1993) 155-162; F.E. Sanders, et al., *Desalin.* 103 (1995) 133 to145; M. Manttari, *J. Membr. Sci.* 137 (1 997) 187 to199; I. Koyuncu, *J. Environ. Sci. Health Part A Tox./Haz. Sub. & Environ. Eng.* 36 (2001) 1321to 1333; S. Sridhar, et al., *J. Membr. Sci.* 205 (2002) 83to 90; S. Sridhar, et al ., *J. Chem. Tech. Biotech.* 78 (2003) 1061to 1067; S.V. Joshi, et al., *Desalin.* 165 (2004) 201 to 208; M. Turan, *Desalin.* 170 (2004) 83 to 90; P. Xu, et al., *Wat. Environ. Res.* 77 (2005) 40 to 48). More recently, interest in forward osmosis (FO) processes inspires the exploration o f novel support membrane structures and chemistries to form interfacial composite membrane s with suitable stability, selectivity, and permeability for applications such desalination, wast ewater purification, sludge concentration, food processing, osmotic pumps, and osmotic ener gy production. (T.Y. Cath, et al., *J. Membr. Sci.* 281 (2006) 70 to 87.) The ideal FO membran e may be an interfacial composite built on a thin, highly porous, hydrophilic support. Howev er, modern RO membranes typically comprise relatively thick, low porosity supports to provi de suitable mechanical stability under high applied pressures. In addition, most successful R O support membranes are made from relatively hydrophobic, chemically stable polymers.

[0053] In general, interfacial composite membranes are formed over porous supports by *in sit u* polycondensation of polyfunctional amine and acid chloride monomers at the interface of t wo immiscible solvents (R.J. Petersen, *J. Membr. Sci.* 83 (1993) 81 to150). Factors influenc ing the physicochemical properties (chemical structure, physical morphology, interfacial prop erties, and separation performance) of composite RO membranes include: support membrane structure and chemistry, monomer structures and concentration, polar and apolar solvent sele ction, catalysts and other additives, reaction temperature and time, curing temperature and ti me, and other post treatments. A key advantage of the thin film composite approach is that th e porous support and thin film can be separately optimized to achieve the best overall separati on performance and membrane stability. In past studies, porous support structures for polya mide composite membranes were prepared from polymers like polysulfone, polyethersulfone, polycarbonate, polyphenylene oxides, poly(styrenecoacrylonitrile), poly(phthalazinone ether sulfone ketone) (PPESK), polyacrylonitrile, polyetherimide, polypropylene and others by con ventional phase inversion techniques (J. Wei, et al, *J. Membr. Sci.* 256 (2005) 116 to 121; IC . Kimet al., *J. Polym. Sci. Part B Polym. Phys.* 40 (2002) 2151 to 2163; S.Verissimo, et al., *J. Membr. Sci.* 264 (2005) 48 to55; A.R. Korikov, et al., *J. Membr. Sci.* 279 (2006) 588 to 600) However, polysulfone appears to be the most popular polymer for fabricating composite RO

membranes because it is widely available, relatively cheap, easy to process, and is fairly stabl e against thermal, mechanical, chemical and bacterial attack. Note that polysulfone is relativ ely hydrophobic compared to most of the other polymers.

[0054] After successful preparation of composite RO membranes from *m*-phenylenediamine (MPD) and trimesoyl chloride (TMC) was demonstrated on polysulfone supports, most research focused on optimizing polyamide chemistry and modifying the surface to improve permeability, selectivity, and fouling-resistance. (A. Kulkarni, et al., *J. Membr. Sci.* 114 (1996) 39-50; I.J. Roh, et al., *J. Polym. Sci. Part B-Polym. Phys.* 36 (1998) 1821-1830; M. Hirose, et al., *J. Membr. Sci.* 121 (1996) 209-215; Y. Song, et al. *J. Membr. Sci.* 251 (2005) 67-79; D. Mukherjee, et al. *J. Membr. Sci.* 97 (1994) 231-249; D. Mukherjee, et al., *Desalin.* 104 (1996) 239-249; V. Freger, et al., *J. Membr. Sci.* 209 (2002) 283-292; J. Benavente, et al., *J. Colloid Interf. Sci.* 297 (2006) 226–234; S. Belfer, et al., *Acta Polym.* 49 (1998) 574 – 582; S. Belfer, et al., *J. Membr. Sci.* 139 (1998) 175 – 181; S. Belfer, et al., *Desalin.* 139 (2001) 169 – 176; T. Kai, et al., *J. Membr. Sci.* 265 (2005) 101–107). Relatively little research has been published on the role of support membrane properties in formation of polyamide composite membranes in recent years (H.I. Kim, et al., *J. Membr. Sci.* 286 (2006) 193–201; P.S. Singh, et al., *J. Membr. Sci.* 278 (2006) 19-25).

The porous support membrane provides a mechanical layer on which to build the composite structure and should be biologically, chemically, mechanically, and thermally stable. In addition, the morphology and chemistry of the support layer may influence the formation of the ultrathin polyamide layer.

[0055] Ghosh et al. (*Journal of Membrane Science* 336 (2009) 140–148) reported that interfacial polymerization of MPD-TMC thin films over polysulfone support membranes with different pore structure and chemistry produced polyamide-polysulfone composite membranes with widely varying separation performance and interfacial properties. Generally, more, large, hydrophobic skin layer pores produced more permeable and rough composite membranes because less polyamide formed within the pores. This produced an overall shorter path length for water and solute transport from the feed side to the permeate side of the polyamide layer. Formation of more polyamide within the pores of relatively porous, hydrophilic support membranes produced thinner, less rough polyamide layers with

significantly lower permeability. These findings have important implications for design of next generation FO membranes, which require highly porous and hydrophilic supports.

[0056] An alternative to traditional RO-TFC membranes has been proposed specifically for small-scale FO processes – the CTA membrane from Hydration Technologies Innovations in Albany, Oregon, USA. It is believed that the membrane comprises a dense cellulose triacetate integrally skinned asymmetric polymer film formed (and embedded) within a woven polyester mesh (to provide mechanical stability) with total film thickness of ~100 μm (Figure 3a) and skin layer thickness of ~10 μm (Figure 3b). The CTA membrane is appropriate for small-scale applications where high water production rates are not required because the thick skin layer gives rise to low water permeability, while the swellable nature of the hydrogel gives rise to low salt selectivity. In addition, cellulosic materials have very poor biological, chemical, mechanical and thermal stability; in fact, they rapidly hydrolyze and dissolve in water at neutral pH or higher. These same issues – low water permeability, salt selectivity and stability – plagued early RO membrane technology based on cellulosic polymers. It is well known that cellulosics are unstable at high temperature and pH, whereas polyamides and polysulfones have much better pH and temperature stability, which in combination with their high flux and selectivity explains their dominance in RO applications.

C. Importance of Internal Concentration Polarization

[0057] The actual (effective) driving force for osmosis is the chemical potential difference, $\Delta\mu_w$, across a semi-permeable osmotic membrane, which fundamentally expresses the concentration of water on either side of the semi-permeable membrane (Figure 4a). A salt and water mixture, therefore, contains less water per unit volume than pure water; the direction of change driving the system towards equilibrium is from high chemical potential to low chemical potential. Hence, water from the solution of higher chemical potential or lower salinity (always designated as the "feed") permeates into the solution of lower chemical potential or higher salinity (always referred to as the "draw"). Internal concentration polarization (ICP) – due to hindered diffusion of salt ions out of the support membrane (Figure 4b) in PRO-mode (concentrative "ICP") or into the support membrane (Figure 4c) in FO-mode ("dilutive ICP")–reduces the effective driving force for water flux across the membrane.

[0058] Experimentally, when the CTA membrane is compared to a commercial TFC membrane in both FO and RO modes of operation the dramatic performance differences are revealed (Figure 5). In RO-mode, the ultra-thin skin layer of the TFC membrane produces higher permeability and selectivity, whereas in FO-mode the low-porosity polysulfone support membrane causes dilutive internal concentration polarization, which decreases water permeability to about ~10X below the CTA membrane. Theoretically, in FO-mode the CTA membrane utilizes the entire driving force for transport, but offers extremely high hydraulic resistance to water permeation because it is so thick (recall Figure 4a), whereas a TFC RO membrane with the dense skin layer facing the feed solution in FO-mode is limited by draw solute dilution inside the porous support (recall Figure 4c).

[0059] Theoretical analysis of hindered diffusion is well established and has been applied to numerous other applications including FO and PRO processes, RO membrane fouling and module design, see E.M.V. Hoek; et al. (Environ. Eng. Sci. 2002, 19, (6), 357-372), E.M.V. Hoek; M. et al. (*Environ. Sci. Technol.* 2003, 37, (24), 5581-5588) and McCutcheon, et al., (*Desalination*, 2005, 174, (1), 1-11). Hindered diffusion in a porous media arises from the excluded volume occupied by the solid fraction of the media (e.g., the solid polymer phase of the support membrane). In addition, the more tortuous path that solutes must follow to exit the porous media also contributes (a straight line is the shortest path length for diffusion, but is not possible due to the tortuous paths that must be taken to migrate the solid volume fraction). Therefore, the "hindered diffusivity" is defined as $D^* = D \cdot \varepsilon_m / \tau_m$, where D is the bulk (unhindered) diffusivity, ε_m is the support membrane porosity, and τ_m ($= 1 - \ln \varepsilon_m^2$) is the support membrane tortuosity (B.P. Boudreau, *Geochim. Cosmochim.* Acc. 1996, 60, 3139). Typically, the porosity of TFC-RO membrane supports is less than ~20%, so the diffusivity is hindered to less than ~5% of the bulk diffusion coefficient for a salt (Figure 6). FO membrane designs begin from the perspective that the support membrane porosity should be as large as possible while maintaining requisite mechanical integrity and stability.

D. Theoretical Basis for High Performance FO Membranes

1. Water and Salt Transport Model

[0060] Transport through polymeric FO/RO membranes (hereafter "osmotic membranes") is generally considered to occur by a solution-diffusion type mechanism where water, J_w, and salt, J_s, flux are described by

$$J_w = P_w(\Delta p - \Delta \pi) \quad (1)$$

$$J_s = P_s \Delta c \quad (2)$$

[0061] Here, Δp is the trans-membrane hydraulic pressure, $\Delta \pi (= f_{os} \Delta c)$ is the trans-membrane osmotic pressure, Δc is the concentration difference across the membrane, f_{os} is the osmotic coefficient (= $2RT$ for NaCl; R = universal gas constant; T = absolute temperature) which converts units of molar concentration into units of osmotic pressure, while P_w and P_s are the apparent water and solute permeability coefficients. In RO processes, Δp is much larger than $\Delta \pi$, so the water flux is in the same direction as the salt flux; however, in FO processes, Δp is much smaller than $\Delta \pi$, so the water flux is in the opposite direction as the salt flux (recall Figure 1).

[0062] Selectivity of osmotic membranes is generally thought to arise from differences in solubility and diffusivity of water and salt in the polymer film comprising the membrane. Therefore, the water and solute permeability coefficients are classically defined by

$$P_w = \frac{D_w S_w}{\Delta x_{eff}} \quad (3)$$

$$P_s = \frac{D_s S_s}{\Delta x_{eff}} \quad (4)$$

where S_w and S_s are the solubility of water and salt in the membrane, D_w and D_s are the diffusivities of water and salt through the membrane, and Δx_{eff} is effective path length for diffusion. It follows that the water and salt permeability should decrease if the effective path length for diffusion increases, but the selectivity of a given membrane is purely due to solubility and diffusivity differences. Hence, the selectivity coefficient for a membrane and a specific solvent/solute pair (e.g., water/NaCl) is

$$\alpha_{w/s} = \frac{P_w}{P_s} = \left(\frac{D_w}{D_s}\right)\left(\frac{S_w}{S_s}\right) \quad (5)$$

[0063] Therefore, an osmotic membrane can be made more selective for water over salt by increasing either the diffusion selectivity (D_w/D_s) or solubility selectivity (S_w/S_s), which requires changing the physical structure or chemical nature of the membrane, respectively.

2. INTERFACIAL COMPOSITE MEMBRANE STRUCTURE-PERFORMANCE MODEL

[0064] Noting that a composite membrane comprises a selective coating film formed over top of a porous support layer, TFC membrane performance must be tied to both selective coating film and porous support layer properties. This is not a new concept in membrane science; a simplified version of a previously developed mechanistic model has been adapted herein H. Lonsdale; et al. (*Membrane processes in industry and biomedicine: proceedings* 1971, 101-122). The effective diffusion path length through the coating film is a direct function of the size and number of pores in the support membrane skin layer – the very top layer of the support membrane on which the coating film rests (Figure 7a). As the support membrane skin layer pore size (r_1) decreases (fixing the number of pores), the effective separation distance between surface pores (r_2) increases (Figure 7b); therefore, the effective path length for diffusion (Δx_{eff}) through the membrane is longer and permeability (for both water and salt) declines. Note the effective film thickness does not influence the selectivity, but rather the overall permeability.

[0065] Assuming a regular cubic arrangement of pores (Figure 7c), the porosity of a single skin layer pore unit cell can be defined from

$$\varepsilon_p = \frac{\pi}{4}\left(\frac{r_1}{r_2}\right)^2 \qquad (6)$$

[0066] Our model assumes the fraction solute and solvent molecules that enter the thin film directly over the skin layer pore is equal to the porosity (ε_p), and this fraction will diffuse in a straight line over a distance Δx. However, solute and solvent molecules that enter the thin film over the skin layer solid volume ($1 - \varepsilon_p$) will experience a longer effective path length to diffuse through the coating film. Therefore, the average path length for diffusion can be approximated by

$$\Delta x_{eff} = \varepsilon_p \Delta x + \left(1 - \varepsilon_p\right)\sqrt{\left(1.118 r_2 - r_1\right)^2 + \Delta x^2} \quad (7)$$

[0067] Applying this equation to explore the relationship between water permeability, coating film thickness, and skin layer pore characteristics a few important relationships emerge. First, thinner coating films are intrinsically more permeable; however, composite membrane permeability also depends on support membrane skin layer pore size and porosity. Specifically, thinner coating films require more porous support membrane skin layers to fully leverage the thin film permeability (Figure 8). For a fixed coating film thickness, support membrane skin layer porosity must increase as skin layer pore size increases (Figure 9). In contrast, as support membrane skin layer pore size decreases the same permeability ratio can be achieved at proportionally lower porosity because a smaller unit cell offers the shorter overall path length for diffusion (Figure 10a) and more unit cells per unit area of coating film (Figure 10b/c). Hence, the overall composite membrane structure is more permeable. For a given coating film structure (i.e., selectivity), a minimum salt rejection is fixed, but the maximum salt rejection is produced by decreasing porosity and increasing pore size (Figure 11a); in contrast, a maximum water flux is fixed and is produced by decreasing support membrane pore size and increasing porosity (Figure 11b). This mechanism explains one aspect of the classic trade-off relationship between high flux and high rejection.

3. Relating Osmotic Membrane Flux to Internal and External CP

[0068] As discussed previously, TFC membranes with porous supports suffer from both internal and external concentration polarization-based mass transfer limitations when operated in FO-mode. The ideal osmotic membrane is a thin, dense film without a porous supporting structure (Figure 12a); hence, only external mass transfer and film permeability/selectivity limit performance. It was ignored above, but the CTA membrane has a porous supporting structure, and hence, suffers from some internal CP although its low flux is largely due to its relatively thick, dense skin layer (Figure 12b). A traditional TFC membrane thin film offers very high flux and selectivity, but suffers from extreme internal CP because of the low porosity polysulfone support as well as some effects of the nonwoven polyester fabric (Figure 12c). The low macrovoid porosity of traditional TFC membrane polysulfone supports can limit their application to forward osmosis processes. Moreover, there is some evidence that the hydrophobicity of polysulfone further limits flux.

[0069] A simplified model of osmotic membrane transport is used here to illustrate the relationship between TFC membrane permeability (P_w), support membrane macrovoid porosity (ε_m) and thickness (δ_m), and water flux through the membrane. Assuming perfect rejection (to simplify this analysis), osmotic flux is described by

$$J_w = P_w\left[\pi_d \exp\left(-\frac{J_w}{k_{\text{int}}}\right) - \pi_f \exp\left(-\frac{J_w}{k_{ext}}\right)\right] \quad (8)$$

where k_{int} (= $D^*/\delta_{m/s}$) and k_{ext} (=$D/\delta_{d/f}$) are the internal and external mass transfer coefficients, D is the bulk diffusivity, and D^* (=$D\varepsilon_m/\tau_m$) is the hindered diffusivity. Note that here the support membrane macrovoid porosity and thickness refer to the entire cross-section of the support membrane rather than the skin layer as discussed above. Here, the TFC osmotic membrane permeability represents the combined effects of support membrane skin layer pore size and porosity plus the coating film structure. Applying the above FO model, the following scenarios were considered: new (hypothetical) TFC-RO membranes with varied support layer porosity, support layer thickness, thin film permeability, and bulk osmotic pressure difference between the feed and draw solutions.

[0070] As observed experimentally, a conventional TFC RO membrane performs very poorly compared to the CTA membrane; however, increasing the support membrane porosity from ~10% to ~50% produces a new TFC osmotic membrane that exhibits ~1.5X the flux of the CTA membrane (Figure 13a). Next, reducing the TFC support membrane thickness from ~150 μm (nonwoven fabric + polysulfone support) down to ~40 μm further increases TFC osmotic membrane flux to ~3X the CTA membrane (Figure 13b). Further optimizing support membrane skin layer and coating film properties can improve the flux to ~4X the CTA membrane (Figure 13c). Finally, depending on the concentration (i.e., osmotic pressure) difference between the feed and draw solutions between 2X and 5X overall productivity enhancements can be achieved (Figure 13d). Note the osmotic pressure difference between seawater and freshwater is ~350 psi at seawater dissolved solids concentrations of ~35 g/L.

E. Results

[0071] Summarizing state-of-the-art knowledge of polyamide composite membrane formation by interfacial polymerization in combination with the structure-performance model

presented above, high-performance osmotic membranes are desirably composite structures comprising: (1) Support membrane skin-layers with: Small pore size (r_p ~10-25 nm; to support 50-250 nm thick coating films), Highly porous (ε_p ~20-30%; to decrease path length for diffusion), Hydrophobic (θ_w> 70 °; to prevent the polyamide coating film from filling support membrane pores as it interfacially polymerizes as described by Ghosh et al. (*J. Membr. Sci.* 2007, 294, (1-2), 1-7), Support membrane cross-sectional characteristics of: Thin (d_m< 40 μm; to reduce path length for diffusion), Highly porous (ε_m> 50 %; ideally vertically aligned macrovoids), Hydrophilic (θ_w< 40 °; to minimize de-wetting and fouling), (3) Coating films that are: Highly permeable (P_w ~ 0.4-0.9×10^{-11} m/Pa-s = 0.05-0.10 gfd/psi), Highly selective (draw solute P_s ~ 0.5-1.0×10^{-8} m/s), Smooth, super-hydrophilic (θ_w< 40 °), uncharged interface (*i.e.*, fouling/cleaning), (4) Composite membrane stability for years when exposed to Periodic exposure to pH <1 or >13 and 1-2 ppm HOCl (cleaning and biogrowth control), Continuous exposure to 5 < T < 60 °C (tolerance to environmental and operational temp swings).

[0072] The disclosed compositions and methods demonstrate the ability to fine-tune performance of a new class of TFC-FO membranes. These first generation materials can comprise a polyamide thin film polymerized *in situ* over porous support membranes comprising different blends of polyaniline and polysulfone polymers. The polyaniline-polysulfone blend membranes can be prepared by phase inversion of the polymer mixtures on top of a polyester nonwoven fabric. PANi-PSf blend ultrafiltration membrane thickness, macrovoid porosity and orientation, skin layer pore size and porosity, and hydrophilicity (Figure 14, Table 1) have been shown to vary as a function of PANi content (G.R. Guillen et al. *Journal of Materials Chemistry* (2010), 20, 4621-4628). Hence, using PANi as an additive in PSf support membranes creates the opportunity to vary all of the theoretically important parameters that are hypothesized to produce high-performance TFC osmotic membranes.

[0073] Separation performance was tested in forward osmosis mode using 32 g/L NaCl solutions as the concentrated draw and deionized water as the dilute feed (Figure 15). Hand-cast PANi-PSf supported TFC-FO membranes were compared with samples of the commercial CTA membrane and a commercial seawater RO membrane (SW30HR, Dow Water Solutions, Midland, Michigan, USA). As noted above, the industry standard seawater RO membrane (noted as TFC-FO in Figure 15) exhibits ~10X lower permeability relative to the CTA membrane when tested in FO-mode. First-generation UCLA hand-cast osmotic

membranes (UCLA-FO1) exhibited similar water and salt permeability as the TFC-FO membrane, which makes sense because both membranes comprise a polyamide thin film coated over a polyester nonwoven fabric supported porous polysulfone membrane. The 2:2 PANi:PSf blended support membrane was more hydrophilic, but not significantly more porous than the pure PSf membrane, but produced significantly increased permeability relative to the TFC-FO membrane. Finally, the 1:3 PANi:PSf blended support membrane was more hydrophilic, thinner, and more porous, and hence, produced significantly enhanced permeability – as good as the CTA membrane. While the disclosed membranes exhibit approximately the same water and salt permeability as the CTA membrane, they exhibit far superior chemical stability when exposed to high pH solutions (representative of the pH of the ammonia-carbon dioxide draw solution).

TABLE 1. SEPARATION PERFORMANCE AND SKIN LAYER PORE MORPHOLOGY OF PANI-PSF UF MEMBRANES

PANi:PSf ratio	L_p ($\mu m \cdot s^{-1} MPa^{-1}$)	r_{NaCl} (%)	r_{MgSO_4} (%)	d_p (r_{MgSO_4}) (nm)	$d_{p,eff}$ (r_{NaCl}) (nm)	$d_{p,ave}$ (SEM) (nm)	$d_{p,max}$ (SEM) (nm)	ε (SEM) (%)	l (SEM) (nm)
1:0	10.492	92	0.2	60	> 6	11	42	2.1	7.8
3:1	3.118	97	1.4	54	> 6	7	20	4.6	22.7
1:1	1.710	> 99%	28	< 48	19	5	25	1.7	7.1
1:3	1.735	> 99%	36	< 48	16	6	23	1.8	10.6
0:1	1.109	> 99%	47	< 48	14	5	23	4.8	30.5

F. FORWARD OSMOSIS MEMBRANES WITH BLENDED SUPPORT STRUCTURES

[0074] In one aspect, the invention uses novel polyaniline-polysulfone (PANi-PSf) blends in the structure supporting a thin polyamide film where the majority of the separation occurs. These novel blends modify the structure and hydrophilicity of the pores in the support membrane. After the PANi-PSf blend is cast onto a non-woven polyester support, it is then coated with a polyamide thin film to enable the membrane to reject salt ions. This membrane

structure can be used in developing FO-based desalination, water purification, drug delivery and PRO osmotic power production processes.

[0075] As explored by Guillen et al., polyaniline alters the structure of polysulfone supports by introducing macrovoids within the support structure, increasing the porosity of the membrane and thereby increasing the water flux through the membrane. By coating a polyamide thin film on the PANi-PSf support an active layer at which the majority of solute rejection occurs. In one aspect, the invention is suited for any FO or PRO applications, but specifically in FO processes in which the solutions are caustic (pH > 10).

[0076] This innovative FO membrane structure is stable under basic conditions (pH >10) whereas the existing commercial CTA membrane degrades within 24 hours under basic conditions. The PANi-PSf supported membrane with a polyamide thin film coating is proven to have relatively constant performance before and after a base bath (pH > 13) for longer than 48 hours.

[0077] Theoretically, engineered osmosis has many potential applications in water and wastewater treatment and renewable energy generation. Companies such as Statkraft in Norway are building pilot plants for pressure retarded osmosis; however, full scale implementation is limited by the lack of an appropriate membrane. This invention is novel because polyaniline has never been used in the support material for osmotic membranes (FO, PRO, or RO). The fact that this FO membrane structure is stable under a wider range of conditions than the state of the art CTA membrane opens its use in applications such as low energy desalination using ammonia/carbon dioxide as the draw solution.

1. MEMBRANE STRUCTURE

[0078] In one aspect, the invention relates to a semi-permeable nanostructured osmosis membrane comprising a polymer film polymerized on a blended support layer. In a further aspect, such a membrane can have an asymmetric structure of three layers: a top thin film active layer (e.g., interfacially polymerized film), a middle polymer support (e.g., blended support layer), and a bottom fabric (e.g., polyester) support.

[0079] In a further aspect, the invention relates to a semi-permeable forward osmosis (FO) membrane comprising having a permeability of from about 0.01 gfd/psi to about 0.10 gfd/psi. The FO membrane can also have a stability for at least about 1 year under periodic exposure

to pH ≤ 1 or pH ≥ 13. In a further aspect, the membrane is compatible with "ammonia - carbon dioxide draw solution"(also referred to herein as a "draw solution") FO process conditions. In a further aspect, the membrane is compatible with continuous exposure to an operating temperature range of from about 5 °C to about 60 °C. For example, the operating temperature can be about 50 °C. In a further aspect, the membrane has a selectivity (R_s) of at least about 99.5% for NaCl, >99.9% for draw solute.

[0080] In a further aspect, the semi-permeable forward osmotic membrane can also have a salt, such as a sodium chloride, permeability (P_s)of less than 10^{-7} m/s , such as a sodium chloride permeability of 10^{-7} m/s to 10^{-8} m/s. For example, the permeable forward osmotic membrane can have a salt, such as a sodium chloride, permeability of about 0.5-1.0×10^{-8} m/s.

[0081] In a further aspect, the permeable forward osmotic membrane can also have a support membrane with deionized water contact angle below 40 degrees. For example, the - permeable forward osmotic membrane can also have a support membrane with deionized water contact angle below 20 degrees. The semi-permeable osmotic membrane can also have up to 50% porosity through the volume of support membrane (flat sheet and hollow fiber) and support fabric (flat sheet only). The semi-permeable osmotic membrane can also have a stability for at least about 1 year under continuous exposure to pH of 10 to 13 (i.e., for the ammonia-carbon dioxide draw solution) and periodic exposure to pH ≤ 1 or pH ≥ 13 (chemical cleaning) and temperatures up to 50 degrees Celsius.

[0082] In one aspect, the membranes can be highly permeable, 0.05-0.10 gfd/psi, be highly selective (draw solute P_s ~ 0.5-1.0×10^{-8} m/s), be smooth, have a super-hydrophilic (θ_w< 40 °), uncharged interface (*i.e.*, fouling/cleaning), the composite membrane can have a stability for years when exposed to Periodic exposure to pH <1 or >13 and 1-2 ppm HOCl (cleaning and biogrowth control), Continuous exposure to 5 < T < 60 °C (tolerance to environmental and operational temp swings).

[0083] In a further aspect, the membrane comprises a polymeric support layer, and a film polymerized on the support layer. In a further aspect, the polymeric support layer comprises a blend of two or more polymers. In a further aspect, the support layer comprises polysulfone. In a further aspect, the support layer comprises polyaniline. In a further aspect, the support layer comprises a blend of polysulfone and polyaniline. In a further aspect, the

support layer comprises at least about 50% polysulfone. In a further aspect, the support layer comprises less than about 50% polyaniline. In a further aspect, the support layer comprises from about 50:50 polyaniline/polysulfone to about 25:75 polyaniline/polysulfone. In a further aspect, the support layer comprises from about 40:60 polyaniline/polysulfone to about 20:80 polyaniline/polysulfone. In a further aspect, the support layer comprises about 1:3 polyaniline/polysulfone.

[0084] In a further aspect, the support layer has: skin-layer average pore size (r_p) of from about 10 nm to about 25 nm, skin-layer porosity (ε_m) of from about 20% to about 30%, skin-layer surface water contact angle of (θ_w) of greater than about 70°, cross-sectional thickness (δ_m) of less than about 50 μm, cross-sectional porosity (ε_m) of greater than about 50%, cross-sectional macrovoid alignment substantially vertical ($\tau_m \approx 1$), and cross-sectional surface water contact angle of (θ_w) of less than about 40°.

[0085] In a further aspect, the film has: cross-sectional thickness of from about 50nm to about 250nm, permeability of from about 0.01 gfd/psi to about 0.10 gfd/psi, and surface water contact angle of (θ_w) of greater than about 70°.

[0086] In a further aspect, the membrane comprises: a polymeric support layer having: skin-layer average pore size (r_p) of from about 10 nm to about 25 nm, skin-layer porosity (ε_m) of from about 20% to about 30%, skin-layer surface water contact angle of (θ_w) of greater than about 70°, cross-sectional thickness (δ_m) of less than about 50 μm, cross-sectional porosity (ε_m) of greater than about 50%, cross-sectional macrovoid alignment substantially vertical ($\tau_m \approx 1$), and cross-sectional surface water contact angle of (θ_w) of less than about 40°; and a film polymerized on the support layer, the film having: cross-sectional thickness of from about 50 nm to about 250 nm, permeability of from about 0.01 gfd/psi to about 0.10 gfd/psi, and surface water contact angle of (θ_w) of greater than about 70°.

[0087] In a further aspect, the membrane comprises a polyaniline/polysulfone blend support layer having: skin-layer average pore size (r_p) of from about 10 nm to about 25 nm, skin-layer porosity (ε_m) of from about 20% to about 30%, skin-layer surface water contact angle of (θ_w) of greater than about 70°, cross-sectional thickness (δ_m) of less than about 50 μm, cross-sectional porosity (ε_m) of greater than about 50%, cross-sectional macrovoid alignment substantially vertical ($\tau_m \approx 1$), and cross-sectional surface water contact angle of (θ_w) of less

than about 40°, such as less than 20°. In a further aspect, the support layer comprises about 1:3 polyaniline/polysulfone.

[0088] In a further aspect, the film comprises at least one of a polyamide, a polyether, a polyether-urea, a polyester, or a polyimide or a copolymer thereof or a mixture thereof. In a further aspect, the film comprises a polyamide. In a further aspect, the polyamide comprises residues of a phthaloyl halide, a trimesoyl halide, or a mixture thereof. In a further aspect, the polyamide comprises residues of diaminobenzene, triaminobenzene, or piperazine or a mixture thereof. In a further aspect, the film comprises an aromatic polyamide. In a further aspect, the film comprises residues of a trimesoyl halide and residues of a diaminobenzene. In a further aspect, the film comprises an interfacially polymerized aromatic polyamide.

[0089] In a further aspect, the membrane is compatible with "ammonia - carbon dioxide" FO process conditions, and comprises an about 1:3 polyaniline/polysulfone blend support layer having: skin-layer average pore size (r_p) of from about 10 nm to about 25 nm, skin-layer porosity (ε_m) of from about 20% to about 30%, skin-layer surface water contact angle of (θ_w) of greater than about 70°, cross-sectional thickness (δ_m) of less than about 50 μm, cross-sectional porosity (ε_m) of greater than about 50%, cross-sectional macrovoid alignment substantially vertical ($\tau_m \approx 1$), and cross-sectional surface water contact angle of (θ_w) of less than about 40°; and a polyamide film interfacially polymerized on the support layer, the film having: cross-sectional thickness of from about 50nm to about 250nm, permeability of from about 0.01 gfd/psi to about 0.10 gfd/psi, and surface water contact angle of (θ_w) of greater than about 70°.

a. DRAW SOLUTION STABILITY OF MEMBRANES

[0090] In one aspect, the FO membranes are more stable in a draw solution than a CTA membrane. For example, the FO membrane can be more stable in a draw solution at pH ≥ 13 than a CTA membrane. In another example, the FO membrane can be more stable in a draw solution at pH 11-13 than a CTA membrane. In another example, the FO membrane can be more stable in a draw solution at pH 9-11 than a CTA membrane. In another example, the FO membrane can be more stable in a draw solution at pH 7-9 than a CTA membrane.

[0091] In a further aspect, the FO membrane can have a draw solution stability of at least about 60 hrs in pH ≥ 13. For example, the FO membrane can have a draw solution stability

of at least about 96 hrs in pH ≥ 13. In another example, the FO membrane can have a draw solution stability of at least about 1 week in pH ≥ 13. In another example, the FO membrane can have a draw solution stability of at least about 1 month in pH ≥ 13. In another example, the FO membrane can have a draw solution stability of at least about 3 months in pH ≥ 13. In another example, the FO membrane can have a draw solution stability of at least about 6 months in pH ≥ 13. In another example, the FO membrane can have a draw solution stability of at least about 1 year in pH ≥ 13. In another example, the FO membrane can have a draw solution stability of at least about 3 years in pH ≥ 13. In another example, the FO membrane can have a draw solution stability of at least about 5 years in pH ≥ 13.

[0092] In a further aspect, the FO membrane can have a draw solution stability of at least about 1 week in pH 11-13. For example, the FO membrane can have a draw solution stability of at least about 3 months in pH 11-13. In another example, the FO membrane can have a draw solution stability of at least about 6 months in pH 11-13. In another example, the FO membrane can have a draw solution stability of at least about 1 year in pH 11-13. In another example, the FO membrane can have a draw solution stability of at least about 3 years in pH 11-13. In another example, the FO membrane can have a draw solution stability of at least about 5 years in pH 11-13.

[0093] In a further aspect, the FO membrane can have a draw solution stability of at least about 3 months in pH 9-11. For example, the FO membrane can have a draw solution stability of at least about 6 months in pH 9-11. In another example, the FO membrane can have a draw solution stability of at least about 1 year in pH 9-11. In another example, the FO membrane can have a draw solution stability of at least about 3 years in pH 9-11. In another example, the FO membrane can have a draw solution stability of at least about 5 years in pH 9-11.

[0094] In a further aspect, the FO membrane can have a draw solution stability of at least about 1 year in pH 7-9. For example, the FO membrane can have a draw solution stability of at least about 3 years in pH 7-9. In another example, the FO membrane can have a draw solution stability of at least about 5 years in pH 7-9.

b. BLENDED SUPPORT LAYER

[0095] In one aspect, the support layer comprises two or more polymers. In a further aspect, the support layer comprises polysulfone. In a further aspect, the support layer comprises polyaniline. In a further aspect, the support layer comprises a blend of polysulfone and polyaniline. In a further aspect, the support layer is nonwoven.

[0096] In various aspects, the blend can comprise up to about 99% polysulfone. For example, the blend can comprise up to about 98%, up to about 97%, up to about 95%, up to about 90%, up to about 85%, up to about 80%, up to about 75%, up to about 70%, up to about 65%, up to about 60%, up to about 55%, up to about 50%, up to about 45%, up to about 40%, up to about 35%, up to about 30%, up to about 25%, up to about 20%, up to about 15%, up to about 10%, up to about 5%, up to about 98%, up to about 3%, up to about 2%, or up to about 1% polysulfone. In one aspect, the blend comprises no polysulfone.

[0097] In further aspects, the blend can comprise up to about 99% polyaniline. For example, the blend can comprise up to about 98%, up to about 97%, up to about 95%, up to about 90%, up to about 85%, up to about 80%, up to about 75%, up to about 70%, up to about 65%, up to about 60%, up to about 55%, up to about 50%, up to about 45%, up to about 40%, up to about 35%, up to about 30%, up to about 25%, up to about 20%, up to about 15%, up to about 10%, up to about 5%, up to about 98%, up to about 3%, up to about 2%, or up to about 1% polyaniline. In one aspect, the blend comprises no polyaniline.

[0098] In yet further aspects, the blend can comprise up to about 99% polyaniline-polysulfone. For example, the blend can comprise up to about 98%, up to about 97%, up to about 95%, up to about 90%, up to about 85%, up to about 80%, up to about 75%, up to about 70%, up to about 65%, up to about 60%, up to about 55%, up to about 50%, up to about 45%, up to about 40%, up to about 35%, up to about 30%, up to about 25%, up to about 20%, up to about 15%, up to about 10%, up to about 5%, up to about 98%, up to about 3%, up to about 2%, or up to about 1% polyaniline-polysulfone. Thus, in certain aspects, the blend can comprise polymers in addition to polyaniline and polysulfone. In such aspects, the ratio of polyaniline to polysulfone can be, for example, 99:1, 98:2, 97:3, 95:5, 90:10, 85:15, 80:20, 75:25, 70:30, 65:35, 60:40, 55:45, 50:50, 45:55, 40:60, 35:65, 30:70, 25:75, 20:80, 15:85, 10:90, 5:95, 3:97, 2:98, or 1:99.

c. POLYMER FILM

[0099] In a further aspect, the film comprises at least one of a polyamide, a polyether, a polyether-urea, a polyester, or a polyimide or a copolymer thereof or a mixture thereof. In a further aspect, the film comprises a polyamide. In a further aspect, the polyamide comprises residues of a phthaloyl halide, a trimesoyl halide, or a mixture thereof. In a further aspect, the polyamide comprises residues of diaminobenzene, triaminobenzene, or piperazine or a mixture thereof. In a further aspect, the film comprises an aromatic polyamide. In a further aspect, the film comprises residues of a trimesoyl halide and residues of a diaminobenzene.

[00100] In a further aspect, the film has an average thickness of from about 50 nm to about 250 nm, from about 50 nm to about 200 nm, from about 100 nm to about 250 nm, or from about 100 nm to about 200 nm. In a further aspect, the film comprises an interfacially polymerized aromatic polyamide.

d. HYDROPHILICITY

[00101] With reference to the disclosed compositions and methods, hydrophilicity can be described in terms of surface water contact angle (θ_w). For example, a membrane (or a discrete part, portion, or section of a membrane) can be described as having a certain surface water contact angle or range of angles. In one aspect, a surface water contact angle can be less than about 40°, less than about 35°, less than about 30°, less than about 25°, less than about 20°, less than about 15°, less than about 10°, or less than about 5°. For example, the membrane can have a surface water contact angle can be less than about 20°.

e. HYDROPHOBICITY

[00102] With reference to the disclosed compositions and methods, hydrophobicity can be described in terms of surface water contact angle (θ_w). For example, a membrane (or a discrete part, portion, or section of a membrane) can be described as having a certain surface water contact angle or range of angles. In one aspect, a surface water contact angle can be greater than about 70°, greater than about 75°, greater than about 80°, greater than about 85°, greater than about 90°, or greater than about 95°.

f. CROSS-SECTIONAL MACROVOID ALIGNMENT

[00103] With reference to the disclosed compositions and methods, cross-sectional alignment of macrovoids within the support layers can be described in terms of deviation from theoretical perpendicularity from the support layer surface. In one aspect, the average cross-sectional macrovoid alignment is substantially parallel to the support layer surface. In a further aspect, cross-sectional alignment of macrovoids within the support layers is substantially vertical ($\tau_m \approx 1$). In a further aspect, τ_m is greater than 0.95, greater than 0.90, greater than 0.85, greater than 0.80, greater than 0.75, or greater than 0.70.

2. METHODS OF MAKING

[00104] In one aspect, the invention relates to a method for preparing a semi-permeable nanostructured osmosis membrane, the method comprising polymerizing a film onto a blended polymeric support layer. In a further aspect, polymerizing is performed interfacially. In a further aspect, the support layer comprises polysulfone. In a further aspect, the support layer comprises polyaniline. In a further aspect, the support layer comprises a blend of polysulfone and polyaniline. In a further aspect, the film comprises at least one of a polyamide, a polyether, a polyether-urea, a polyester, or a polyimide or a copolymer thereof or a mixture thereof. In a further aspect, the film comprises a polyamide. In a further aspect, the support layer is produced by phase inversion of a polymer blend solution or suspension.

[00105] In one aspect, the invention comprises the steps of providing a polar mixture comprising a polar liquid and a first monomer that is miscible with the polar liquid; providing an apolar mixture comprising an apolar liquid substantially immiscible with the polar liquid and a second monomer that is miscible with the apolar liquid; and contacting the polar mixture and the apolar mixture at a temperature sufficient to react the first monomer with the second monomer, thereby interfacially-polymerizing the first monomer and the second monomer to form a polymer matrix film.

[00106] By "miscible," it is meant that the respective phases can mix and form a homogeneous mixture or dispersion at the relevant temperature and pressure. Unless otherwise specified, the relevant temperature and pressure are at room temperature and at atmospheric pressure. By "immiscible," it is meant that the respective phases do not

appreciably mix and do not appreciably form a homogeneous mixture at the relevant temperature and pressure. Two liquids can be termed immiscible if neither liquid is appreciably soluble in the other liquid. An example of two immiscible liquids is hexane and water.

a. APOLAR LIQUID

[00107] While it is contemplated that the apolar liquid can be any apolar liquid known to those of skill in the art, typically, an apolar liquid of the invention is selected such that it is immiscible with a particular polar liquid used in a method of the invention.

[00108] In one aspect, the apolar liquid can comprise at least one of a C_5 to C_{24} hydrocarbon. The hydrocarbon can be an alkane, an alkene, or an alkyne. The hydrocarbon can be cyclic or acyclic. The hydrocarbon can be straight chain or branched. The hydrocarbon can be substituted or unsubstituted. In further aspects, the apolar liquid can comprise at least one of a linear hydrocarbon, a branched hydrocarbon, a cyclic hydrocarbon, naptha, heavy naptha, paraffin, or isoparaffin or a mixture thereof. In one aspect, the apolar liquid comprises hexane.

b. POLAR LIQUID

[00109] While it is contemplated that the polar liquid can be any polar liquid known to those of skill in the art, typically, a polar liquid of the invention is selected such that it is immiscible with a particular apolar liquid used in a method of the invention.

[00110] In one aspect, the polar liquid can comprise at least one of a C_5 to C_{24} alcohol. The alcohol can be an alkane, an alkene, or an alkyne. The alcohol can be cyclic or acyclic. The alcohol can be straight chain or branched. The alcohol can be substituted or unsubstituted. In a further aspect, the polar liquid comprises water.

c. BLENDED SUPPORT LAYER

[00111] The support membrane can comprise a polymer blend. That is, the support membrane can comprise two or more polymers. In a further aspect, the support membrane comprises polysulfone. In a further aspect, the support membrane comprises polyaniline. In a further aspect, the support membrane comprises a blend of polysulfone and polyaniline. In

a further aspect, the support membrane is cast onto a nonwoven fabric. In a further aspect, the support membrane is cast into a woven fabric.

d. MONOMERS

[00112] Generally, the polymer matrix of the invention is prepared by reaction of two or more monomers. In one aspect, the first monomer is a dinucleophilic or a polynucleophilic monomer and the second monomer is a dielectrophilic or a polyelectrophilic monomer. That is, each monomer can have two or more reactive (*e.g.*, nucleophilic or electrophilic) groups. Both nucleophiles and electrophiles are well known in the art, and one of skill in the art can select suitable monomers for use in the methods of the invention. In one aspect, the first and second monomers can be chosen so as to be capable of undergoing an interfacial polymerization reaction to form a polymer matrix (*i.e.*, a three-dimensional polymer network) when brought into contact. In a further aspect, the first and second monomers can be chosen so as to be capable of undergoing a polymerization reaction when brought into contact to form a polymer product that is capable of subsequent crosslinking by, for example, exposure to heat, light radiation, or a chemical crosslinking agent.

[00113] In one aspect, a first monomer is selected so as to be miscible with a polar liquid and, with the polar liquid, can form a polar mixture. The first monomer can optionally also be selected so as to be immiscible with an apolar liquid. Typically, the first monomer is a dinucleophilic or a polynucleophilic monomer. In a further aspect, the first monomer can comprise a diaminobenzene. For example, the first monomer can comprise *m*-phenylenediamine. As a further example, the first monomer can comprise a triaminobenzene. In a yet further aspect, the polar liquid and the first monomer can be the same compound; that is, the first monomer is not dissolved in a separate polar liquid.

[00114] In one aspect, a second monomer is selected so as to be miscible with an apolar liquid and, with the apolar liquid, can form an apolar mixture. The second monomer can optionally also be selected so as to be immiscible with a polar liquid. Typically, the second monomer is a dielectrophilic or a polyelectrophilic monomer. In a further aspect, the second monomer can comprise a trimesoyl halide. For example, the second monomer can comprise trimesoyl chloride. As a further example, the second monomer can comprise a phthaloyl halide. In a yet further aspect, the apolar liquid and the second monomer can be the same compound; that is, the second monomer is not dissolved in a separate apolar liquid.

[00115] Generally, the difunctional or polyfunctional nucleophilic monomer used in the present invention can have primary or secondary amino groups and may be aromatic (*e.g.*, *m*-phenylenediamine, *p*-phenyenediamine, 1,3,5-triaminobenzene, 1,3,4-triaminobenzene, 3,5-diaminobenzoic acid, 2,4-diaminotoluene, 2,4-diaminoanisole, and xylylenediamine) or aliphatic (*e.g.*, ethylenediamine, propylenediamine, and *tris*(2-diaminoethyl)amine). Examples of suitable amine species include primary aromatic amines having two or three amino groups, for example *m*-phenylene diamine, and secondary aliphatic amines having two amino groups, for example piperazine. The amine can typically be applied to the microporous support as a solution in a polar liquid, for example water. The resulting polar mixture typically includes from about 0.1 to about 20 weight percent, for example from about 0.5 to about 6 weight percent, amine. Once coated on the microporous support, excess polar mixture may be optionally removed. The polar mixture need not be aqueous but is typically immiscible with the apolar liquid.

[00116] Generally, difunctional or polyfunctional electrophilic monomer is preferably coated from an apolar liquid, although the monomer can optionally be delivered from a vapor phase (for monomers having sufficient vapor pressure). The electrophilic monomer can be aromatic in nature and can contain two or more, for example three, electrophilic groups per molecule. In the case of acyl halide electrophilic monomers, because of the relatively lower cost and greater availability, acyl chlorides are generally more suitable than the corresponding bromides or iodides. A suitable polyfunctional acyl halide is trimesoyl chloride (TMC). The polyfunctional acyl halide can be dissolved in an apolar organic liquid in a range of, for example, from about 0.01 to about 10.0 weight percent or from about 0.05 to about 3 weight percent, and delivered as part of a continuous coating operation. Suitable apolar liquids are those which are capable of dissolving the electrophilic monomers, for example polyfunctional acyl halides, and which are immiscible with a polar liquid, for example water. In particular, suitable polar and apolar liquids can include those which do not pose a threat to the ozone layer and yet are sufficiently safe in terms of their flashpoints and flammability to undergo routine processing without having to undertake extreme precautions. Higher boiling hydrocarbons, *i.e.*, those with boiling points greater than about 90 °C, such as C_8 –C_{24} hydrocarbons and mixtures thereof, have more suitable flashpoints than their C_5 -C_7 counterparts, but they are less volatile.

[00117] Once brought into contact with one another, the electrophilic monomer and nucleophilic monomer react at the surface interface between the polar mixture and the apolar mixture to form a polymer, for example polyamide, discriminating layer. The reaction time is typically less than one second, but contact time is often longer, for example from one to sixty seconds, after which excess liquid may optionally be removed, *e.g.*, by way of an air knife, water bath(s), dryer, and the like. The removal of the excess polar mixture and/or apolar mixture can be conveniently achieved by drying at elevated temperatures, *e.g.*, from about 40 °C to about 120 °C, although air drying at ambient temperatures may be used, or by immersing into water at elevated temperatures, *e.g.*, from about 40 °C to about 120 °C.

[00118] Through routine experimentation, those skilled in the art will appreciate the optimum concentration of the monomers, given the specific nature and concentration of the other monomer, reaction conditions, and desired membrane performance.

3. Methods for Using

[00119] In a further aspect, the invention relates to a method for osmotically-driven separation, the method comprising creating an osmotic pressure gradient across a semi-permeable forward osmosis membrane comprising a film polymerized on a blended support layer. In a further aspect, the semi-permeable forward osmosis membrane exhibits a water permeability of about 1×, about 2×, or about 5× that of a commercial "CTA" membrane. In a further aspect, the semi-permeable forward osmosis membrane exhibits a salt passage of about 1×, about 0.1×, or about 2× that of a commercial "CTA" membrane. In a further aspect, purified water is produced. In a further aspect, electricity is produced.

G. Synthesis of Porous Membranes

[00120] Membranes comprising the compositions disclosed herein can be produced by a number of procedures known in the art. Typical processes and reagents known in the art include those described for example in Fan et al., J. Membr. Sci., 2008, 320, 363-371; Ball et al., Membr. Sci., 2000,174,161-176; Anderson et al., Science, 1991,252, 1412-1415; U.S. Patent No. 5,096,586; U.S. Provisional Patent Application No. 61/260,365; WO 2009/039467; WO 2006/098872; U.S. Patent Publication No. 20050270442; U.S. Patent Application No. 11/927,521; and U.S. Patent Application No. 11/364,885, the contents of which are incorporated by reference.

[00121] Phase inversion is a common method used to synthesize porous membranes. Polymers are controllably transformed from a liquid state to a solid state by this process. Solidification is initiated by the formation of two liquid phases from a single liquid phase.

[00122] This is known as liquid-liquid demixing. During liquid-liquid demixing, the high polymer concentration phase begins to solidify and form a matrix. Membrane structure can be tailored by controlling liquid-liquid demixing. Phase inversion covers several specific techniques such as vapor phase precipitation, solvent evaporation, thermal precipitation, and immersion precipitation. Immersion precipitation is the most common technique used to produce phase inversion membranes (see, e.g. Mulder, M., Basic Principles of Membrane Technology. 2nd Edition ed.; Kluwer Academic Publishers: Dordrecht, The 25 Netherlands, 2003).

[00123] Factors that influence phase inversion membrane morphology include: (1) the choice of solvent/nonsolvent system; (2) the composition of the polymer solution, which includes the polymer selected, its concentration and molecular weight distribution plus addition of other polymers or nonsolvent; (3) the composition of the coagulation bath, which is generally limited to adding solvent up to the binodal; and (4) film casting conditions such as polymer solution and coagulation bath temperature, film thickness, immersion in a non-solvent with low mutual affinity to the solvent or use of an evaporation step before immersing into the nonsolvent. The latter two techniques of item (4) are generally used to produce integrally skinned membranes for gas separation, vapor permeation, or pervaporation. Immersion precipitation membranes are typically formed by casting a polymer solution as a thin film on a support or by extruding a hollow fiber through a spinneret with an appropriate bore liquid. The polymer solution, or dope, is composed of polymer, solvent, and may contain some additives. The cast thin film and support or extruded hollow fiber are immersed in a coagulation bath. A coagulation bath consists of the nonsolvent and may contain additives. Solvent diffuses out of the polymer/solvent phase and into the coagulation bath while nonsolvent diffuses into the polymer/solvent phase. This continues until the polymer/solvent/nonsolvent system becomes thermodynamically unstable and demixing, or polymer precipitation, occurs and a solid polymeric membrane is formed. The time to the demixing step determines the ultimate membrane structure. Delayed demixing results in membranes with a dense, nonporous top layer. These membranes are typically used in gas separation and pervaporation applications. Instantaneous demixing results in membranes with

relatively porous top layers useful as microfiltration or ultrafiltration membranes, or as support membranes used in creation of composite osmotic membranes via interfacial polymerization of a dense film.

[00124] The choice of solvent/nonsolvent system in porous membrane synthesis can be significant. The polymer is typically soluble or easily dispersible in the chosen solvent. There are usually several solvents that are compatible with a given polymer. However, the solvent can also be paired with a nonsolvent in which it is miscible. Listed below are several solvents, which are compatible with polysulfone and are miscible with water.

Solvents compatible with polysulfone/water system

Polymer /nonsolvent solvent	Solvent
polysulfone/water	dimethylformamide (DMF)
	dimethylacetamide (DMAc)
	dimethylsulfoxide (DMSO)
	formylpiperidine (FP)
	morpholine (MP)
	N-methylpyrrolidone (NMP)

H. PORE-STRUCTURE, HYDROPHILICITY, AND PARTICLE FILTRATION CHARACTERISTICS OF POLYANILINE–POLYSULFONE ULTRAFILTRATION MEMBRANES

[00125] A highly processable form of polyaniline was synthesized and used to form pure polyaniline and polyaniline–polysulfone ultrafiltration membranes by nonsolvent induced phase inversion. Blends containing up to 75% polyaniline were 10–20% more permeable than pure polysulfone membranes, while pure polyaniline membranes were 10 times more permeable and extremely hydrophilic. A novel scanning electron microscope imaging technique was combined with characterization data and the Hagen–Poiseuille pore-flow model to elucidate that increasing polyaniline content increased the apparent membrane pore size and hydrophilicity, while decreasing skin layer thickness and porosity. Pure polyaniline membranes exhibited relatively larger, shorter pores that combined with the increased hydrophilicity to produce the observed separation performance enhancements. Herein, we present physical and chemical characteristics of pure polysulfone (PSf), pure

PANi and PANi–PSf blend membranes, which indicate this highly processable form of polyaniline can open up new opportunities for engineering advanced membrane materials.

I. EXPERIMENTAL

[00126] The following examples are put forth so as to provide those of ordinary skill in the art with a complete disclosure and description of how the compounds, compositions, articles, devices and/or methods claimed herein are made and evaluated, and are intended to be purely exemplary of the invention and are not intended to limit the scope of what the inventors regard as their invention. Efforts have been made to ensure accuracy with respect to numbers (*e.g.*, amounts, temperature, etc.), but some errors and deviations should be accounted for. Unless indicated otherwise, parts are parts by weight, temperature is in °C or is at ambient temperature, and pressure is at or near atmospheric.

1. EXAMPLE 1

a. MATERIALS

[00127] Ammonium peroxydisulfate (APS) (Prod. No. A682, ACS grade, 98.0%), acetone (Prod. No. 268310010, HPLC grade, 99.8%), and sodium hydroxide (Prod. No. S612) were purchased from Fisher. Aniline (Prod. No. 10400, ACS grade, 99.5%), sulfuric acid (Prod. No. 320501, ACS grade, 95.0–98.0%), methanol (Prod. No. 179957, laboratory grade, 99.6%), potassium bromide (Prod. No. 221864, FT-IR grade, 99%), polysulfone beads (Prod. No. 182443, Mnz22 kDa), bovine serum albumin (BSA) (Prod. No. A9647, 96%), and 1-methyl-2-pyrrolidinone (NMP) (Prod. No. 442778, ACS grade, 99.0%) were purchased from Aldrich. Silica nanoparticles (SNOWTEX-20L) were purchased from Nissan Chemical Corp. All materials were used as received.

b. MEMBRANE FORMATION AND CHARACTERIZATION

[00128] Polymer solutions were prepared with PANi:PSf weight ratios of 1:0 (pure polyaniline), 3:1, 1:1, 1:3, and 0:1 (pure polysulfone). The total polymer concentration was 18 wt% in all cases. Films were cast on a commercial nonwoven polyester support layer and immersed in 18 MΩ laboratory deionized water at room temperature to induce precipitation. Polysulfone was chosen as the base membrane and blend polymer because it is a well studied ultrafiltration membrane material. Permeability and rejection tests were conducted in a dead-

end flow cell (HP4750 Stirred Cell, Sterlitech Corp.) using 4 cm diameter membrane samples taken from membranes cast on different days and prepared from different casting solutions.

[00129] Pure water permeability was determined for each membrane by measuring volumetric water flux at pressures ranging from 5–20 psi. The water flux (J_v) is proportional to the applied pressure drop (Δp) via a permeability coefficient (L_p) according to:

$$J_v = L_p \Delta p = \frac{\varepsilon d_p^2}{32 \mu l} \Delta p \quad (9)$$

where ε is the membrane porosity, d_p is the membrane pore diameter, μ is the liquid dynamic viscosity, and l is the effective membrane thickness. For integrally skinned asymmetric membranes, ε is skin layer porosity, l is skin layer thickness (i.e., apparent pore length including tortuosity), and Δp is the pressure drop across the skin layer.

[00130] Silica nanoparticles and BSA were used to evaluate the membrane separation performance. The nanoparticle concentration was measured using a turbidimeter (Z100AN, Hach Company). A UV-vis spectrophotometer (Lambda 20, Perkin Elmer) was used to determine the BSA concentration. Solute particle rejection (r) was calculated from:

$$r = 1 - \frac{c_p}{c_f} \quad (10)$$

where c_p and c_f are solute particle concentrations in the permeate and feed streams, respectively. Dynamic light scattering (Zeta-PALS, Brookhaven) confirmed that BSA and silica nanoparticles had diameters of 6 nm and 48 nm, respectively. Hence, membrane pore size was approximated from solute particle rejection by using the following relationship:

$$r = 1 - 2(1 - \lambda)^2 + (1 - \lambda)^4 \quad (11)$$

where $\lambda = d_s/d_p$; d_s and d_p are solute particle diameter and membrane pore diameter, respectively. Membrane samples were prepared for SEM (Nova 600 NanoLab DualBeam"-SEM/FIB, FEI Company) analysis by soaking in pH 1 H_2SO_4 solutions for 1 h and drying

overnight in a desiccator. Membranes containing polyaniline were made electrically conductive by this doping step, so surface coating (by gold, palladium, platinum, etc.) prior to imaging was unnecessary. Pure polysulfone membranes were sputter-coated with gold to prevent charging. Membrane cross-sections were prepared by freeze fracturing using liquid nitrogen. Membrane surface milling was achieved by a focused ion beam (FIB) operated using a gallium source at a current of 10 nA, accelerating voltage of 30 kV, and a magnification of 5000X.

[00131] Membrane pore size and surface porosity were determined by image analyses of scanning electron micrographs using NIH ImageJ software. High magnification grey-scale surface images were converted to black and white images (Figure 16) following a previously described procedure. Surface porosity was calculated by dividing the sum of the black pixels (A_{black}) by the total pixels in an image. Average pore diameter ($d_{p,avg}$) was calculated by the following equation:

$$d_{\mathrm{p,avg}} = \sqrt{\frac{4A_{\mathrm{black}}}{n\pi}} \qquad (12)$$

where n is the number of continuous dark areas (pores) counted by the software. Maximum pore diameter ($d_{p,max}$) was estimated similarly, but using the largest individual black spot observed. Membrane surface roughness was measured using atomic force microscopy (AFM) (Synergy ESPM 3-D, Novascan). Air dried membranes were scanned in tapping mode in 500 nm X 500 nm sections. Water contact angles were measured using a goniometer (DSA10, Kruss). The captive bubble technique was employed here rather than the sessile drop technique due to the porous and hydrophilic nature of pure polyaniline films. Ten drops were measured for each membrane with the highest and lowest values being discarded. Surface roughness-corrected solid–liquid free energy ($-\Delta G_{13}$)—a better measure of the intrinsic hydrophilicity of a material than raw contact angle values—was calculated as previously described using a water surface tension value of 72.8 $mJ.m^{-2}$. Fourier transform infrared (FTIR) (FT/IR-420, JASCO) spectra were measured for each polymer composite. Films were cast without a polyester support layer and dried. Dry films and KBr were then ground into fine powders using a mortar and pestle and pressed into pellets for FTIR analysis.

2. RESULTS

[00132] Scanning electron microscopy reveals that the polyaniline synthesized as described above produced an agglomerated polymer structure. Polymer dispersions with agglomerated polyaniline weight fractions as high as 18% in NMP have been created. Membranes of varying polyaniline and polysulfone content were formed using the immersion precipitation technique. Images of each membrane are shown in Figure 17. Water permeability and nanoparticle and protein rejection were measured for polyaniline–polysulfone composite membranes. Pure polyaniline membranes are an order of magnitude more permeable than pure polysulfone and composite membranes, i.e., there is a sharp decrease in permeability when polysulfone is introduced.

[00133] Membranes have comparable rejection for 48 nm silica particles. Membranes containing large fractions of polyaniline showed little or no BSA rejection, while the pure polysulfone membrane showed greater than 45% BSA rejection. Error bars in membrane performance data reflect batch-to-batch variability.

[00134] Fourier transform infrared analyses were performed for each polymer composite. Spectra are shown in Figure 18. Sulfones and secondary aromatic amines both have strong absorption bands at 1350–1300 cm^{-1}. Sulfones also have an absorption band at 1160–1120 cm^{-1}. This peak (highlighted in Figure 18) diminishes as the polysulfone content decreases in each composite membrane.

[00135] Atomic force microscopy was used to measure surface roughness for each composite membrane. Roughness data are presented in Table 2. Average roughness (Ra) and root mean squared (RMS) roughness values are similar for all composite membranes. The surface area difference (SAD), which is the difference in actual membrane surface area and planar area, is lowest for the pure polysulfone membrane. The surface area difference increases with increasing polyaniline content until a maximum SAD is reached for the 1:1 PANi:PSf composite membrane, beyond which SAD decreases with increasing polyaniline content.

Table 2 Physical-chemical properties of PANi-PSf membranes

PANi : PSf ratio	R_{avg}/nm	R_{max}/nm	SAD (%)	θ_w/°	$-\Delta G_{13}$/mJ m^{-2}
1 : 0	4.1 ± 5.6	47.2	16.4	24.2 ± 2.1	129.8
3 : 1	3.0 ± 3.8	30.7	37.8	25.3 ± 2.1	120.6
1 : 1	3.7 ± 4.6	35.9	85.3	32.0 ± 3.3	106.1
1 : 3	2.1 ± 2.8	27.4	24.9	43.0 ± 4.7	115.5
0 : 1	4.1 ± 5.4	40.6	6.6	64.7 ± 3.8	102.0

[00136] Captive bubble contact angles were measured using deionized water on all composite membranes. Contact angle values and surface energies for each membrane composition are given in Table 2. As expected, the pure polysulfone membrane is the most hydrophobic, and membrane hydrophilicity generally increases with increasing polyaniline content. When surface roughness is considered, the free energy of cohesion for the 1:1 PANi:PSf membrane approaches that of the hydrophobic pure polysulfone membrane. Scanning electron micrographs (SEM) were taken for each composite membrane (Figure 14). Images show varied membrane morphology based on polymer composition. Cross-sectional SEM images of the composite membranes reveal that surface skin layers are thinnest for the pure polymer membranes (1:0 and 0:1), thickest for the equal polymer blend membrane (1:1), and of intermediate thickness for the other blend membranes (3:1 and 1:3). Pure polyaniline (PANi) and polysulfone (PSf) membranes have a more open structure with many large, fingerlike macrovoids. The 3:1 and 1:3 PANi:PSf composite membranes have fewer finger-like macrovoids. The 1:1 PANi:PSf membrane has a sponge-like substructure with few macrovoids. Scanning electron micrographs were taken while simultaneously exposing composite membrane surfaces to a focused ion beam (FIB). The FIB removes surface material by bombarding the surface with gallium ions. Time step images in Figure 19 show varied membrane surface resistance to the FIB due to some combination of membrane chemical composition and skin layer thickness.

[00137] Membrane pore size was calculated using silica nanoparticle and BSA rejection data and eqn (12). Approximate pore diameters for each membrane are shown in Table 3.

Table 3 Membrane pore-structure analyses

PANi : PSf ratio	L_p/μm s^{-1} MPa^{-1}	r_{SiO_2} (%)	r_{BSA} (%)	d_p (r_{SiO_2})/nm	d_p (r_{BSA})/nm
1 : 0	10 492	92	0.2	60	>6
3 : 1	3118	97	1.4	54	>6
1 : 1	1710	>99	28	<48	19
1 : 3	1735	>99	36	<48	16
0 : 1	1109	>99	47	<48	14

Table 3 (Continued)

PANi : PSf ratio	$d_{p,avg}$ (SEM)/nm	$d_{p,max}$ (SEM)/nm	ε (SEM) (%)	l (SEM)/nm
1 : 0	11	42	2.1	7.8
3 : 1	7	20	4.6	22.7
1 : 1	5	25	1.7	7.1
1 : 3	6	23	1.8	10.6
0 : 1	5	23	4.8	30.5

[00138] Partial silica nanoparticle rejection (r_{SiO2}) by the pure polyaniline membrane translates into an average pore diameter of 60 nm, classifying this membrane as a "loose" ultrafiltration membrane. Complete nanoparticle rejection, however, gives an incomplete picture of membrane pore diameter; pore diameter is less than the particle diameter. Partial BSA rejection indicates that the pure polysulfone membrane is a much tighter ultrafiltration membrane with an average pore diameter of 14 nm.

[00139] Membrane average pore diameter, maximum pore diameter, and surface porosity were approximated by analyzing surface SEM images of composite membranes (Table 3). Average membrane pore diameters ranging from 5–11 nm were found for composite polyaniline–polysulfone membranes. Pore diameter was found to decrease with increasing polysulfone content. Maximum observed pore diameters were typically 3–5 times greater than average pore diameters for each membrane, which may have affected solute rejection and permeability. Surface porosity ranged from 2–5%, and did not follow a

noticeable trend with relative polymer content. Effective pore length was calculated using eqn (1) and was found to generally increase with increasing polysulfone content.

3. Discussion

a. Polyaniline processability

[00140] Concentrated solutions are needed if polyaniline is to be used in fiber spinning and conventional film casting techniques. Yang added secondary amines to NMP to disperse high molecular weight polyaniline in NMP up to concentrations of 15 wt%, which is about the minimum concentration required to form an ultrafiltration membrane by nonsolvent induced phase inversion. We report a synthesis of polyaniline that produces a material that is stable in NMP solution up to 18 wt% without the use of any co-solvent additives. Although we have not experimentally determined the molecular weight of our as synthesized polyaniline, the similarity in synthetic conditions between our synthesis and those reported by Adams et al. and those reported by Tran et al. leads us to anticipate the molecular weight to be around Mn of 10 (8–12) kDa and Mw of 25 (20–40) kDa. The room temperature synthesis of polyaniline using APS has been shown to produce nanofibers of controlled diameters when the acid and conditions for nucleation are controlled. Li et al. have shown that nanofibers are formed early during the chemical polymerization of aniline and that minor modifications of these conditions have a drastic impact on the morphology and dispersability of the resultant material.37 Adams et al. have shown that controlling the rate of oxidant addition and the reaction temperature has a profound influence on the structural regularity and molecular weight of the resultant polymer. They used ^{13}C NMR to reveal irregularities, termed "defects," in the molecular structure of polyaniline synthesized at room temperature by a rapid addition of the oxidant solution. Their finding, that performing the synthesis at reduced temperature with a dropwise addition of the oxidant solution leads to a more regular structure, has led the polyaniline community to accept the low temperature synthesis method as the standard method for producing "high-quality" polyaniline. However, for applications where conductivity is not a figure of merit other synthetic methods should be considered.

[00141] Here, we have created a high defect density polyaniline that is resistant to gel formation in NMP solution by rapid addition of the oxidant at room temperature followed by intentional disruption of the nucleation process by stirring for 1 hour. This is significant, as previous reports and our own experience with polyaniline have shown that polyaniline

solutions in NMP gel at concentrations as low as 5–10 wt%. Yang and Mattes attribute gel formation in polyaniline to strong hydrogen bonding interactions between the amine and imine nitrogens on neighboring polymer chains as polymer chains are more closely in contact with one another in concentrated solutions. We hypothesize that our high defect density polyaniline chains are unable to pack as closely to one another, preventing the interchain hydrogen bonding interactions from reaching a critical stage where the fluidity of the system is lost and the gel formation process is irreversible. One can imagine drawing a parallel between a "high defect density" polyaniline and a cis-fatty acid in biochemistry. As opposed to a linear polyaniline (which can be thought of as a straight-chain hydrocarbon), the increased kinks and bends in the chain prohibit strong inter-chain interactions and lead to improved processability.

b. MEMBRANE MORPHOLOGY AND STRUCTURE

[00142] According to the Hagen–Poiseuille pore-flow model of porous membranes (eqn (9)), water permeability is proportional to the square of the pore diameter. Pore diameters calculated from silica and BSA rejection over-predict the difference in water permeability between the pure polyaniline and polysulfone membranes [$L_{p,1:0}/L_{p,0:1} = 9.5$; $(d_{p,1:0}/d_{p,0:1})^2 = 19$]. Also, the pure polyaniline membrane structure factor (ε/l^1) is half that of the pure polysulfone membrane, which indicates the PANi membrane is less porous and has longer pores. However, using solute particle rejection data to describe membrane pore size has a few limitations. Fouling of the membrane due to solute–membrane interactions may cause higher solute rejection, which can result in the calculation of a smaller pore diameter; however, this may not be the case for very hydrophilic membranes that resist fouling. Solutes such as BSA may deform when under stress and can squeeze through pores smaller than their hydrodynamic radii, which can result in the calculation of a larger pore diameter. Membrane porosity and pore length cannot be independently determined from such an analysis. Several other factors may also play a role in membrane performance and morphology. Membrane hydrophilicity is known to affect membrane performance. An increase in polyaniline content leads to an increase in membrane hydrophilicity and may be partially responsible for the increased water permeability. These effects cannot be quantified from the physical membrane permeability model.

[00143] Average membrane pore diameters determined from analysis of SEM surface images were smaller than those determined from solute particle rejection. However, maximum observed membrane pore diameters were similar in value to those calculated from solute particle rejection. A few larger pores may have had a large influence on solute particle retention by the membranes. An advantage of SEM image analysis is the ability to quantify membrane surface porosity. Pure polysulfone average membrane pore diameter is less than half that of the pure polyaniline membrane, but the surface porosity is more than twice that of the pure polyaniline membrane. Pure polyaniline membrane permeability is 9.5 times greater than pure polysulfone membrane permeability. Differences in pore diameter, porosity, and effective pore area (εd_p^2) do not explain the difference in membrane permeability between pure polyaniline and pure polysulfone membranes [$L_{p,1:0}/L_{p,0:1} = 9.5$; $(d_{pore,1:0}/d_{pore,0:1})^2 = 5.5$; $\varepsilon_{1:0}/\varepsilon_{0:1} \times (d_{pore,1:0}/d_{pore,0:1})^2 = 2.4$]. Using the effective pore length (l) as a fitting parameter for membrane permeabilities produces the values of l given in Table 3. The pure PANi membrane had an effective pore length that was nearly 4 times shorter than that of the pure PSf membrane; thus, providing a more mechanistic, membrane structure-based explanation for the performance. It remains possible that the fitted pore-length is underestimated due to the extremely hydrophilic nature of PANi membranes.

[00144] Surface SEM images (Figure 14) show dark regions in the pure polyaniline membrane, which appear to be macrovoids under a thin, semi-transparent skin layer. These features are easily visible as dark regions in the pure polyaniline membrane surface image and are visible, but less pronounced, in pure polysulfone and 3:1 PANi:PSf membranes. Macrovoids are not visible in the surface SEM images of 1:1 and 1:3 PANi:PSf composite membranes. The macrovoids visible in the pure polyaniline membranes appear in clusters and display some spatial ordering.

[00145] Full SEM cross-sections reveal that each membrane has fingerlike macrovoids. The 1:1 composite membrane is an exception as it appears to have a mixture of sponge-like and finger-like morphology.

[00146] Membrane skin layer thickness was analyzed from the time sequence of FIB-SEM images. The pure polyaniline membrane had the shortest erosion time (thinnest skin layer) of the composite membranes. The majority of the skin layer was removed after only 5 min. The pure polysulfone and 3:1 PANi:PSf membrane showed marked erosion near the 10

min mark indicating that their skin layers are thinner than those of the 1:1 and 1:3 PANi:PSf membranes. These results mirror the results of the skin layer SEM images. The FIB-SEM images allow for positive identification of macrovoids under the thin, transparent skin layers of the pure polyaniline, pure polysulfone, and 3:1 PANi:PSf membranes. The darker regions visible at t = 0 in these membranes become macrovoids after several minutes under the FIB. The 1:1 PANi:PSf membrane shows slight pitting after 10 min, which may be the exposed sponge-like sublayer. The 1:3 PANi:PSf membrane shows very slight pitting only after 15 min of FIB irradiation. An obvious limitation to this analysis lies in the assumption that each polymer has similar physical/thermal resistance to the FIB, whereby skin layer thickness is proportional to erosion time.

4. EXAMPLE 2

[00147] Various thin-film composite membranes were formed by forming a thin polyamide film on top of PSf and PANi-blended membranes and tested in FO-mode under the same conditions (Figure 20). Blend 1 comprises of 1:3 PANi:PSf, while Blend 2 comprises of a 1:1 PANi:PSf blend. The data shows that as the amount of PANi increases in the support membrane, the water permeability and salt passage increases, as compared to the relatively more hydrophobic PSf membrane. However, the data shows that using PANi-blended support membranes do not reach the permeability and selectively of the commercial FO CTA membrane.

[00148] From contact angle measurements, membranes with PANi were shown to be more hydrophilic than pure PSf membranes; previously, it was shown that hydrophilic support membranes produce relatively low permeability polyamide composite RO membranes. Table 4 shows absorption data of MPD and water by different blends of membranes, which shows that PANi-containing membranes take up slightly lower but similar amounts of MPD and ~100X more water, as compared to a pure PSf membrane. This data indicates after the membrane is immersed in the aqueous MPD solution as part of the thin-film formation process, the concentration of MPD in the membrane is more diluted for a PANi membrane than for a PSf membrane. Thus, a change in the polyamide thin-film formation chemistry and/or polymerization conditions is required to achieve high permeability and selectivity.

TABLE 4. Absorption Data showing the amount of MPD and Water taken up by PANi-PSf Blended Membranes

Increasing Amount of PSf ↓	Unsupported Membrane	Mass MPD / Mass of Membrane (g MPD/g Membrane)	Mass Water / Mass of Membrane (g Water/g Membrane)
	Pure PANi	0.088 ± 0.076	1.86 ± 0.16
	Blend 1	0.057 ± 0.016	2.02 ± 0.17
	Blend 2	0.090 ± 0.066	1.80 ± 0.10
	Pure PSf	0.109 ± 0.025	0.01 ± 0.00

[00149] Such properties can be improved by changing the organic solvent that the trimesoyl chloride is dissolved in the subsequent thin-film formation step. By switching from an isoparaffin hydrocarbon solvent (Isopar-G, Exxon Mobil Chemical, Houston, TX) to hexane, the resulting thin-film composite membrane outperformed the CTA membrane in terms of water permeability and selectivity when tested under the same conditions (PRO-mode, 32 g/L NaCl draw solution, deionized water feed solution, and constant temperature 20°C) (Figure 21). The difference in performance could be attributed to several factors, including the difference in MPD solubility and diffusivity and the boiling points of the two organic solvents. The lower solubility of MPD in hexane allowed for less MPD to partition from the support into the reaction zone (presumably on the hexane side of the aqueous hexane interface) during interfacial polymerization. The higher diffusivity of MPD in hexane gives rise to faster film formation, generally producing a thinner (more permeable) coating film with a high cross-linking density. The lower boiling point of hexane compared to isopar enabled a lower curing temperature, which prevented the pores of the PANi-blended support membrane from contracting by annealing such as may happen when curing at higher temperature which is required for membranes formed using high boiling point solvents like isopar.

J. References

[00150] The following publications listed below are incorporated herein by reference to disclose and describe the methods and/or materials in connection with which the

publications are cited. The publications discussed herein are provided solely for their disclosure prior to the filing date of the present application. Nothing herein is to be construed as an admission that the present invention is not entitled to antedate such publication by virtue of prior invention. Further, the dates of publication provided herein may be different from the actual publication dates, which can require independent confirmation.

[00151] A. C. Haddix, Emerging Infect. Dis., 2003, 9, 426–431.

[00152] A. G. Macdiarmid, J. C. Chiang, A. F. Richter and A. J. Epstein, Synth. Met., 1987, 18, 285–290.

[00153] A. K. Ghosh, B. H. Jeong, X. F. Huang and E. M. V. Hoek, J. Membr. Sci., 2008, 311, 34–45.

[00154] A. Achilli.; T. Y. Cath.; E. A. Marchand.; A. E. Childress., The forward osmosis membrane bioreactor: A low fouling alternative to mbr processes. Desalination 2009, 239, (1-3), 10-21.

[00155] B. Yao, G. C. Wang, J. K. Ye and X. W. Li, Mater. Lett., 2008, 62, 1775–1778.

[00156] J. E Cadotte.; R. J. Petersen; R. E. Larson.; E. E. Erickson, New thin-film composite seawater reverse-osmosis membrane. Desalination 1980, 32, (1-3), 25-31.

[00157] T. Y. Cath; A. E. Childress; M. Elimelech, Forward osmosis: Principles, applications, and recent developments. J. Membr. Sci. 2006, 281, (1-2), 70-87.

[00158] D. C. Trivedi and S. K. Dhawan, Synth. Met., 1993, 59, 267–272.

[00159] D. Li, J. X. Huang and R. B. Kaner, Acc. Chem. Res., 2009, 42, 135–145.

[00160] D. M. Mohilner, W. J. Argersinger and R. N. Adams, J. Am. Chem. Soc., 1962, 84, 3618–3622.

[00161] D. Yang and B. R. Mattes, Synth. Met., 1999, 101, 746–749.

[00162] D. Yang, PhD Thesis, University of California, Los Angeles, 1999.

[00163] E. M. Genies, A. Boyle, M. Lapkowski and C. Tsintavis, Synth. Met., 1990, 36, 139–182.

[00164] V. Freger, Nanoscale heterogeneity of polyamide membranes formed by interfacial polymerization. Langmuir 2003, 19, (11), 4791-4797.

[00165] V. Freger; J. Gilron; S. Belfer, Tfc polyamide membranes modified by grafting of hydrophilic polymers: An ft-ir/afm/tem study. Journal of Membrane Science 2002, 209, (1), 283-292.

[00166] G.R. Guillen; T.P. Farrell; R.B. Kaner; E.M.V. Hoek, Pore-structure, hydrophilicity, and particle filtration characteristics of polyaniline-polysulfone ultrafiltration membranes. J. Mater. Chem. 2010, 20, 4621-4628.

[00167] H. D. Tran, I. Norris, J. M. D'Arcy, H. Tsang, Y. Wang, B. R. Mattes and R. B. Kaner, Macromolecules, 2008, 41, 7405–7410.

[00168] H. Letheby, J. Chem. Soc., 1862, 15, 161–163.

[00169] H. Hachisuka; K. Ikeda, Reverse osmosis composite membrane and reverse osmosis treatment method for water using the same. U.S. Patent 6,413,425, Issued July 2, 2002.

[00170] J. Herron, Asymmetric forward osmosis membranes USPTO, Editor. 2005, Hydration technologies Inc. (Albany, OR).

[00171] M. Hirose; H. Ito; Y. Kamiyama, Effect of skin layer surface structures on the flux behaviour of RO membranes. J. Membrane Sci. 1996, 121, (2), 209-215.

[00172] R. W. Holloway; A. E. Childress; K. E. Dennett; T. Y. Cath, Forward osmosis for concentration of anaerobic digester centrate. Water Res. 2007, 41, (17), 4005-4014.

[00173] I. J. Ball, S. C. Huang, K. J. Miller, R. A. Wolf, J. Y. Shimano and R. B. Kaner, Synth. Met., 1999, 102, 1311–1312.

[00174] I. J. Ball, S. C. Huang, R. A. Wolf, J. Y. Shimano and R. B. Kaner, J. Membr. Sci., 2000, 174, 161–176.

[00175] I. J. Ball, S. C. Huang, T. M. Su and R. B. Kaner, Synth. Met., 1997, 84, 799–800.

[00176] J. Alam, U. Riaz and S. Ahmad, Polym. Adv. Technol., 2008, 19, 882–888.

[00177] J. C. Crittenden, R. R. Trussel, D. W. Hand, K. J. Howe and G. Tchobanoglous, Water Treatment: Principles and Design, John Wiley & Sons, Inc., Hoboken, New Jersey, 2nd edn, 2005.

[00178] J. Desilvestro, W. Scheifele and O. Haas, J. Electrochem. Soc., 1992, 139, 2727–2736.

[00179] J. Joo and A. J. Epstein, Appl. Phys. Lett., 1994, 65, 2278–2280.

[00180] J. X. Huang and R. B. Kaner, J. Am. Chem. Soc., 2004, 126, 851–855.

[00181] J. X. Huang, S. Virji, B. H. Weiller and R. B. Kaner, J. Am. Chem. Soc., 2003, 125, 314–315.

[00182] C. K. Kim; J. H. Kim; I. J. Roh; J. J. Kim, The changes of membrane performance with polyamide molecular structure in the reverse osmosis process. Journal of Membrane Science 2000, 165, (2), 189-199.

[00183] I. C. Kim; K. H Lee, Preparation of interfacially synthesized and silicone-coated composite polyamide nanofiltration membranes with high performance. Industrial & Engineering Chemistry Research 2002, 41, (22), 5523-5528.

[00184] M. Kurihara; Y. Fusaoka; T. Sasaki; R. Bairinji; T. Uemura, Development of cross-linked fully aromatic polyamide ultra-thin composite membranes for seawater desalination. Desalination 1994, 96, (1-3), 133-143.

[00185] S. Y. Kwak, Relationship of relaxation property to reverse osmosis permeability in aromatic polyamide thin-film-composite membranes. Polymer 1999, 40, (23), 6361-6368.

[00186] S. Y. Kwak; D. W. Ihm, Use of atomic force microscopy and solid-state nmr spectroscopy to characterize structure-property-performance correlation in high-flux reverse osmosis (ro) membranes. J. Membrane Sci. 1999, 158, (1-2), 143-153.

[00187] S. Y. Kwak; S. G Jung.; S. H. Kim, Structure-motion-performance relationship of flux-enhanced reverse osmosis (RO) membranes composed of aromatic polyamide thin films. Environmental Science & Technology 2001, 35, (21), 4334-4340.

[00188] S. Y. Kwak; S. G Jung.; Y. Yoon; D. W. Ihm, Details of surface features in aromatic polyamide reverse osmosis membranes characterized by scanning electron and atomic force microscopy. Journal of Polymer Science Part B-Polymer Physics 1999, 37, (13), 1429-1440.

[00189] S. Y. Kwak.; S. H. Kim.; S. S. Kim., Hybrid organic/inorganic reverse osmosis (RO) membrane for bactericidal anti-fouling. 1. Preparation and characterization of tio2 nanoparticle self-assembled aromatic polyamide thin- film-composite (TFC) membrane. Environmental Science & Technology 2001, 35, (11), 2388-2394.

[00190] S. Loeb, Large-scale power production by pressure-retarded osmosis, using river water and sea water passing through spiral modules (vol 143, pg 115, 2002). Desalination 2002, 150, (2), 205-205.

[00191] M. Cheryan, Ultrafiltration and Microfiltration Handbook, Technomic Publishing Company, Inc., Lancaster, PA, 1998.

[00192] M. Mulder, Basic Principles of Membrane Technology, Kluwer Academic Publishers, Dordrecht, The Netherlands, 2nd edn, 2003.

[00193] M. R. Anderson, B. R. Mattes, H. Reiss and R. B. Kaner, Science, 1991, 252, 1412–1415.

[00194] M. Sairam, X. X. Loh, K. Li, A. Bismarck, J. H. G. Steinke and A. G. Livingston, J. Membr. Sci., 2009, 330, 166–174.

[00195] C. R. Martinetti; A. E. Childress; T. Y. Cath, High recovery of concentrated ro brines using forward osmosis and membrane distillation. J. Membr. Sci. 2009, 331, (1-2), 31-39.

[00196] J. R. McCutcheon; M. Elimelech, Influence of concentrative and dilutive internal concentration polarization on flux behavior in forward osmosis. J. Membr. Sci. 2006, 284, (1-2), 237-247.

[00197] J. R. McCutcheon; M. Elimelech, Influence of membrane support layer hydrophobicity on water flux in osmotically driven membrane processes. J. Membr. Sci. 2008, 318, (1-2), 458-466.

[00198] J. R. McCutcheon; M. Elimelech, Modeling water flux in forward osmosis: Implications for improved membrane design. Aiche J. 2007, 53, (7), 1736-1744.

[00199] J. R. McCutcheon; R. L. McGinnis; M. Elimelech, A novel ammonia-carbon dioxide forward (direct) osmosis desalination process. Desalination, 2005. 174(1): p.1-11.

[00200] J. R. McCutcheon; R. L. McGinnis, and M. Elimelech, Desalination by ammonia-carbon dioxide forward osmosis: Influence of draw and feed solution concentrations on process performance. Journal of Membrane Science, 2006, 278: p. 114-123.

[00201] R. L. McGinnis, and M. Elimelech, Global challenges in energy and water supply: The promise of engineered osmosis. Environ. Sci. Technol. 2008, 42, (23), 8625-8629.

[00202] G. D. Mehta; S. Loeb, Internal polarization in the porous substructure of a semipermeable membrane under pressure-retarded osmosis. J. Membr. Sci. 1978, 4, (2), 261-265.

[00203] W. E. Mickols, Composite membrane and method for making the same. May 13, 2003.

[00204] NRC, Identifying future drinking water contaminants, in Water Science and Technology Board, National Research Council, National Academy Press, Washington, DC, 1999.

[00205] P. Chapman, X. X. Loh, A. G. Livingston, K. Li and T. A. C. Oliveira, J. Membr. Sci., 2008, 309, 102–111.

[00206] P. N. Adams, P. J. Laughlin, A. P. Monkman and A. M. Kenwright, Polymer, 1996, 37, 3411–3417.

[00207] P. S. Corso, M. H. Kramer, K. A. Blair, D. G. Addiss, J. P. Davis and

[00208] R. J. Petersen, Composite reverse-osmosis and nanofiltration membranes. Journal of Membrane Science 1993, 83, (1), 81-150.

[00209] R. L. Droste, Theory and Practice of Water and Wastewater Treatment, John Wiley & Sons, Inc., New York, NY, 1997, pp.416–451.

[00210] R. M. Silverstein, G. C. Bassler and T. C. Merrill, Infrared spectroscopy, in Spectrometric Identification of Organic Compounds, John Wiley & Sons, Inc., New York, 1991, ch. 3, pp. 91–164.

[00211] A. P. Rao; S. V. Joshi; J. J. Trivedi; C. V. Devmurari; V. J. Shah, Structure-performance correlation of polyamide thin film composite membranes: Effect of coating conditions on film formation. Journal of Membrane Science 2003, 211, (1), 13-24.

[00212] I. J. Roh; S. Y. Park; J. J. Kim; C. K. Kim, Effects of the polyamide molecular structure on the performance of reverse osmosis membranes. Journal of Polymer Science Part B-Polymer Physics 1998, 36, (11), 1821-1830.

[00213] S. C. Huang, I. J. Ball and R. B. Kaner, Macromolecules, 1998, 31, 5456–5464.

[00214] S. T. Kang, A. Subramani, E. M. V. Hoek, M. A. Deshusses and M. R. Matsumoto, J. Membr. Sci., 2004, 244, 151–165.

[00215] S. E. Skilhagen; J. E. Dugstad; R. J. Aaberg, Osmotic power - power production based on the osmotic pressure difference between waters with varying salt gradients. Desalination 2008, 220, (1-3), 476-482.

[00216] T. M. Su, I. J. Ball, J. A. Conklin, S. C. Huang, R. K. Larson, S. L. Nguyen, B. M. Lew and R. B. Kaner, Synth. Met., 1997, 84, 801–802.

[00217] W. J. Feast, J. Tsibouklis, K. L. Pouwer, L. Groenendaal and E. W. Meijer, Polymer, 1996, 37, 5017–5047.

[00218] W. K. Lu, R. L. Elsenbaumer and B. Wessling, Synth. Met., 1995, 71, 2163–2166.

[00219] World Health Organization, 2004, http://www.who.int/water_sanitation_health/publications/facts2004/en/index.html, accessed 26 October 2009.

[00220] Z. F. Fan, Z. Wang, M. R. Duan, J. X. Wang and S. C. Wang, J. Membr. Sci., 2008, 310, 402–408.

[00221] Z. F. Fan, Z. Wang, N. Sun, J. X. Wang and S. C. Wang, J. Membr. Sci., 2008, 320, 363–371.

[00222] T.Y. Cath; A.E. Childress; M. Elimelech, Forward osmosis: Principles, applications, and recent developments. J. Membr. Sci. 2006, 281, (1-2), 70-87.

[00223] J.R. Mccutcheon; R.L. Mcginnis; M. Elimelech, A novel ammonia-carbon dioxide forward (direct) osmosis desalination process. Desalination 2005, 174, (1), 1-11.

[00224] J.R. Mccutcheon; R.L. Mcginnis; M. Elimelech, Desalination by ammonia-carbon dioxide forward osmosis: Influence of draw and feed solution concentrations on process performance. J. Membr. Sci. 2006, 278, (1-2), 114-123.

[00225] R.L. Mcginnis; M. Elimelech, Energy requirements of ammonia-carbon dioxide forward osmosis desalination. Desalination 2007, 207, (1-3), 370-382.

[00226] K.L. Lee; R.W. Baker; H.K. Lonsdale, Membranes for power-generation by pressure-retarded osmosis. J. Membr. Sci. 1981, 8, (2), 141-171.

[00227] S. Loeb, Energy production at the dead sea by pressure-retarded osmosis: Challenge or chimera? Desalination 1998, 120, (3), 247-262.

[00228] S. Loeb, One hundred and thirty benign and renewable megawatts from great salt lake? The possibilities of hydroelectric power by pressure-retarded osmosis. Desalination 2001, 141, (1), 85-91.

[00229] S. Loeb, Large-scale power production by pressure-retarded osmosis, using river water and sea water passing through spiral modules. Desalination 2002, 143, (2), 115-122.

[00230] A. Achilli; T.Y. Cath; E.A. Marchand; A.E. Childress, The forward osmosis membrane bioreactor: A low fouling alternative to mbr processes. Desalination 2009, 239, (1-3), 10-21.

[00231] J.L. Cartinella; T.Y. Cath; M.T. Flynn; G.C. Miller; K.W. Hunter; A.E. Childress, Removal of natural steroid hormones from wastewater using membrane contactor processes. Environ. Sci. Technol. 2006, 40, (23), 7381-7386.

[00232] T.Y. Cath; D. Adams; A.E. Childress, Membrane contactor processes for wastewater reclamation in space ii. Combined direct osmosis, osmotic distillation, and membrane distillation for treatment of metabolic wastewater. J. Membr. Sci. 2005, 257, (1-2), 111-119.

[00233] T.Y. Cath; S. Gormly; E.G. Beaudry; M.T. Flynn; V.D. Adams; A.E. Childress, Membrane contactor processes for wastewater reclamation in space part i. Direct osmotic concentration as pretreatment for reverse osmosis. J. Membr. Sci. 2005, 257, (1-2), 85-98.

[00234] R.W. Holloway; A.E. Childress; K.E. Dennett; T.Y. Cath, Forward osmosis for concentration of anaerobic digester centrate. Water Res. 2007, 41, (17), 4005-4014.

[00235] J.R. Mccutcheon; M. Elimelech, Influence of concentrative and dilutive internal concentration polarization on flux behavior in forward osmosis. J. Membr. Sci. 2006, 284, (1-2), 237-247.

[00236] J.R. Mccutcheon; M. Elimelech, Modeling water flux in forward osmosis: Implications for improved membrane design. Aiche J. 2007, 53, (7), 1736-1744.

[00237] J.R. Mccutcheon; M. Elimelech, Influence of membrane support layer hydrophobicity on water flux in osmotically driven membrane processes. J. Membr. Sci. 2008, 318, (1-2), 458-466.

[00238] G.D. Mehta; S. Loeb, Internal polarization in the porous substructure of a semipermeable membrane under pressure-retarded osmosis. J. Membr. Sci. 1978, 4, (2), 261-265.

[00239] E.M.V. Hoek; M. Elimelech, Cake-enhanced concentration polarization: A new fouling mechanism for salt-rejecting membranes. Environ. Sci. Technol. 2003, 37, (24), 5581-5588.

[00240] E.M.V. Hoek; A.S. Kim; M. Elimelech, Influence of crossflow membrane filter geometry and shear rate on colloidal fouling in reverse osmosis and nanofiltration separations. Environ. Eng. Sci. 2002, 19, (6), 357-372.

[00241] A.K. Ghosh; B.H. Jeong; X.F. Huang; E.M.V. Hoek, Impacts of reaction and curing conditions on polyamide composite reverse osmosis membrane properties. J. Membr. Sci. 2008, 311, (1-2), 34-45.

[00242] B.H. Jeong; E.M.V. Hoek; Y.S. Yan; A. Subramani; X.F. Huang; G. Hurwitz; A.K. Ghosh; A. Jawor, Interfacial polymerization of thin film nanocomposites: A new concept for reverse osmosis membranes. J. Membr. Sci. 2007, 294, (1-2), 1-7.

[00243] M.L. Lind; A.K. Ghosh; G. Guillen; E.M.V. Hoek, Impacts of zeolite surface chemistry on zeolite-polyamide thin film nanocomposite membranes. Desalination 2010, submitted, March.

[00244] M.L. Lind; A.K. Ghosh; A. Jawor; X.F. Huang; W. Hou; Y. Yang; E.M.V. Hoek, Influence of zeolite crystal size on zeolite-polyamide thin film nanocomposite membranes. Langmuir 2009, 25, (17), 10139-10145.

[00245] M.L. Lind; B.H. Jeong; A. Subramani; X.F. Huang; E.M.V. Hoek, Effect of mobile cation on zeolite-polyamide thin film nanocomposite membranes. J. Mater. Res. 2009, 24, (5), 1624-1631.

[00246] M.L. Lind; D. Suk; E.M.V. Hoek, Tailoring the Structure of Thin Film Nanocomposite Membranes to Achieve Seawater RO Membrane Performance. Environ. Sci. Technol., 44, 2010, 8230-8235.

[00247] F. Peng; X. Huang; A. Jawor; E.M.V. Hoek, Transport, structural, and interfacial properties of poly(vinyl alcohol)-polysulfone composite nanofiltration membranes. J. Membr. Sci. 2010, 353, 169-176.

[00248] F. Peng; Z.-Y. Jiang; E.M.V. Hoek, Tuning the molecular structure, separation performance and interfacial properties of poly(vinyl alcohol)-polysulfone composite membranes. J. Membr. Sci., 2011, 368, 26-33.

[00249] H. Lonsdale; R. Riley; C. Lyons; D. Carosella Jr, Transport in composite reverse osmosis membranes. Membrane processes in industry and biomedicine: proceedings 1971, 101-122.

[00250] E.M.V. Hoek; G.R. Guillen; T.P. Farrell; R.B. Kaner Membrane compositions and methods for making and using them. December 11, 2009, 2009.

[00251] A.K. Ghosh; E.M.V. Hoek, Impacts of support membrane structure and chemistry on polyamide-polysulfone interfacial composite membranes. J. Membr. Sci. 2009, 336, (1-2), 140-148.

[00252] M.L. Lind; A.K. Ghosh; X. Huang; W. Hou; Y. Yang; E.M. Hoek, Influence of zeolite crystal size on zeolite-polyamide thin film nanocomposite membranes. Langmuir 2009, 25, 10139-10145.

[00253] M.L. Lind; B.H. Jeong; A. Subramani; E.M.V. Hoek, Effect of mobile cation on zeolite-polyamide thin film nanocomposite membranes. J. Mater. Res. 2009, 24, 1624-1631.

[00254] G. Guillen; E.M.V. Hoek, Modeling the impacts of feed spacer geometry on reverse osmosis and nanofiltration processes. Chem. Eng. J. 2009, 149, (1-3), 221-231.

[00255] S. Kim; E.M.V. Hoek, Modeling concentration polarization in reverse osmosis processes. Desalination 2005, 186, (1-3), 111-128.

[00256] A. Subramani; S. Kim; E.M.V. Hoek, Pressure, flow, and concentration profiles in open and spacer-filled membrane channels. J. Membr. Sci. 2006, 277, (1-2), 7-17.

[00257] It will be apparent to those skilled in the art that various modifications and variations can be made in the present invention without departing from the scope or spirit of the invention. Other aspects of the invention will be apparent to those skilled in the art from consideration of the specification and practice of the invention disclosed herein. It is

intended that the specification and examples be considered as exemplary only, with a true scope and spirit of the invention being indicated by the following claims.

CLAIMS

What is claimed is:

1. A semi-permeable forward osmosis (FO) membrane having a permeability of from about 0.01 gfd/psi to about 0.10 gfd/psi or about 0.07 x 10^{-11} m/Pa-s to about 0.7 x 10^{-11} m/Pa-s, a sodium chloride permeability less than 10^{-7} m/s and a draw solution stability of: at least about 60 hrs in pH $\geq$ 13, at least about 1 week in pH 11-13, at least about 3 months in pH 9-11, and at least about 1 year in pH 7-9.

2. The FO membrane of claim 1, wherein the membrane has a draw solution stability of at least about 3 months in pH $\geq$ 13.

3. The FO membrane of claim 1, wherein the membrane has a sodium chloride permeability of about 0.5-1.0x 10^{-8} m/s.

4. The membrane of claim 1, wherein the membrane is compatible with "ammonia - carbon dioxide" FO process conditions.

5. The membrane of claim 1, wherein the membrane is compatible with continuous exposure to an operating temperature range of from about 5 °C to about 60 °C.

6. The membrane of claim 1, wherein the membrane has a selectivity (R_s) of at least about 99.5% for NaCl, >99.9% for draw solute.

7. The membrane of claim 1, wherein the membrane comprises:

    a. a polymeric support layer, and

    b. a film polymerized on the support layer.

8. The membrane of claim 7, wherein the polymeric support layer comprises a blend of two or more polymers.

9. The membrane of claim 8, wherein the support layer comprises polysulfone.

10. The membrane of claim 8, wherein the support layer comprises polyaniline.

11. The membrane of claim 8, wherein the support layer comprises a blend of polysulfone and polyaniline.

12. The membrane of claim 11, wherein the support layer comprises at least about 50% polysulfone.

13. The membrane of claim 11, wherein the support layer comprises less than about 50% polyaniline.

14. The membrane of claim 11, wherein the support layer comprises from about 50:50 polyaniline/polysulfone to about 25:75 polyaniline/polysulfone.

15. The membrane of claim 11, wherein the support layer comprises from about 40:60 polyaniline/polysulfone to about 20:80 polyaniline/polysulfone.

16. The membrane of claim 11, wherein the support layer comprises about 1:3 polyaniline/polysulfone.

17. The membrane of claim 7, wherein the support layer has:

    a. skin-layer average pore size (r_p) of from about 10 nm to about 25 nm,

    b. skin-layer porosity (ε_m) of from about 20% to about 30%,

    c. skin-layer surface water contact angle of (θ_w) of less than about 40°,

    d. cross-sectional thickness (δ_m) of less than about 50 μm,

    e. cross-sectional porosity (ε_m) of greater than about 50%, and

    f. cross-sectional macrovoid alignment substantially vertical ($\tau_m \approx 1$).

18. The membrane of claim 7, wherein the film has:

    a. cross-sectional thickness of from about 50 nm to about 250 nm,

    b. permeability of from about 0.01 gfd/psi to about 0.10 gfd/psi, and

    c. surface water contact angle of (θ_w) of less than about 40°.

19. The membrane of claim 1, comprising:

a. a polymeric support layer having:

i. skin-layer average pore size (r_p) of from about 10 nm to about 25 nm,

ii. skin-layer porosity (ε_m) of from about 20% to about 30%,

iii. skin-layer surface water contact angle of (θ_w) of less than about 40°,

iv. cross-sectional thickness (δ_m) of less than about 50 μm,

v. cross-sectional porosity (ε_m) of greater than about 50%,

vi. cross-sectional macrovoid alignment substantially vertical ($\tau_m \approx 1$),

and

b. a film polymerized on the support layer, the film having:

i. cross-sectional thickness of from about 50 nm to about 250 nm,

ii. permeability of from about 0.01 gfd/psi to about 0.10 gfd/psi, and

iii. surface water contact angle of (θ_w) of less than about 70°.

20. The membrane of claim 1, comprising a polyaniline/polysulfone blend support layer having:

i. skin-layer average pore size (r_p) of from about 10 nm to about 25 nm,

ii. skin-layer porosity (ε_m) of from about 20% to about 30%,

iii. skin-layer surface water contact angle of (θ_w) of less than about 40°,

iv. cross-sectional thickness (δ_m) of less than about 50 μm,

v. cross-sectional porosity (ε_m) of greater than about 50%,

vi. cross-sectional macrovoid alignment substantially vertical ($\tau_m \approx 1$).

21. The membrane of claim 20, wherein the support layer comprises about 1:3 polyaniline/polysulfone.

22. The membrane of claim 1, wherein the film comprises at least one of a polyamide, a polyether, a polyether-urea, a polyester, or a polyimide or a copolymer thereof or a mixture thereof.

23. The membrane of claim 1, wherein the film comprises a polyamide.

24. The membrane of claim 23, wherein the polyamide comprises residues of a phthaloyl halide, a trimesoyl halide, or a mixture thereof.

25. The membrane of claim 23, wherein the polyamide comprises residues of diaminobenzene, triaminobenzene, or piperazine or a mixture thereof.

26. The membrane of claim 23, wherein the film comprises an aromatic polyamide.

27. The membrane of claim 1, wherein the film comprises residues of a trimesoyl halide and residues of a diaminobenzene.

28. The membrane of claim 1, wherein the film comprises an interfacially polymerized aromatic polyamide.

29. The membrane of claim 1, compatible with "ammonia - carbon dioxide" FO process conditions, and comprising:

    a. an about 1:3 polyaniline/polysulfone blend support layer having:

        i. skin-layer average pore size (r_p) of from about 10 nm to about 25 nm,

        ii. skin-layer porosity (ε_m) of from about 20% to about 30%,

        iii. skin-layer surface water contact angle of (θ_w) of less than about 40°,

        iv. cross-sectional thickness (δ_m) of less than about 50 μm,

        v. cross-sectional porosity (ε_m) of greater than about 50%, and

        vi. cross-sectional macrovoid alignment substantially vertical ($\tau_m \approx 1$)

and

b. a polyamide film interfacially polymerized on the support layer, the film having:

i. cross-sectional thickness of from about 50 nm to about 250 nm,

ii. permeability of from about 0.01 gfd/psi to about 0.10 gfd/psi, and

iii. surface water contact angle of (θ_w) of less than about 70°.

30. A method for preparing a semi-permeable osmosis membrane, the method comprising polymerizing a film onto a blended polymeric support layer.

31. The method of claim 30, wherein polymerizing is performed interfacially.

32. The method of claim 30, wherein the support layer comprises polysulfone.

33. The method of claim 30, wherein the support layer comprises polyaniline.

34. The method of claim 30, wherein the support layer comprises a blend of polysulfone and polyaniline.

35. The method of claim 30, wherein the film comprises at least one of a polyamide, a polyether, a polyether-urea, a polyester, or a polyimide or a copolymer thereof or a mixture thereof.

36. The method of claim 30, wherein the film comprises a polyamide.

37. The method of claim 30, wherein the support layer is provide by phase inversion of a polymer blend solution or suspension.

38. The product produced by the method of any of claims 30 to 37.

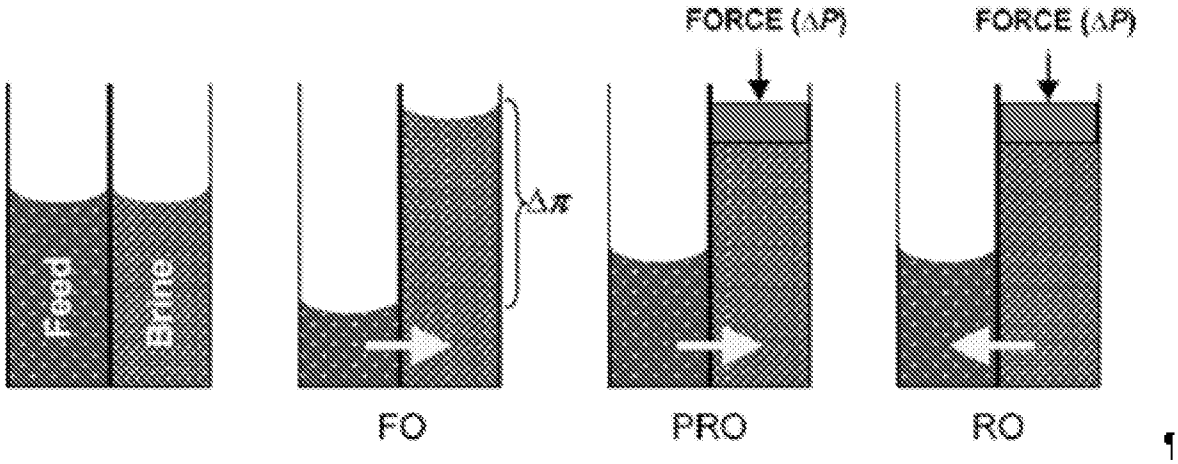
39. A method for osmotically-driven separation, the method comprising creating an osmotic pressure gradient across a semi-permeable forward osmosis membrane comprising a film polymerized on a blended support layer.

40. The method of claim 39, wherein the semi-permeable forward osmosis membrane exhibits a water permeability of about 1×, about 2×, or about 5× that of a commercial "CTA" membrane.

41. The method of claim 39, wherein the semi-permeable forward osmosis membrane exhibits a salt passage of about 1×, about 0.1×, or about 2× that of a commercial "CTA" membrane.

42. The method of claim 39, wherein purified water is produced.

43. The method of claim 39, wherein electricity is produced.



¶

Figure 1

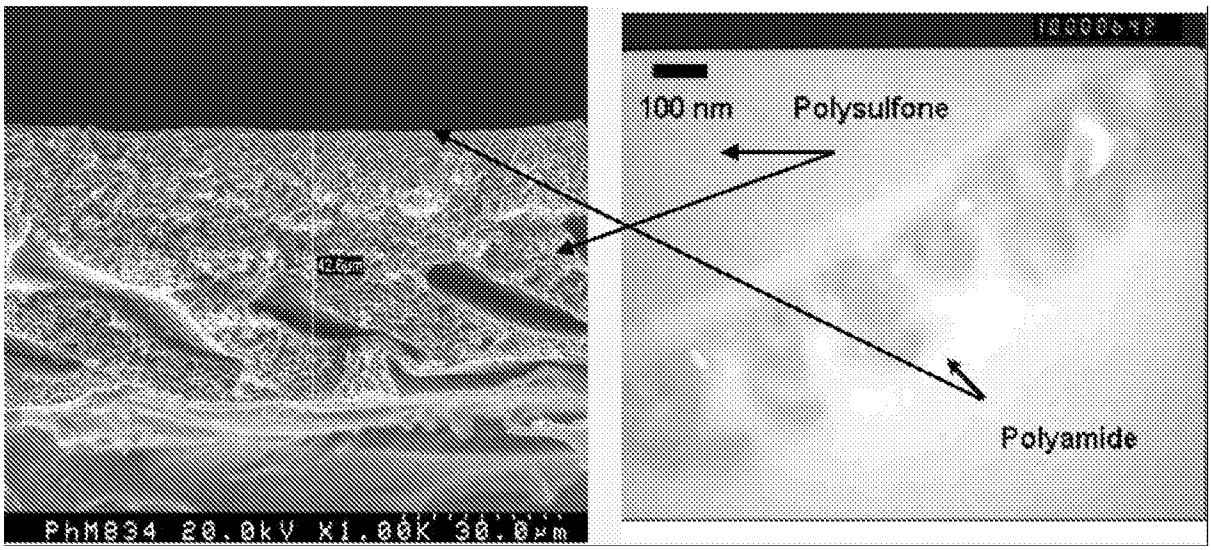


FIGURE 2

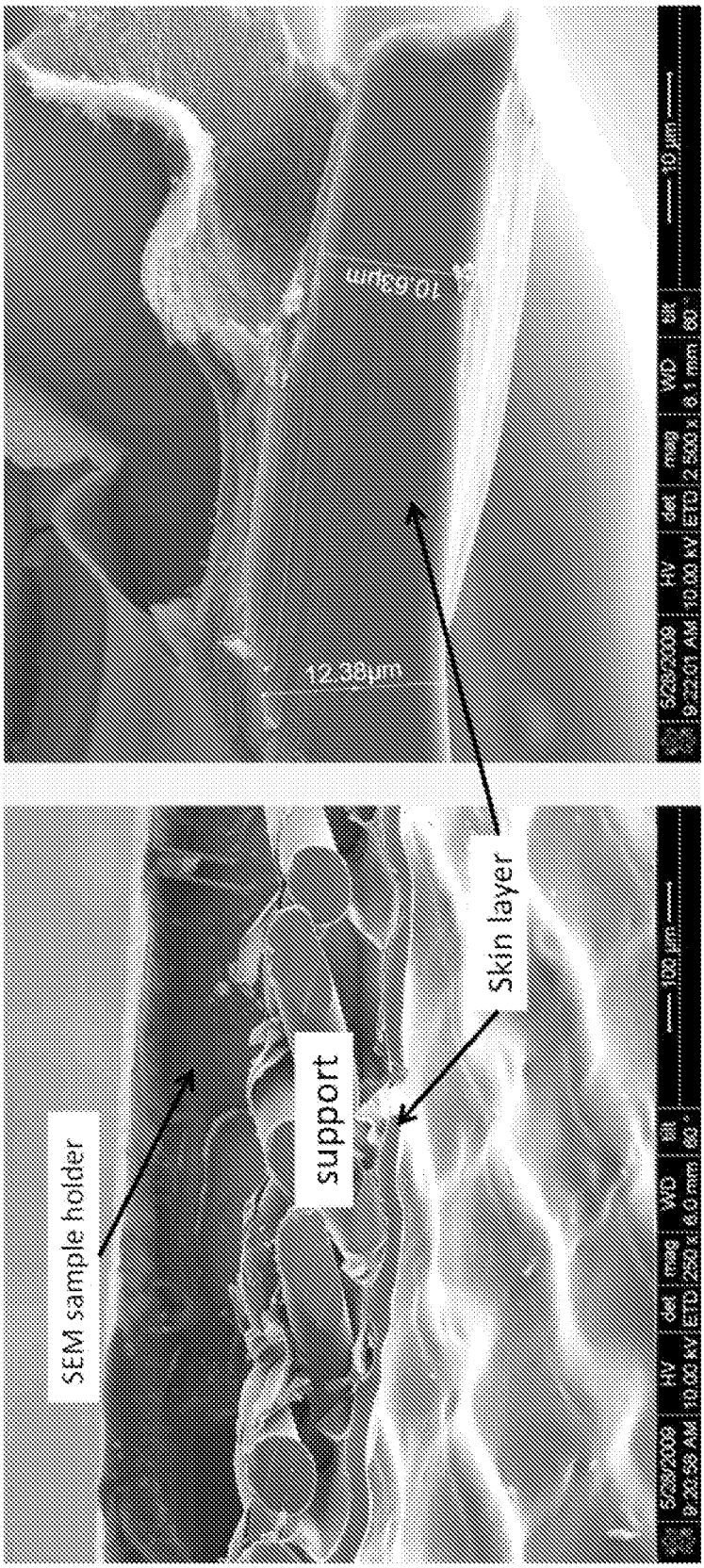


FIGURE 3

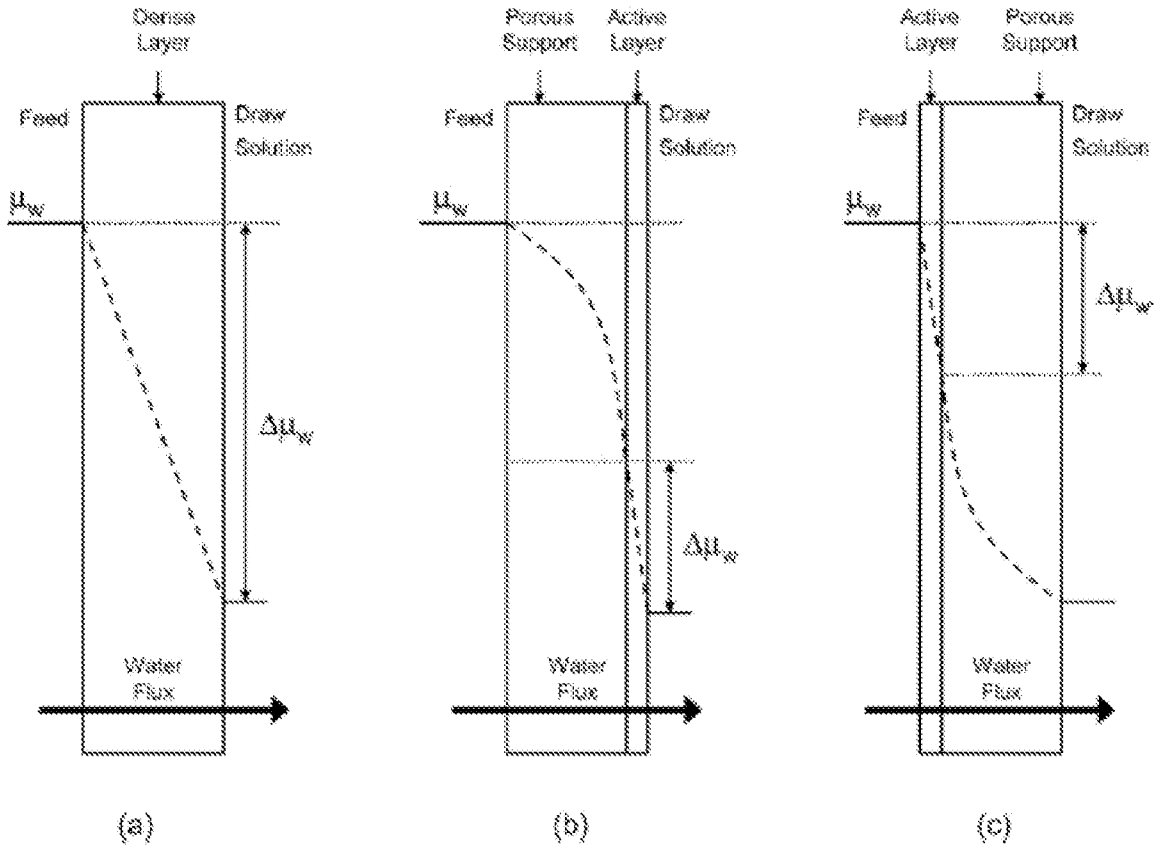

Dense Layer
Feed
Draw Solution
μ_w
$\Delta\mu_w$
Water Flux
(a)
Porous Support
Active Layer
Feed
Draw Solution
μ_w
$\Delta\mu_w$
Water Flux
(b)
Active Layer
Porous Support
Feed
Draw Solution
μ_w
$\Delta\mu_w$
Water Flux
(c)

FIGURE 4

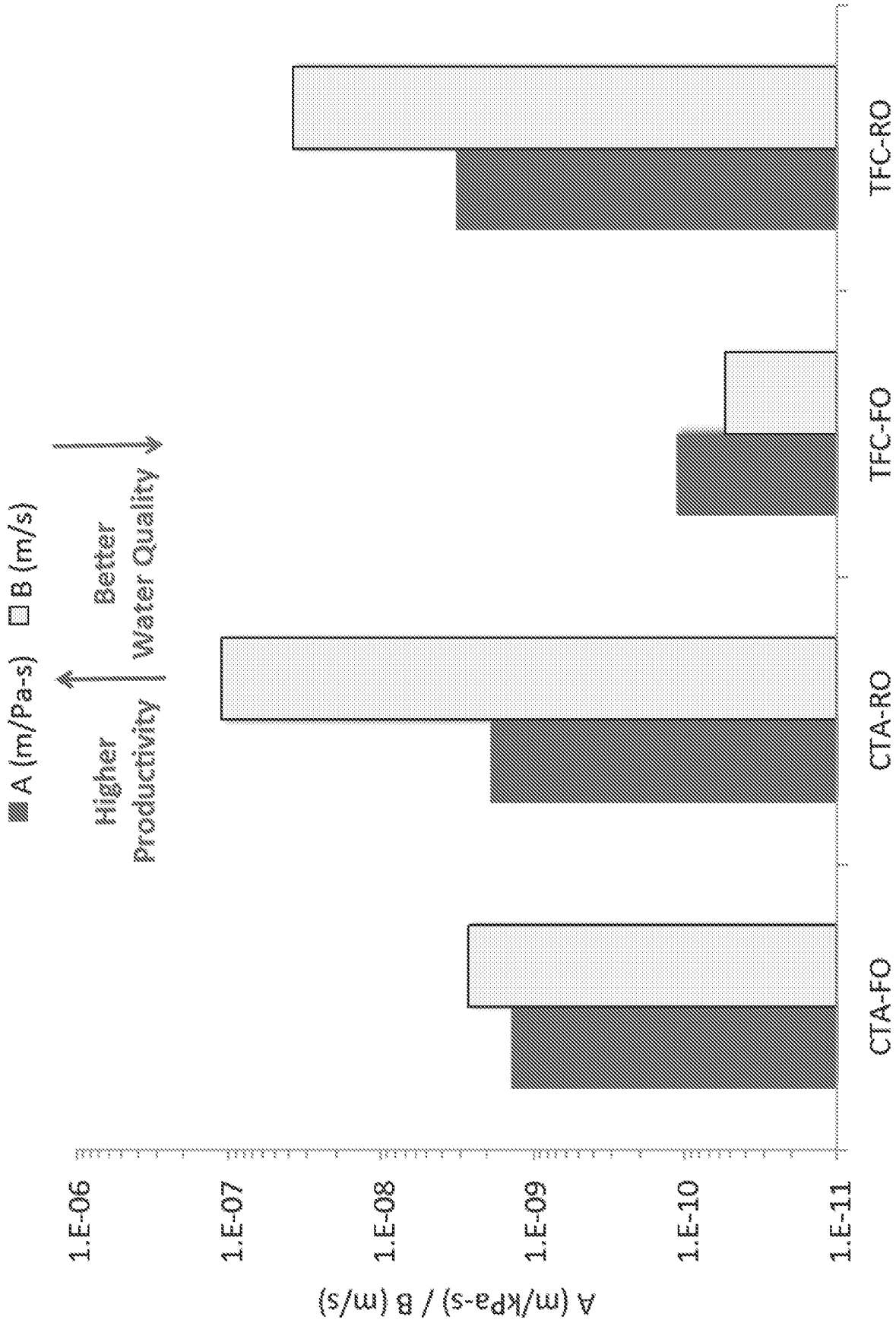

A (m/Pa-s)
B (m/s)
Higher Productivity
Better Water Quality
A (m/kPa-s) / B (m/s)
1.E-06
1.E-07
1.E-08
1.E-09
1.E-10
1.E-11
CTA-FO
CTA-RO
TFC-FO
TFC-RO

FIGURE 5

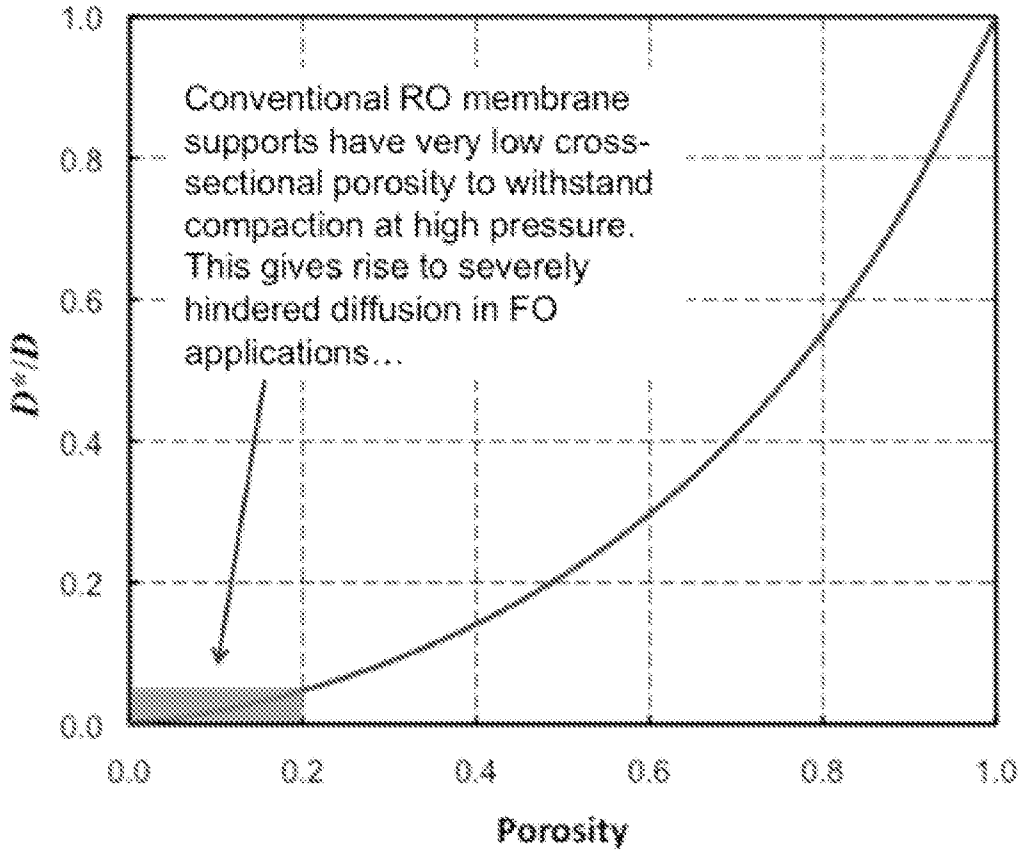

Conventional RO membrane supports have very low cross-sectional porosity to withstand compaction at high pressure. This gives rise to severely hindered diffusion in FO applications…
D*/D
Porosity
1.0
0.8
0.6
0.4
0.2
0.0
0.0
0.2
0.4
0.6
0.8
1.0

Figure 6

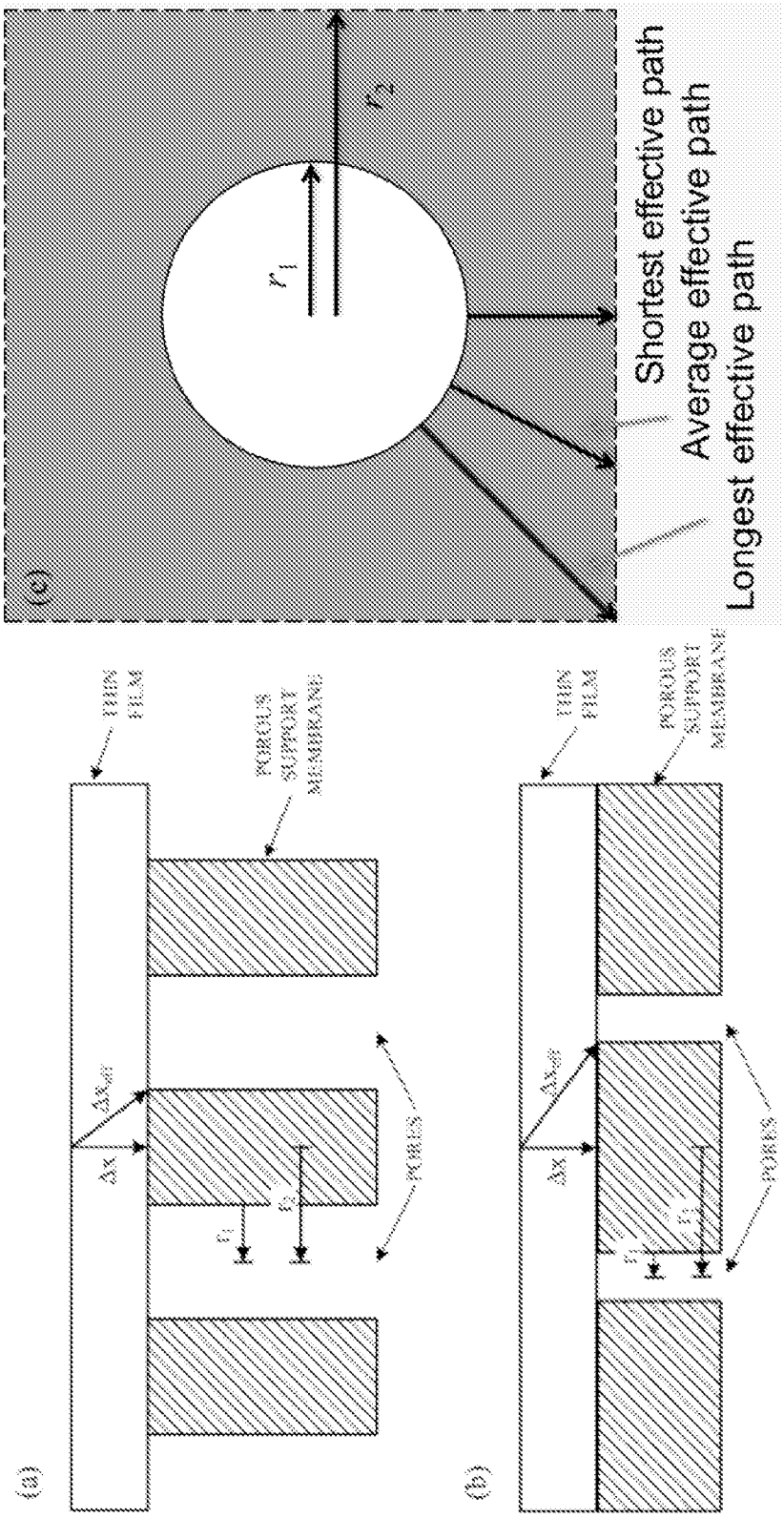

(c)
r_1
r_2
Shortest effective path
Average effective path
Longest effective path
(a)
THIN FILM
POROUS SUPPORT MEMBRANE
Δx_{eff}
Δx
r_1
r_2
PORES
(b)
THIN FILM
POROUS SUPPORT MEMBRANE
Δx_{eff}
Δx
r_1
r_2
PORES

FIGURE 7

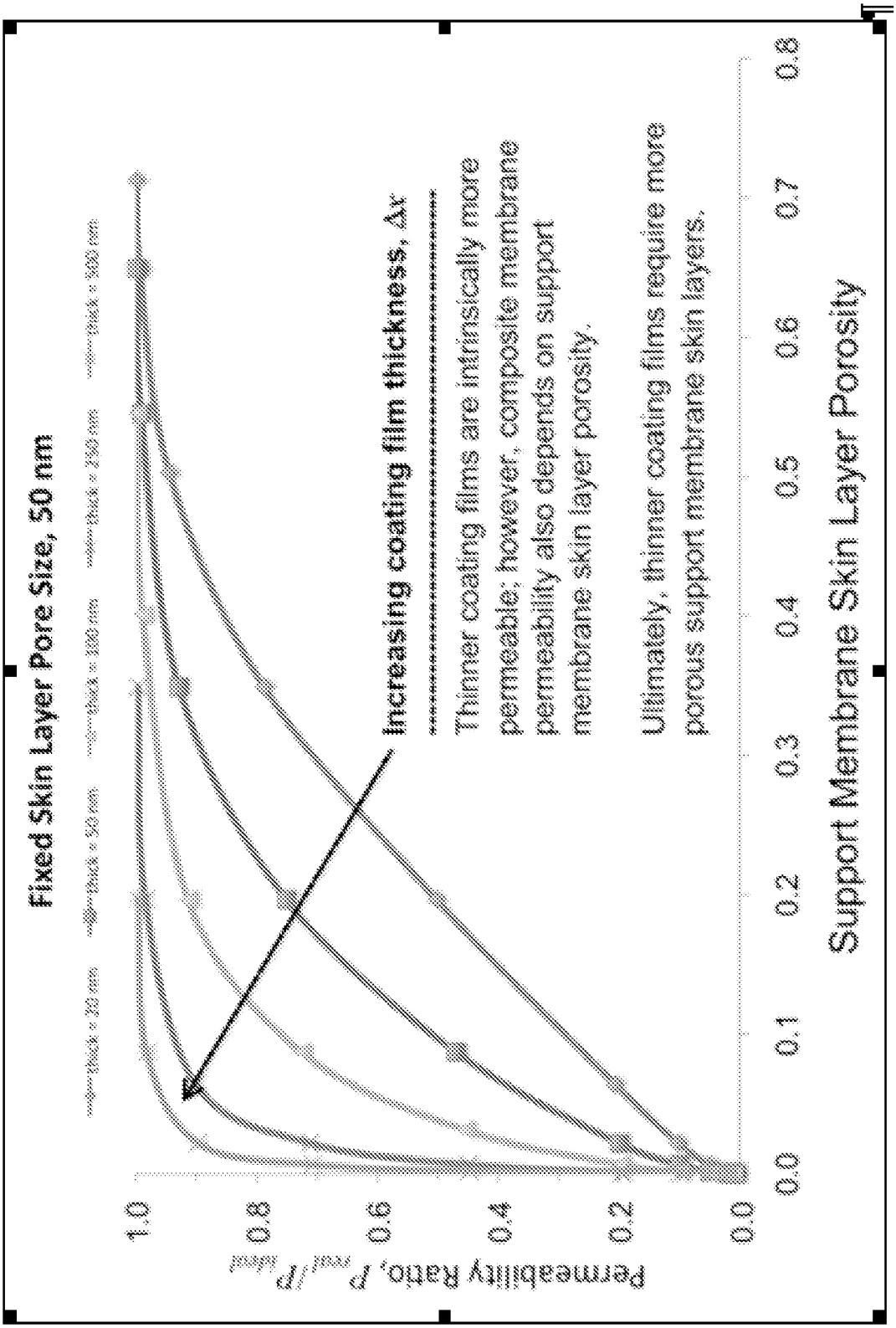

Fixed Skin Layer Pore Size, 50 nm
Increasing coating film thickness, Δx
Thinner coating films are intrinsically more permeable; however, composite membrane permeability also depends on support membrane skin layer porosity.
Ultimately, thinner coating films require more porous support membrane skin layers.
Permeability Ratio, P_{mul}/P_{skin}
Support Membrane Skin Layer Porosity
0.0
0.2
0.4
0.6
0.8
1.0
0.1
0.3
0.5
0.7

FIGURE 8

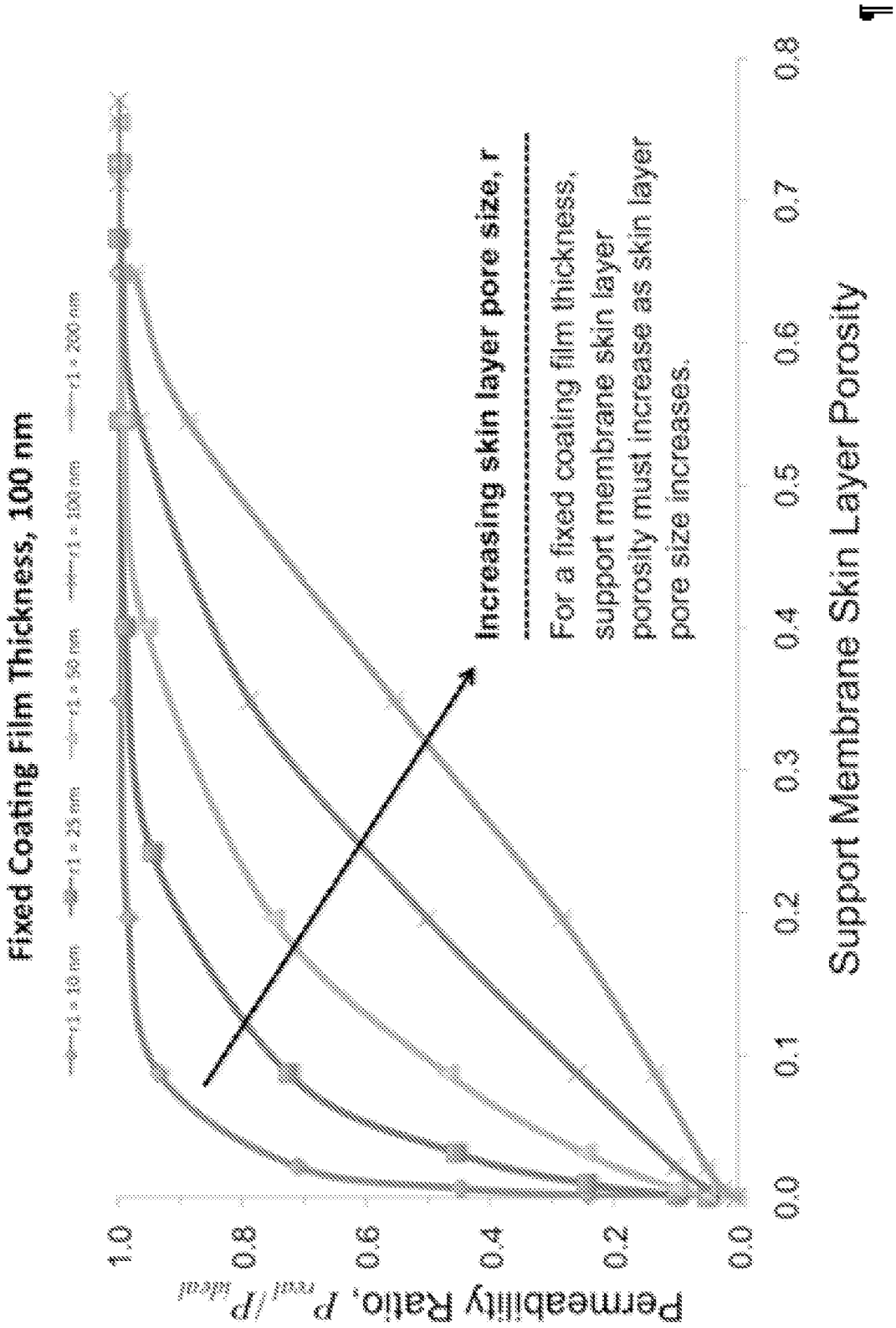

Fixed Coating Film Thickness, 100 nm
r = 10 nm
r = 25 nm
r = 50 nm
r = 100 nm
r = 200 nm
Increasing skin layer pore size, r
For a fixed coating film thickness, support membrane skin layer porosity must increase as skin layer pore size increases.
Permeability Ratio, P_{real}/P_{ideal}
Support Membrane Skin Layer Porosity
0.0
0.2
0.4
0.6
0.8
1.0
0.0
0.1
0.2
0.3
0.4
0.5
0.6
0.7
0.8

FIGURE 9

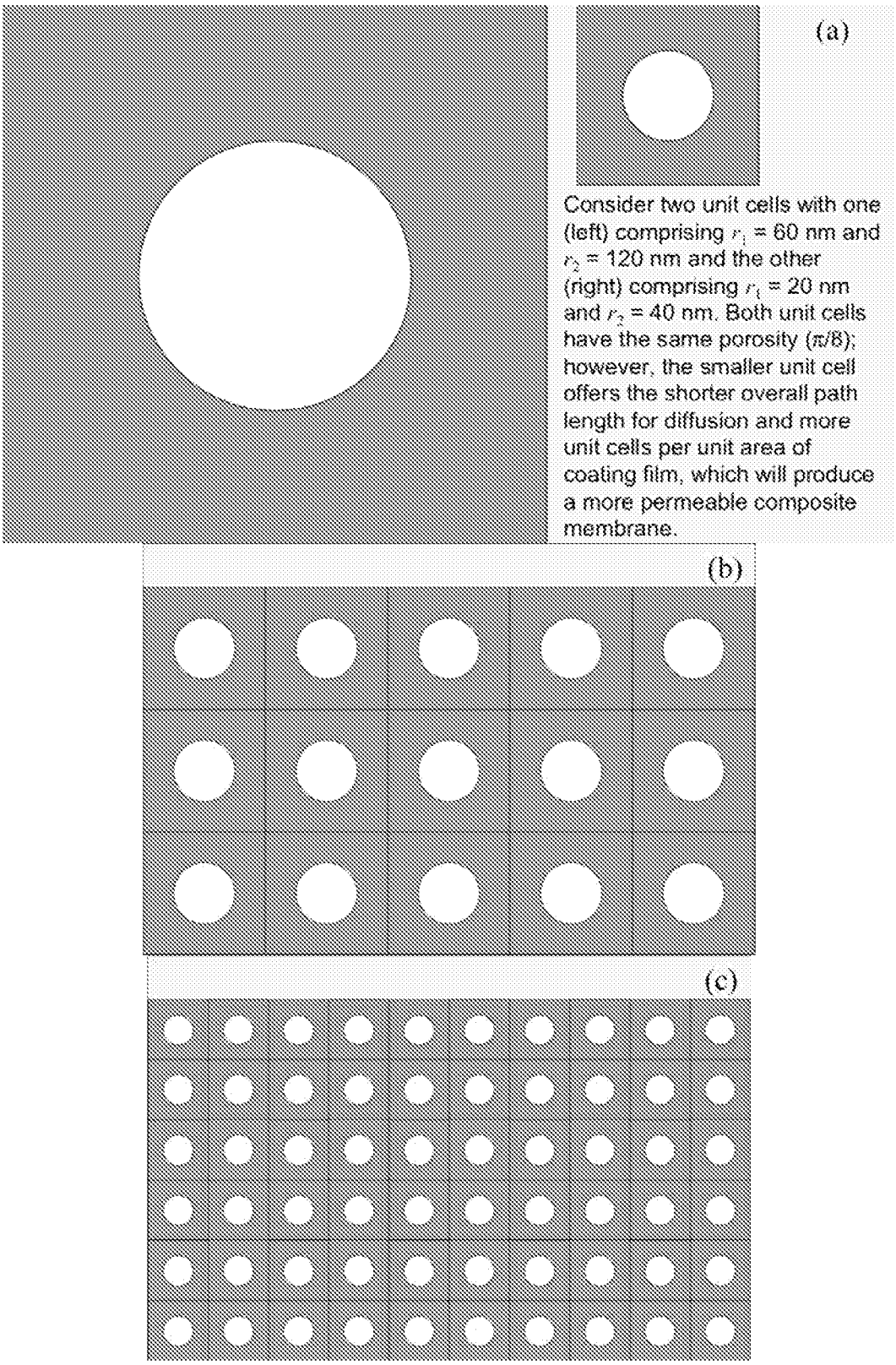

(a)
Consider two unit cells with one (left) comprising r_1 = 60 nm and r_2 = 120 nm and the other (right) comprising r_1 = 20 nm and r_2 = 40 nm. Both unit cells have the same porosity ($\pi/8$); however, the smaller unit cell offers the shorter overall path length for diffusion and more unit cells per unit area of coating film, which will produce a more permeable composite membrane.
(b)
(c)

FIGURE 10

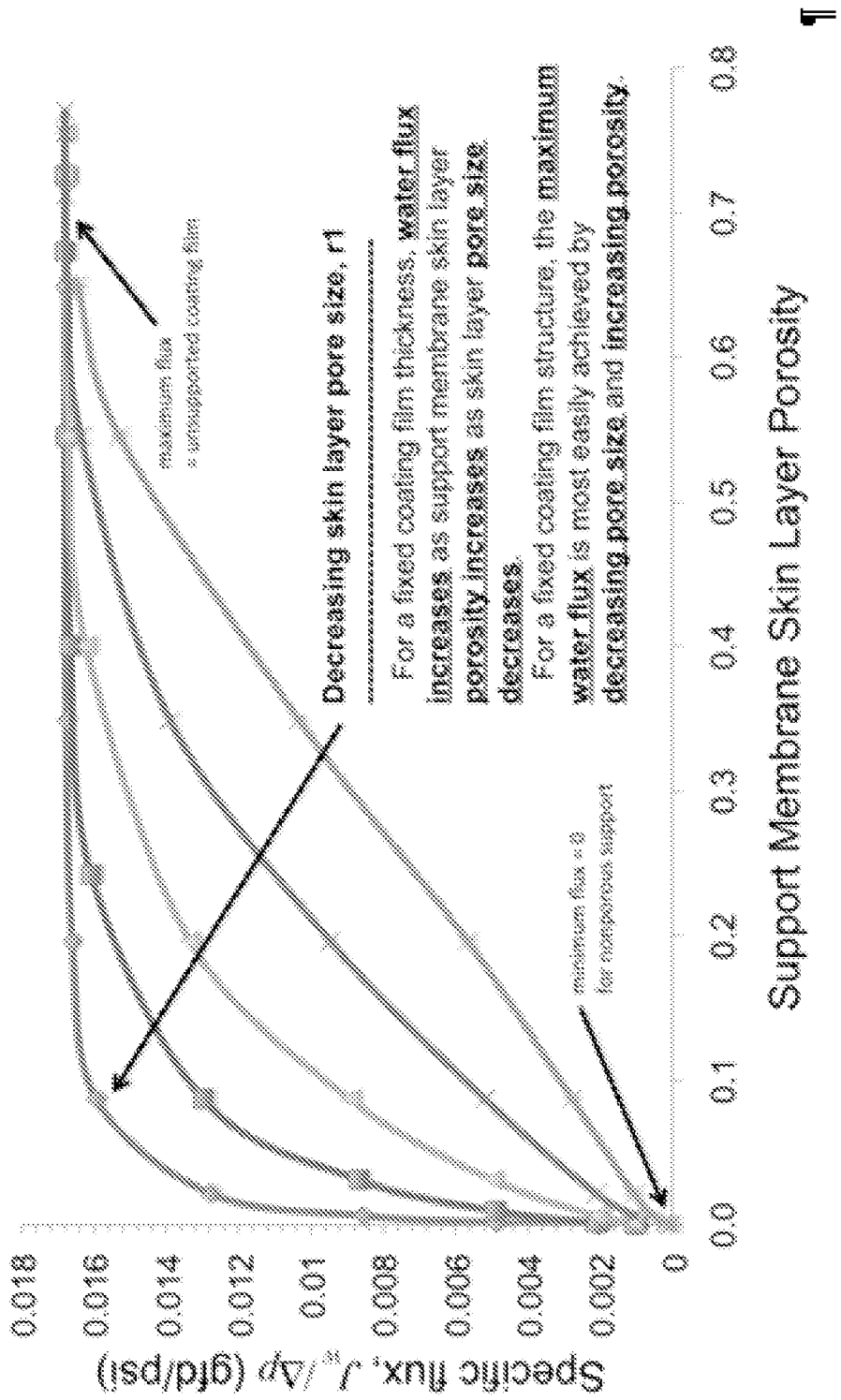

Fixed Coating Film Thickness, 100 nm
r1 = 10 nm
r1 = 25 nm
r1 = 50 nm
r1 = 100 nm
r1 = 200 nm
Specific flux, $J_w/\Delta p$ (gfd/psi)
0.018
0.016
0.014
0.012
0.01
0.008
0.006
0.004
0.002
0
0.0
0.1
0.2
0.3
0.4
0.5
0.6
0.7
0.8
Support Membrane Skin Layer Porosity
maximum flux
= unsupported coating film
resistance flux = 0
for nonporous support
Decreasing skin layer pore size, r1
For a fixed coating film thickness, water flux increases as support membrane skin layer porosity increases as skin layer pore size decreases.
For a fixed coating film structure, the maximum water flux is most easily achieved by decreasing pore size and increasing porosity.

FIGURE 11A

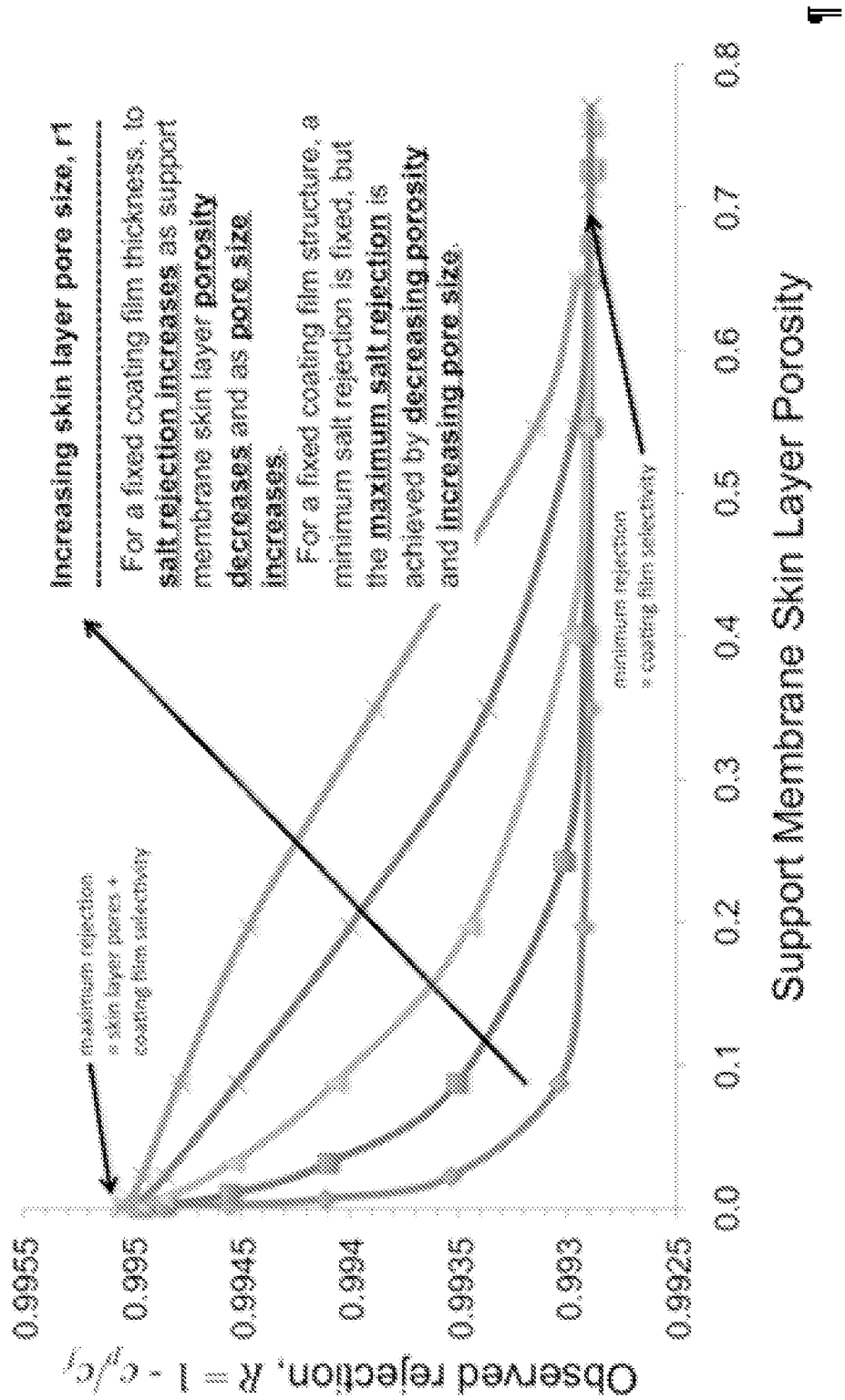

Fixed Coating Film Thickness, 100 nm
r1 = 10 nm
r1 = 25 nm
r1 = 50 nm
r1 = 100 nm
r1 = 200 nm
maximum rejection
= skin layer porosity *
coating film selectivity
Increasing skin layer pore size, r1
For a fixed coating film thickness, to salt rejection increases as support membrane skin layer porosity decreases and as pore size increases.
For a fixed coating film structure, a minimum salt rejection is fixed, but the maximum salt rejection is achieved by decreasing porosity and increasing pore size.
minimum rejection
= coating film selectivity
Observed rejection, R = 1 - cp/cf
0.9955
0.995
0.9945
0.994
0.9935
0.993
0.9925
0.0
0.1
0.2
0.3
0.4
0.5
0.6
0.7
0.8
Support Membrane Skin Layer Porosity

FIGURE 11B

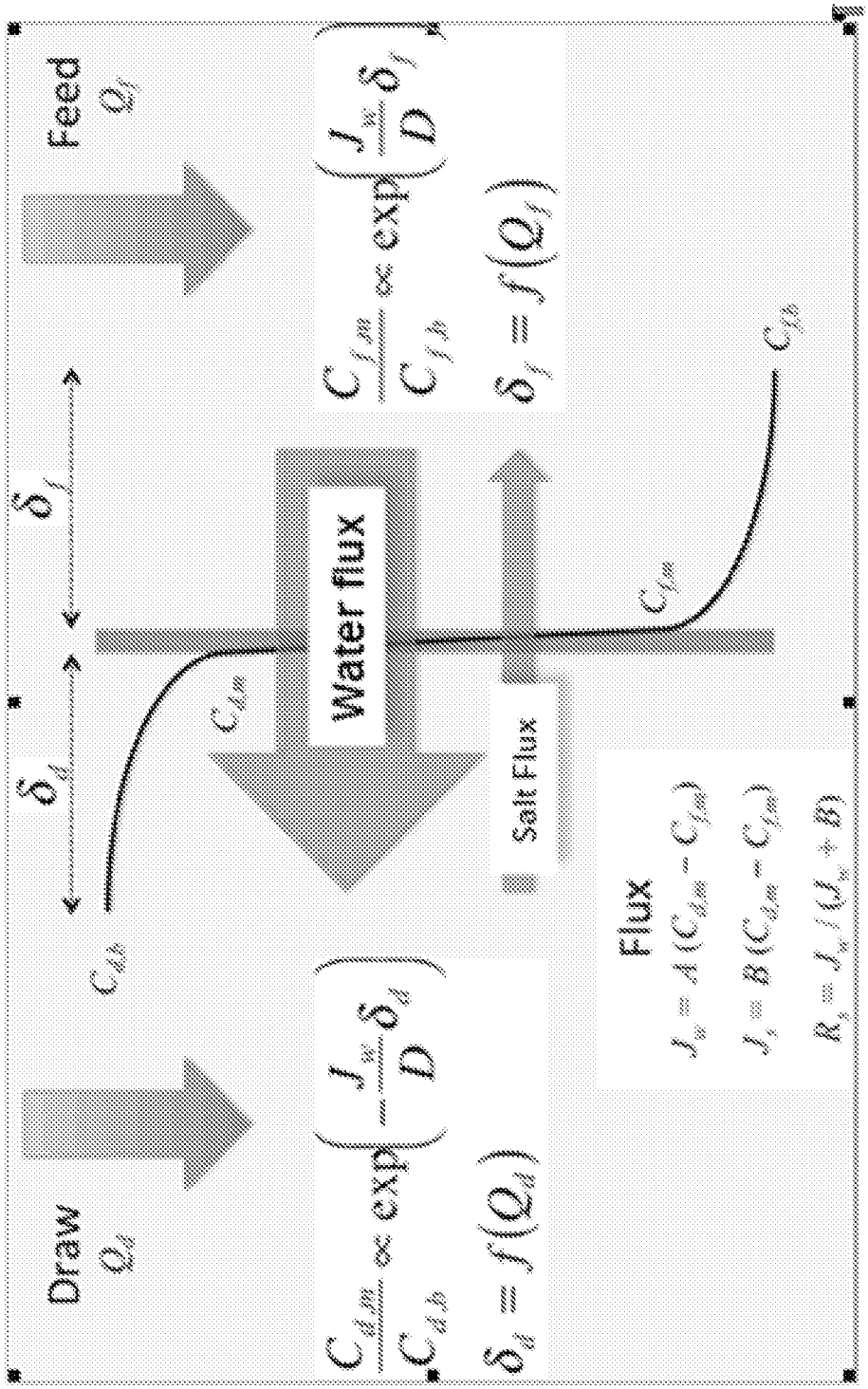

Draw
Q_d
Feed
Q_f
δ_d
δ_f
$C_{d,b}$
$C_{d,m}$
Water flux
Salt Flux
$C_{f,m}$
$C_{f,b}$
$\frac{C_{d,m}}{C_{d,b}} \propto \exp\left(-\frac{J_w}{D}\delta_d\right)$
$\delta_d = f(Q_d)$
$\frac{C_{f,m}}{C_{f,b}} \propto \exp\left(\frac{J_w}{D}\delta_f\right)$
$\delta_f = f(Q_f)$
Flux
$J_w = A(C_{d,m} - C_{f,m})$
$J_s = B(C_{d,m} - C_{f,m})$
$R_s = J_s / (J_w + B)$

FIGURE 12A

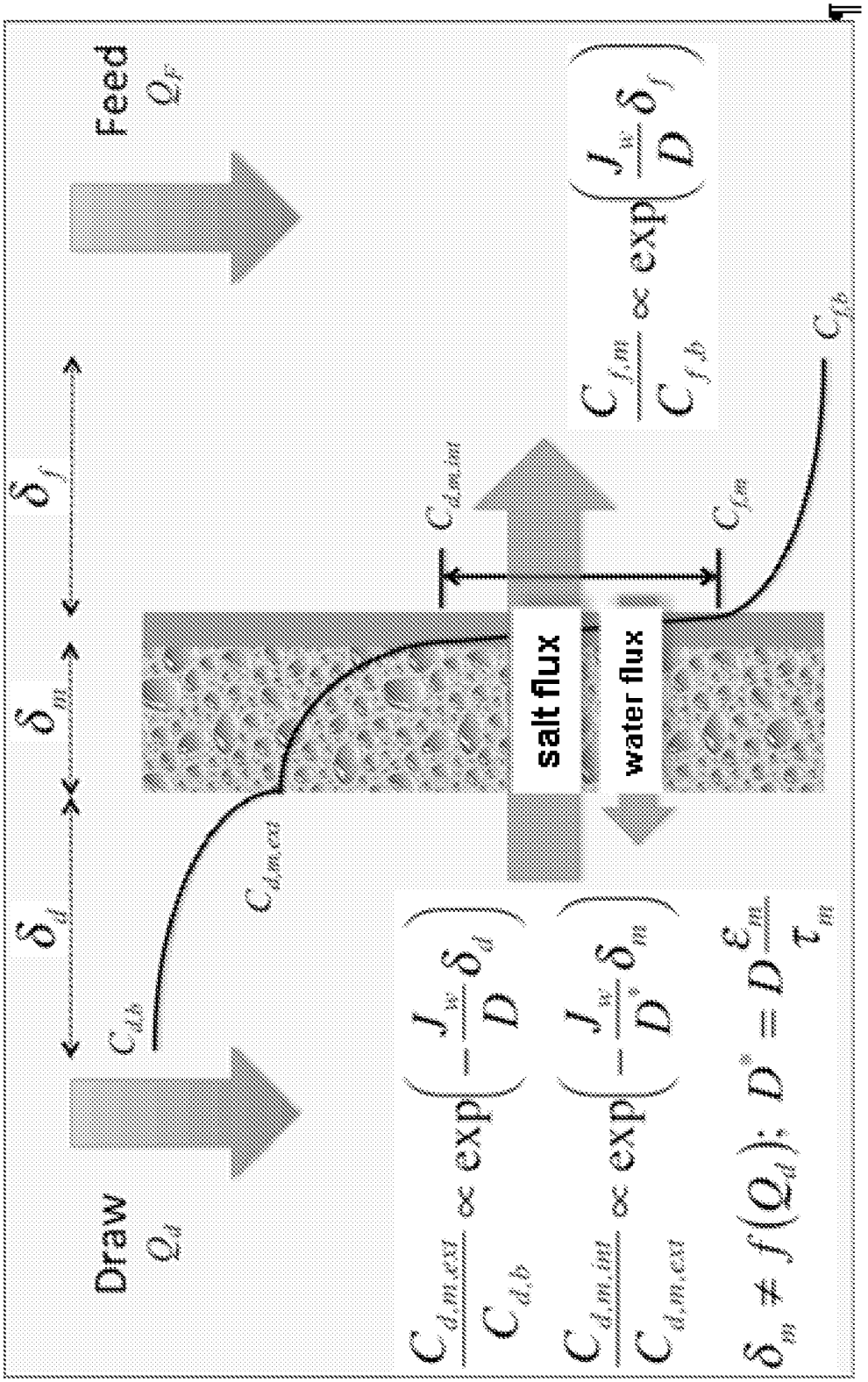

Draw
Q_d
Feed
Q_F
δ_d
δ_m
δ_f
$C_{d,b}$
$C_{d,m,ext}$
$C_{d,m,int}$
$C_{f,m}$
$C_{f,b}$
salt flux
water flux
$\frac{C_{d,m,ext}}{C_{d,b}} \propto \exp\left(-\frac{J_w}{D}\delta_d\right)$
$\frac{C_{d,m,int}}{C_{d,m,ext}} \propto \exp\left(-\frac{J_w}{D^*}\delta_m\right)$
$\frac{C_{f,m}}{C_{f,b}} \propto \exp\left(\frac{J_w}{D}\delta_f\right)$
$\delta_m \neq f(Q_d);\ D^* = D\frac{\varepsilon_m}{\tau_m}$

FIGURE 12B

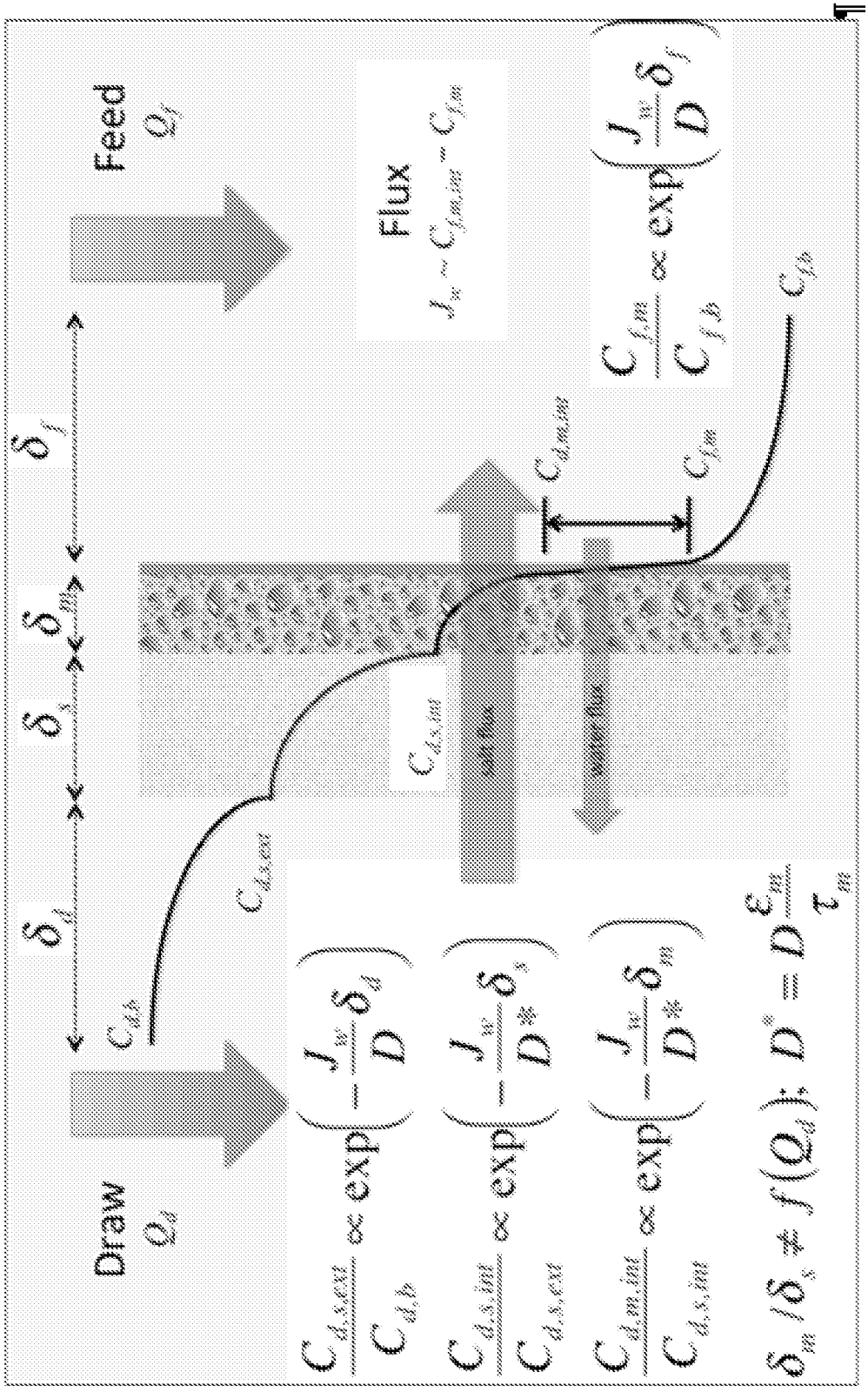

Draw
Q_d
Feed
Q_f
δ_d
δ_s
δ_m
δ_f
$C_{d,b}$
$C_{d,s,ext}$
$C_{d,s,int}$
$C_{d,m,int}$
$C_{f,m}$
$C_{f,b}$
Flux
$J_w \sim C_{f,m,int} - C_{f,m}$
$\frac{C_{d,s,ext}}{C_{d,b}} \propto \exp\left(-\frac{J_w}{D}\delta_d\right)$
$\frac{C_{d,s,int}}{C_{d,s,ext}} \propto \exp\left(-\frac{J_w}{D^*}\delta_s\right)$
$\frac{C_{d,m,int}}{C_{d,s,int}} \propto \exp\left(-\frac{J_w}{D^*}\delta_m\right)$
$\frac{C_{f,m}}{C_{f,b}} \propto \exp\left(\frac{J_w}{D}\delta_f\right)$
$\delta_m / \delta_s \neq f(Q_d)$; $D^* = D\frac{\varepsilon_m}{\tau_m}$

FIGURE 12C

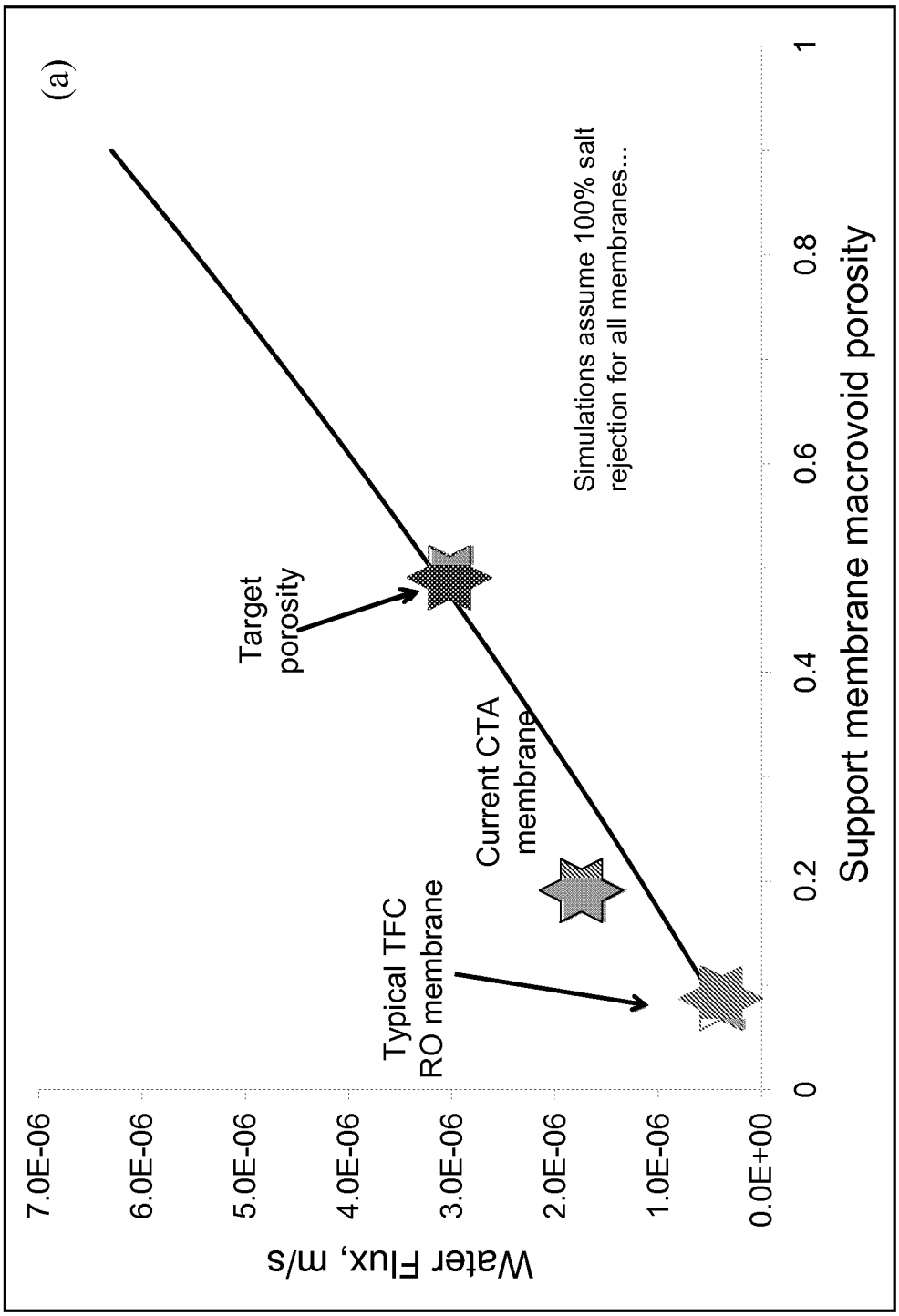

(a)
Water Flux, m/s
7.0E-06
6.0E-06
5.0E-06
4.0E-06
3.0E-06
2.0E-06
1.0E-06
0.0E+00
0
0.2
0.4
0.6
0.8
1
Support membrane macrovoid porosity
Simulations assume 100% salt rejection for all membranes...
Target porosity
Current CTA membrane
Typical TFC RO membrane

FIGURE 13A

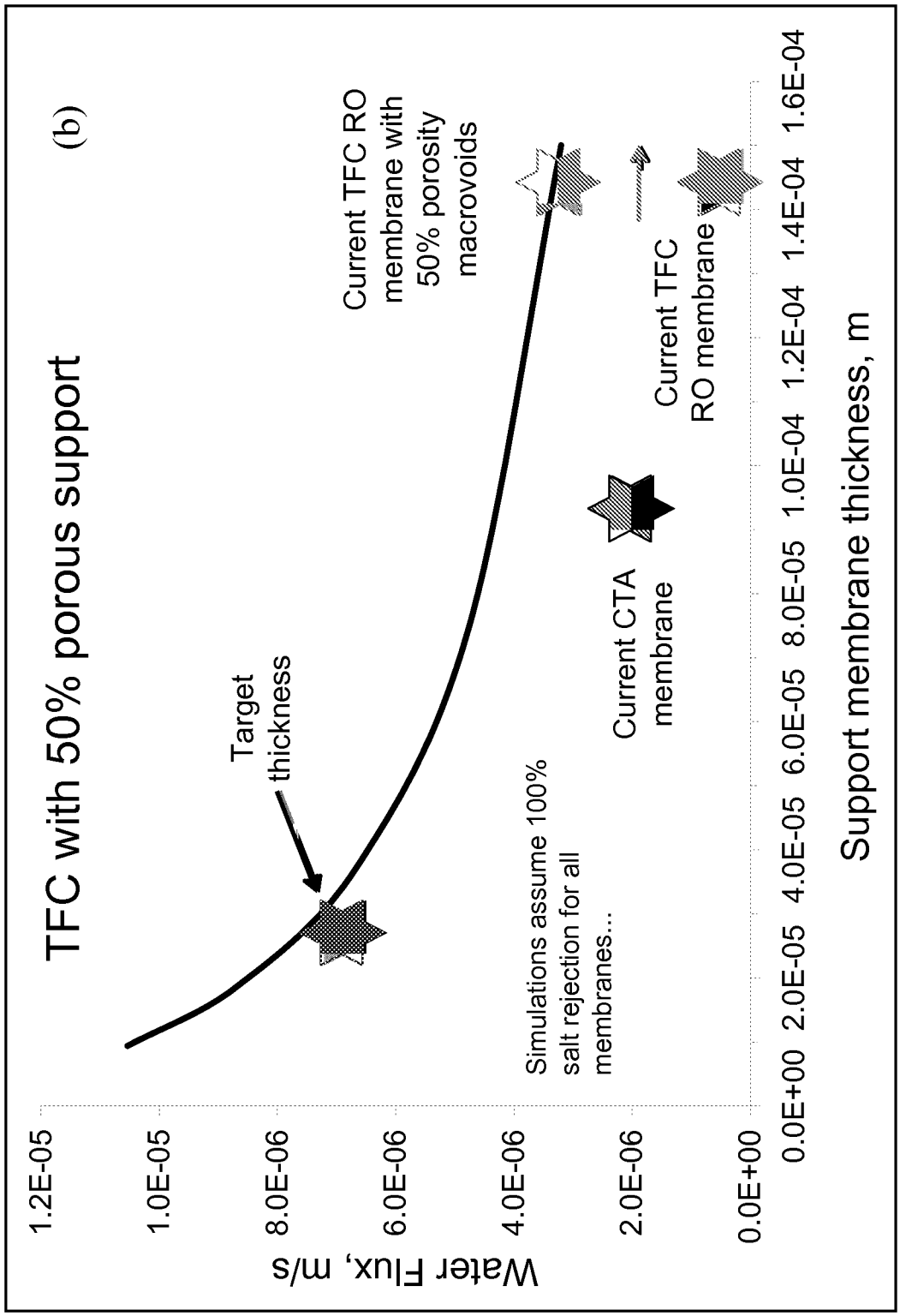

TFC with 50% porous support
(b)
Water Flux, m/s
1.2E-05
1.0E-05
8.0E-06
6.0E-06
4.0E-06
2.0E-06
0.0E+00
0.0E+00 2.0E-05 4.0E-05 6.0E-05 8.0E-05 1.0E-04 1.2E-04 1.4E-04 1.6E-04
Support membrane thickness, m
Target thickness
Simulations assume 100% salt rejection for all membranes...
Current CTA membrane
Current TFC RO membrane
Current TFC RO membrane with 50% porosity macrovoids

FIGURE 13B

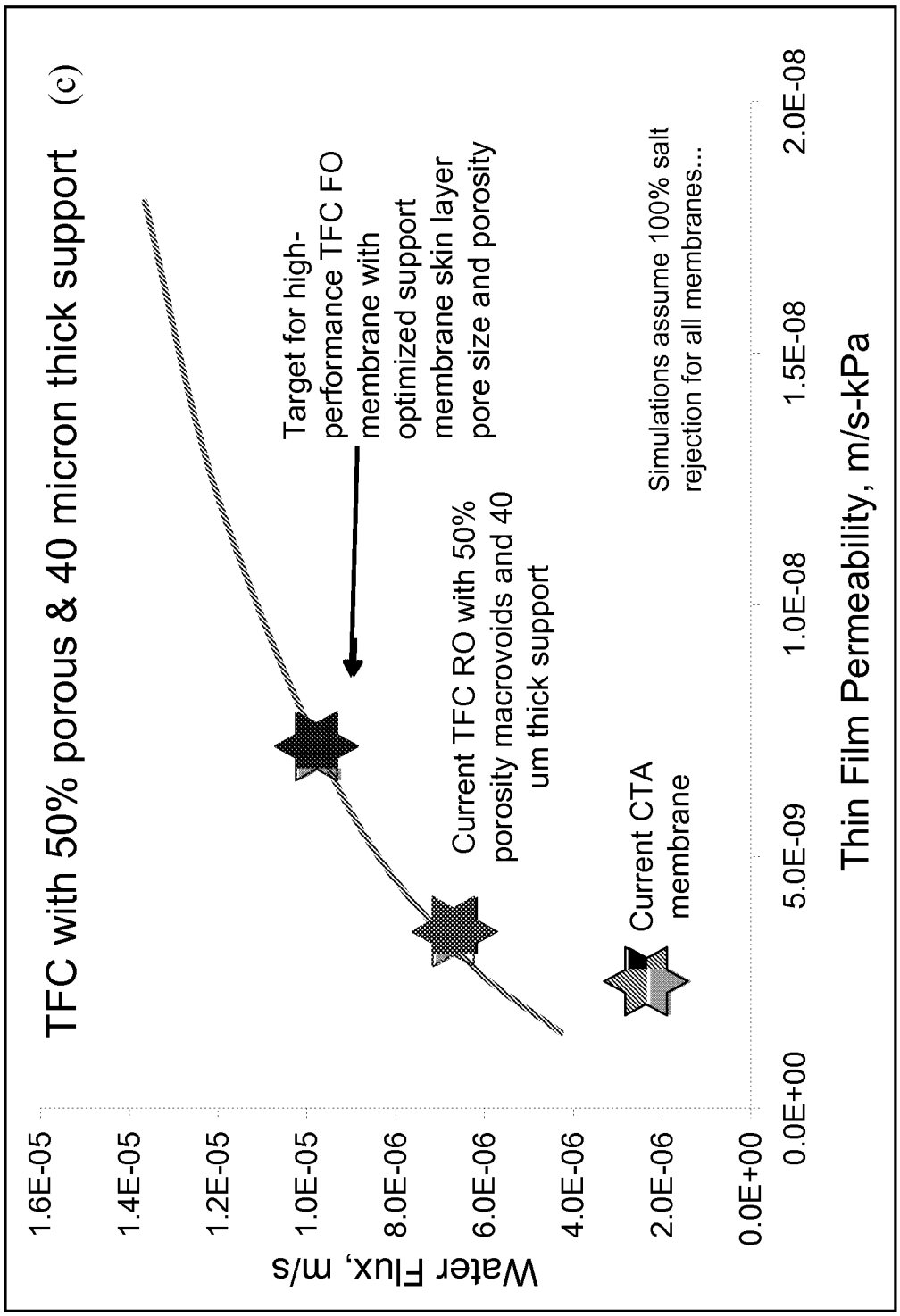

TFC with 50% porous & 40 micron thick support (c)
Water Flux, m/s
Thin Film Permeability, m/s-kPa
1.6E-05
1.4E-05
1.2E-05
1.0E-05
8.0E-06
6.0E-06
4.0E-06
2.0E-06
0.0E+00
0.0E+00
5.0E-09
1.0E-08
1.5E-08
2.0E-08
Target for high-performance TFC FO membrane with optimized support membrane skin layer pore size and porosity
Current TFC RO with 50% porosity macrovoids and 40 um thick support
Current CTA membrane
Simulations assume 100% salt rejection for all membranes...

FIGURE 13C

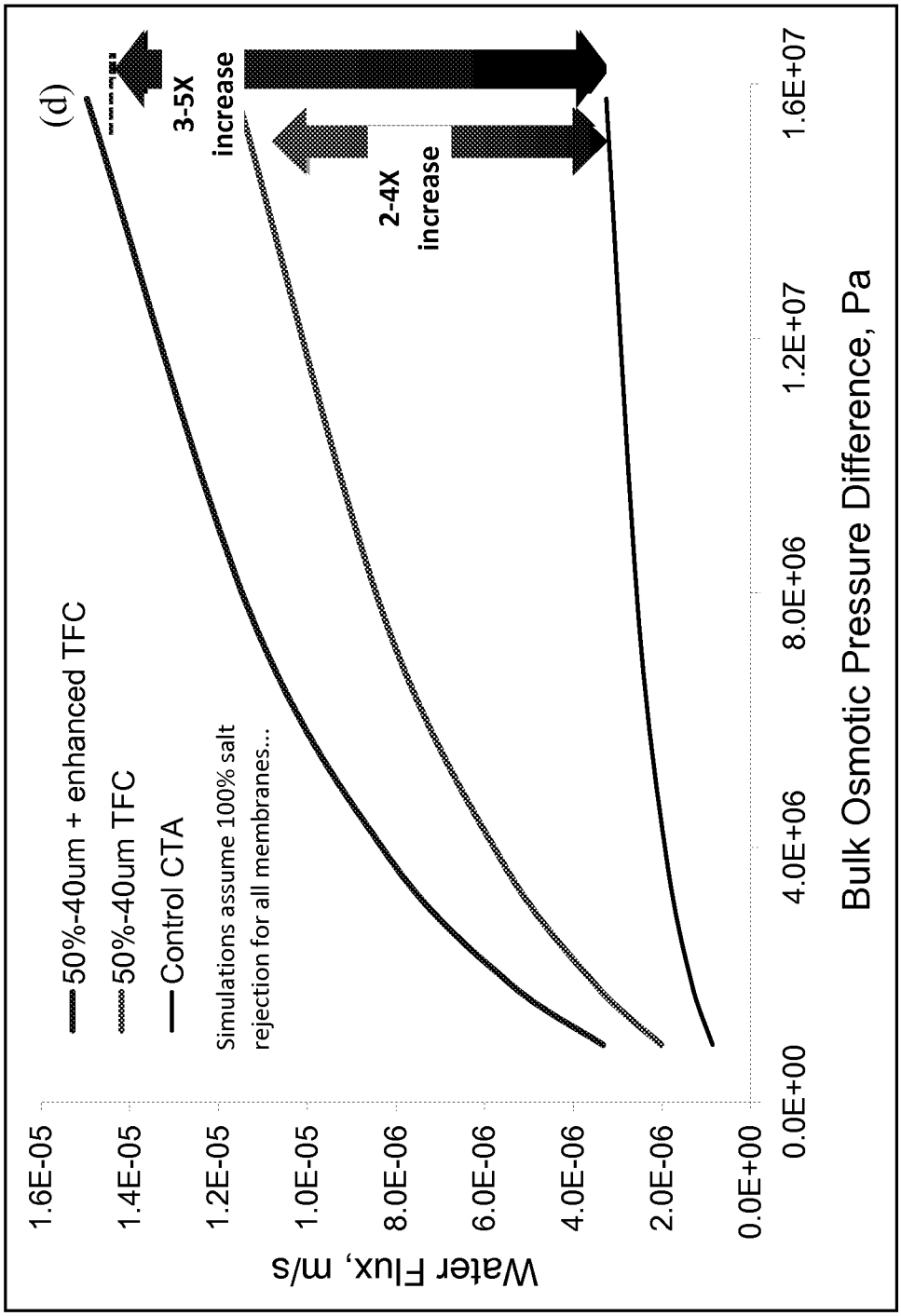

(d)
50%-40um + enhanced TFC
50%-40um TFC
Control CTA
Simulations assume 100% salt rejection for all membranes...
3-5X increase
2-4X increase
Water Flux, m/s
Bulk Osmotic Pressure Difference, Pa
0.0E+00
2.0E-06
4.0E-06
6.0E-06
8.0E-06
1.0E-05
1.2E-05
1.4E-05
1.6E-05
0.0E+00
4.0E+06
8.0E+06
1.2E+07
1.6E+07

FIGURE 13D

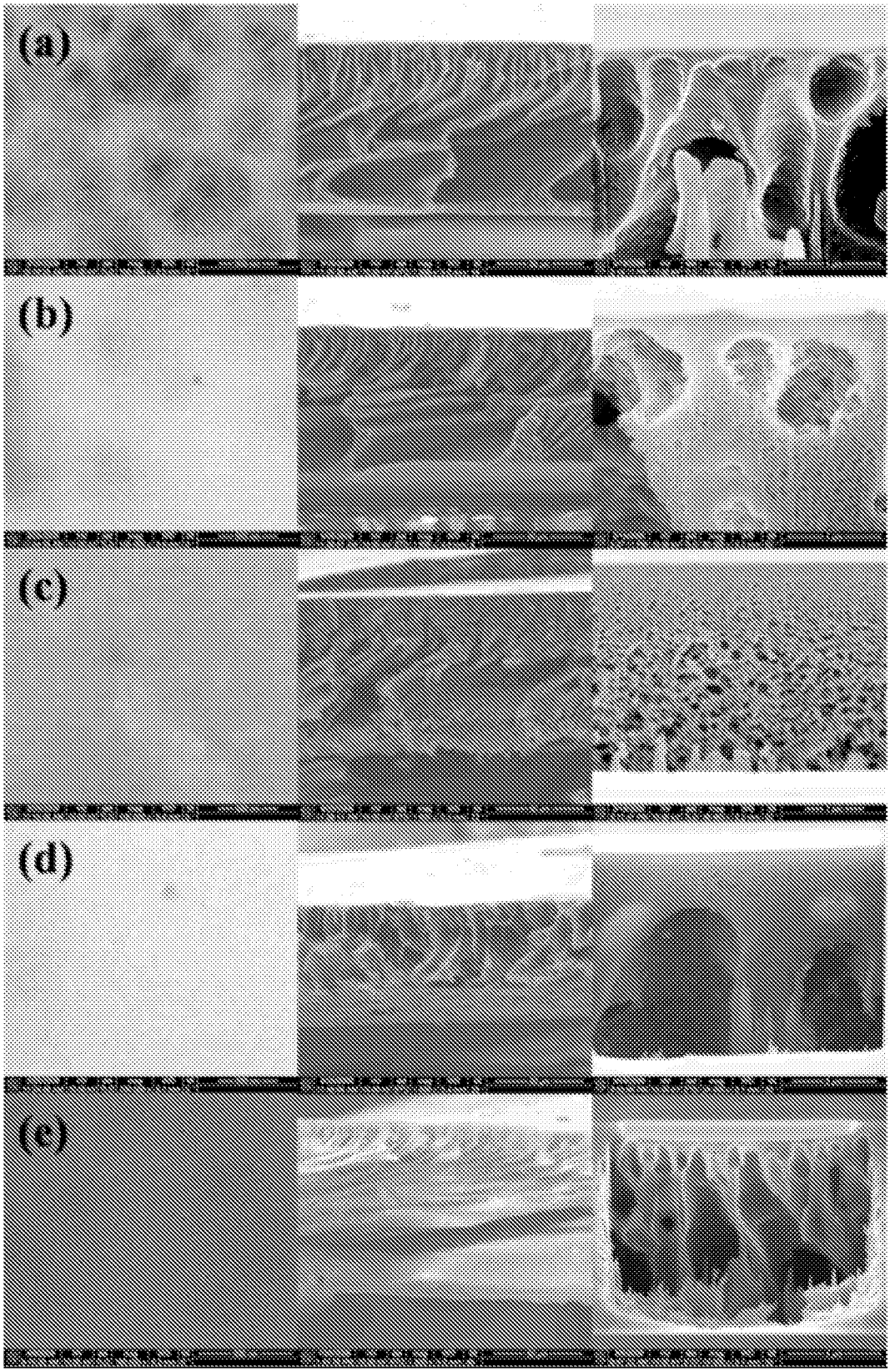


FIGURE 14

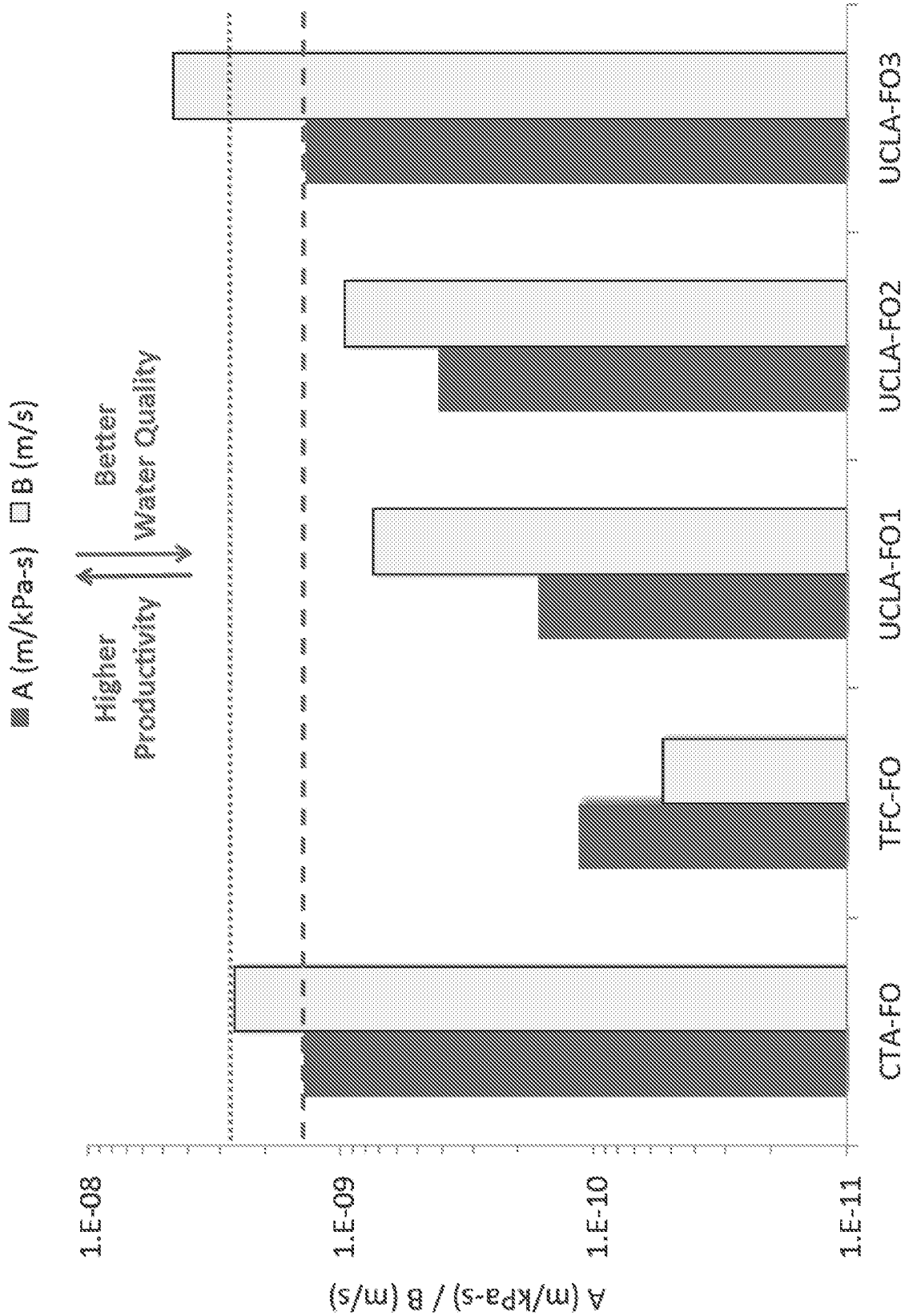

A (m/kPa-s) / B (m/s)
1.E-08
1.E-09
1.E-10
1.E-11
A (m/kPa-s)
B (m/s)
Higher Productivity
Better Water Quality
CTA-FO
TFC-FO
UCLA-FO1
UCLA-FO2
UCLA-FO3

FIGURE 15

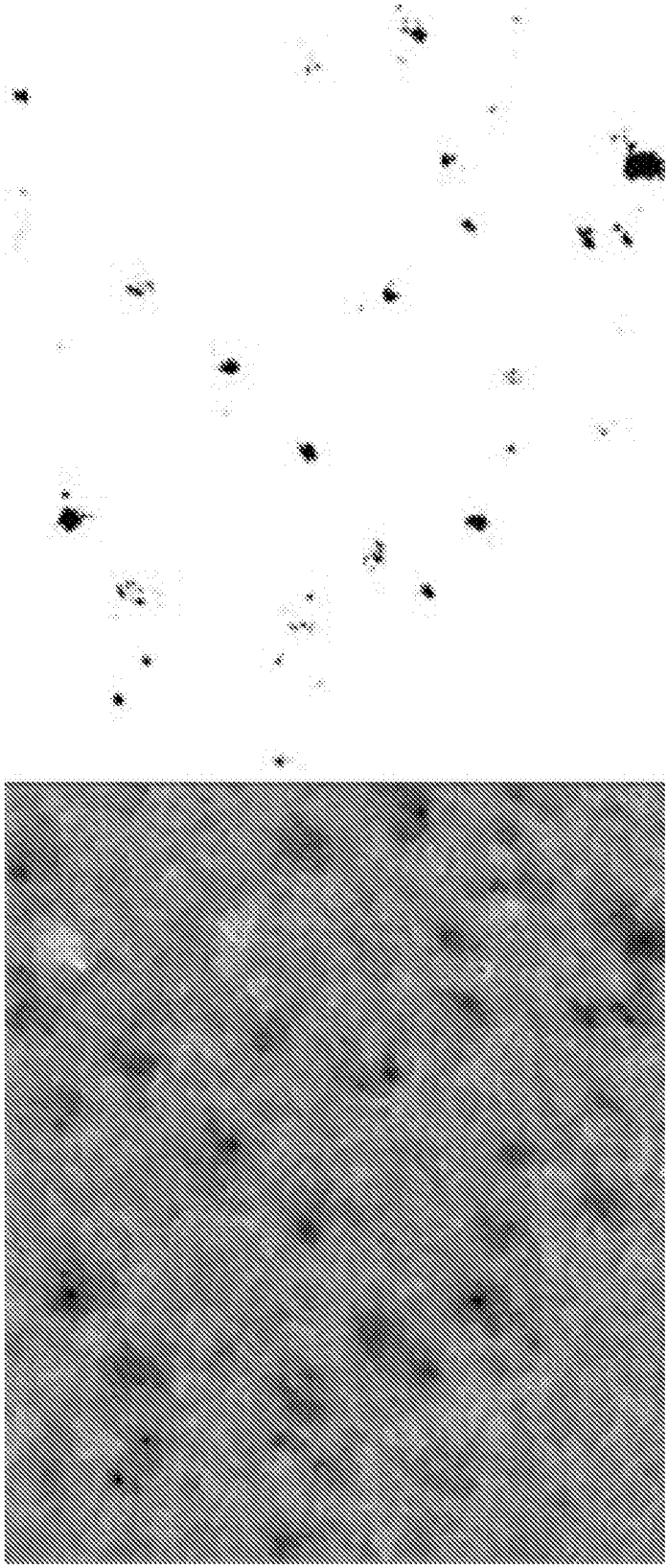


FIGURE 16

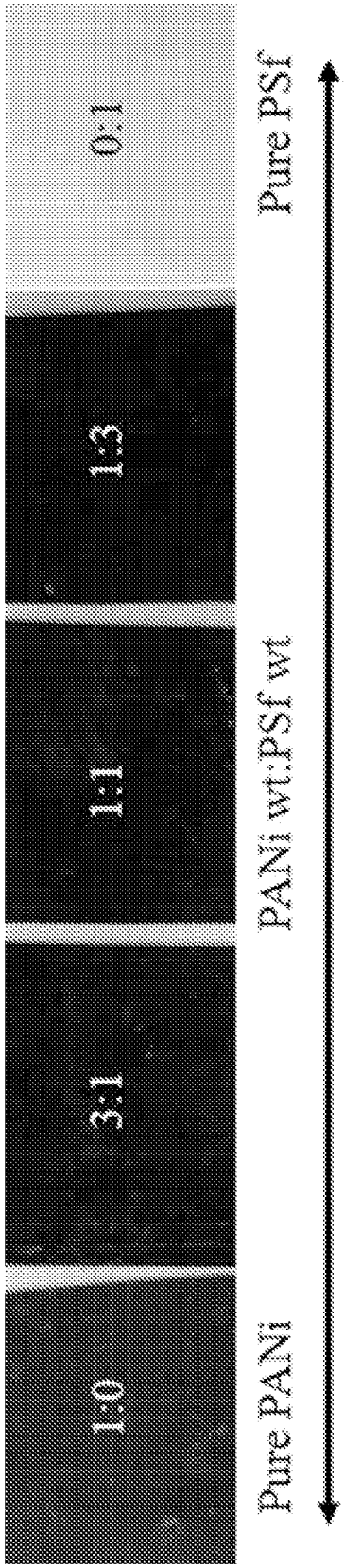


FIGURE 17

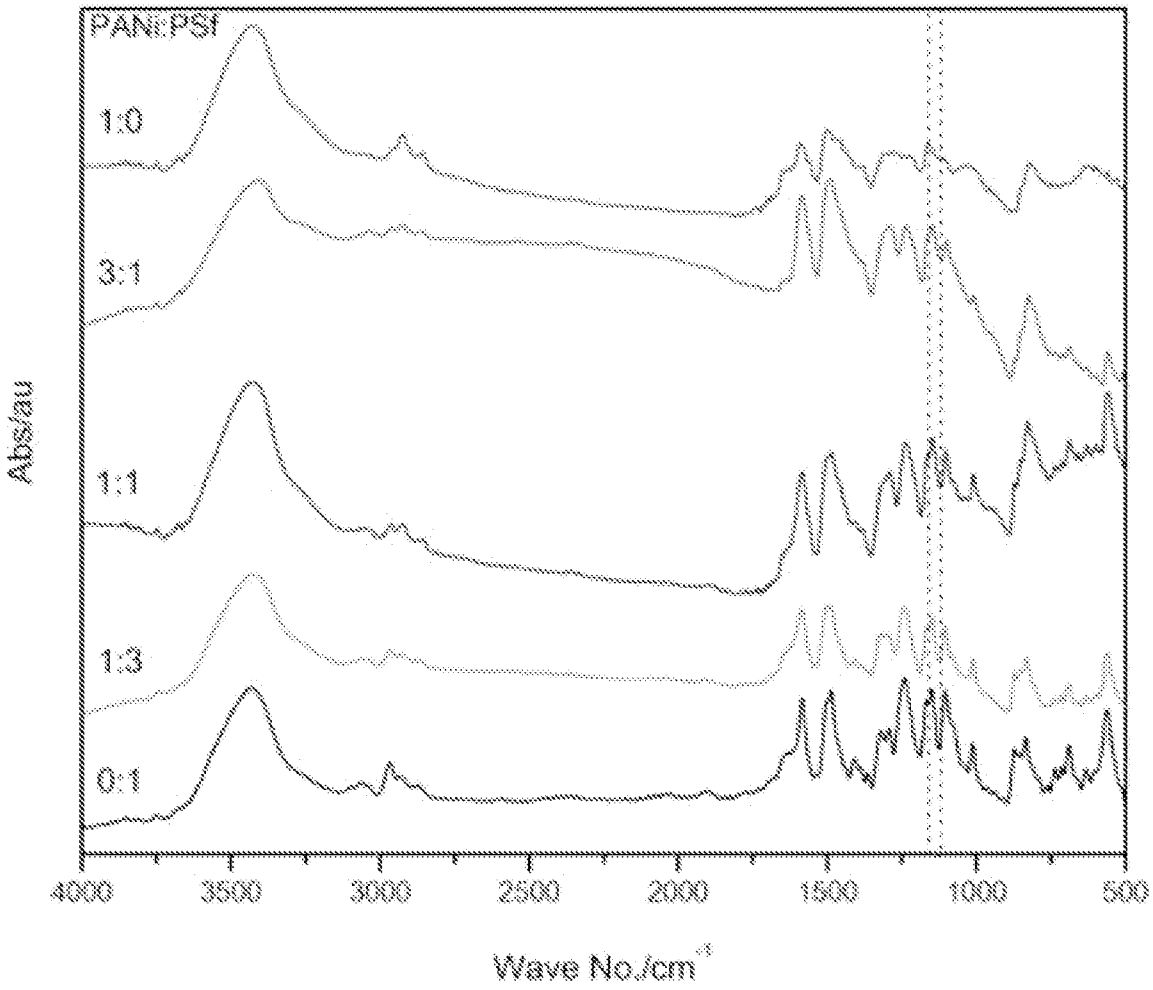

PAN:PSf
1:0
3:1
1:1
1:3
0:1
Abs/au
4000
3500
3000
2500
2000
1500
1000
500
Wave No./cm-1

Figure 18

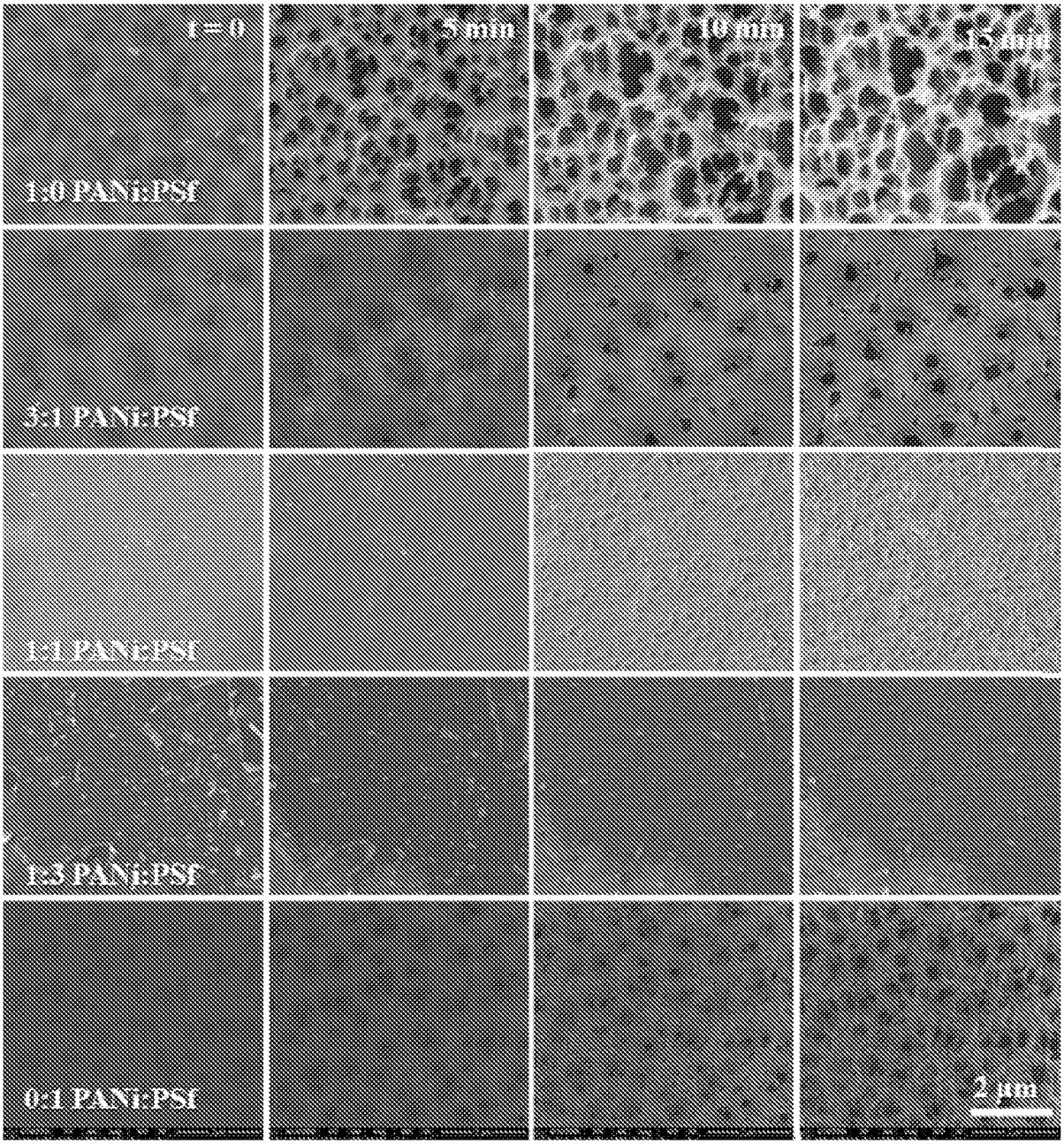

t = 0
5 min
10 min
15 min
1:0 PANi:PSf
3:1 PANi:PSf
1:1 PANi:PSf
1:3 PANi:PSf
0:1 PANi:PSf
2 μm

Figure 19

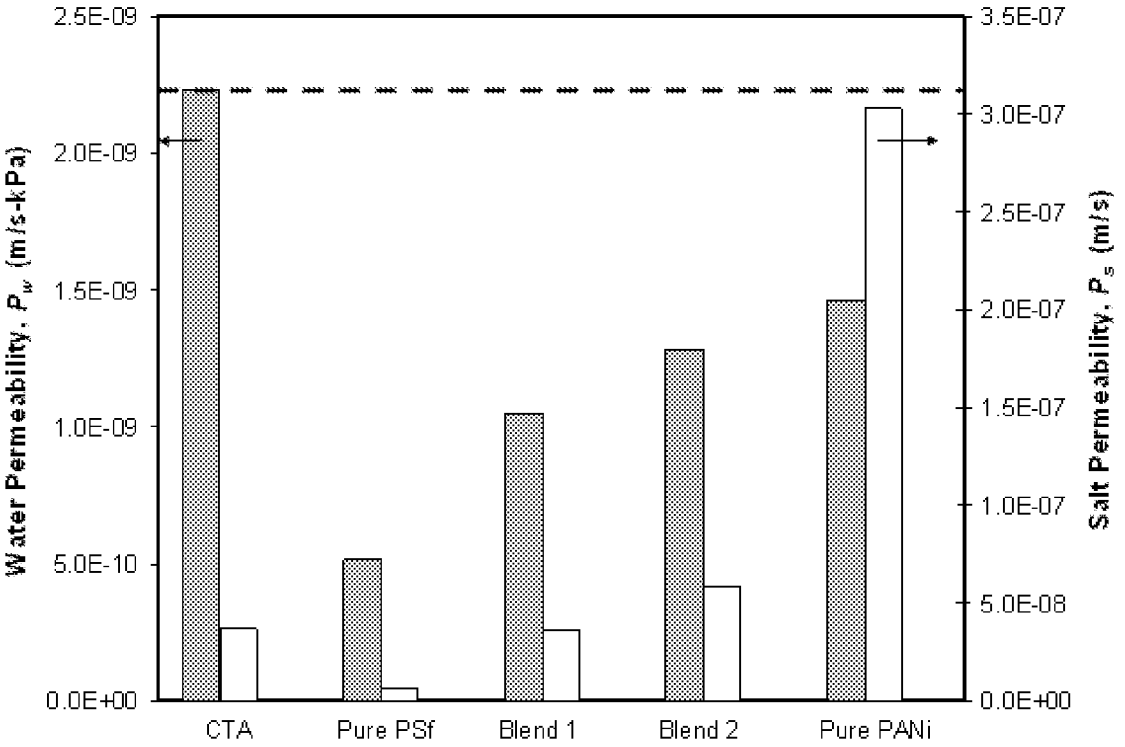


FIGURE 20

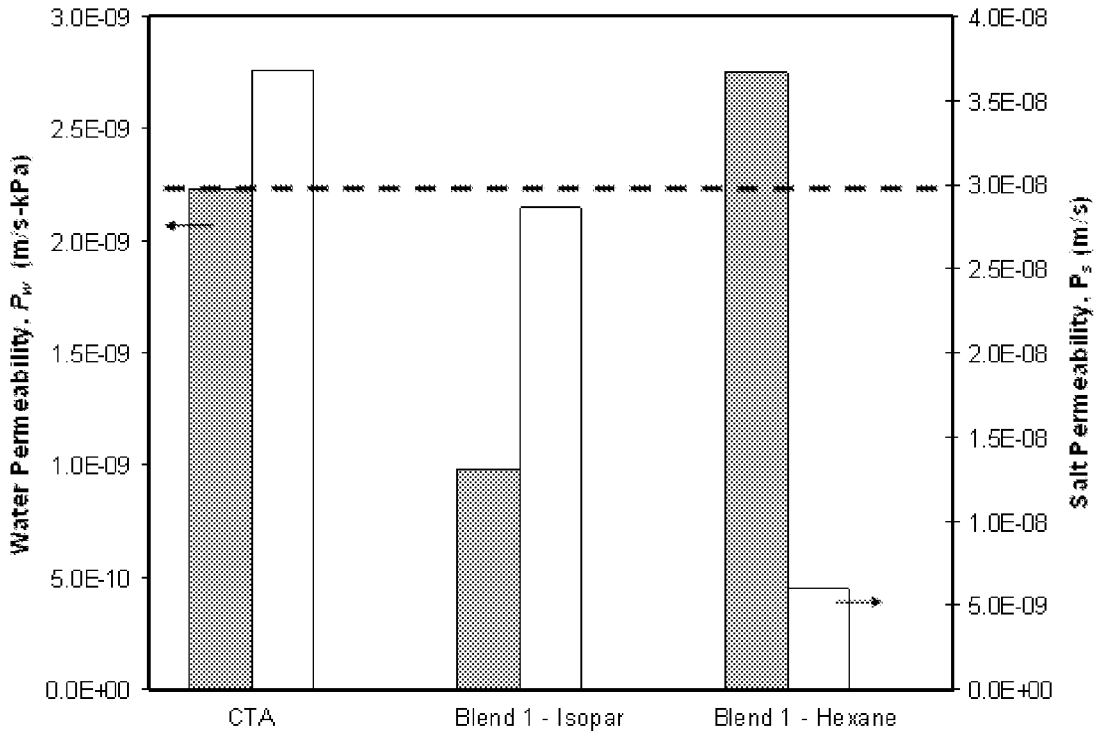


Figure 21

INTERNATIONAL SEARCH REPORT

International application No.
PCT/US 12/35188

A. CLASSIFICATION OF SUBJECT MATTER
IPC(8) - B01D 71/06 (2012.01)
USPC - 210/490, 500.21
According to International Patent Classification (IPC) or to both national classification and IPC

B. FIELDS SEARCHED

Minimum documentation searched (classification system followed by classification symbols)
IPC(8): B01D 71/06 (2012.01); USPC: 210/490, 500.21

Documentation searched other than minimum documentation to the extent that such documents are included in the fields searched
USPC: 210/490, 500.21

Electronic data base consulted during the international search (name of data base and, where practicable, search terms used)
Google Scholar, Google Patents, PubWEST (PGPB,USPT,EPAB,JPAB) (Membrane, forward, osmosis, permeable, desalinate, drug, delivery, food, beverage, dehydrate, water, phthaloyl, trimesoyl, aminobenzene, contact, angle, macrovoid, ammonia, carbon, dioxide)

C. DOCUMENTS CONSIDERED TO BE RELEVANT

Category*	Citation of document, with indication, where appropriate, of the relevant passages	Relevant to claim No.
X Y	US 2003/0162939 A1 (Wang, et al.) 28 Aug 2003 (28.08.2003) paragraphs [0007], [0013], [0026]-[0032], [0042]-[0047], [0076]-[0077]	30-38 1-29
X Y	US 2010/0224555 A1 (Hoek, et al.) 09 Sep 2010 (09.09.2010) paragraphs [0184], [0202], [0213], [0226], [0305], [0318], [0353]-[0356], [0408], [0531]	39-43 17-21, 24, 27, 29
Y	US 2011/0017666 A1 (Cath, et al.) 27 Jan 2011 (27.01.2011) paragraphs [0020], [0057], [0065], [0077], [0094], [0117]	1-29

☐ Further documents are listed in the continuation of Box C. ☐

* Special categories of cited documents:
"A" document defining the general state of the art which is not considered to be of particular relevance
"E" earlier application or patent but published on or after the international filing date
"L" document which may throw doubts on priority claim(s) or which is cited to establish the publication date of another citation or other special reason (as specified)
"O" document referring to an oral disclosure, use, exhibition or other means
"P" document published prior to the international filing date but later than the priority date claimed
"T" later document published after the international filing date or priority date and not in conflict with the application but cited to understand the principle or theory underlying the invention
"X" document of particular relevance; the claimed invention cannot be considered novel or cannot be considered to involve an inventive step when the document is taken alone
"Y" document of particular relevance; the claimed invention cannot be considered to involve an inventive step when the document is combined with one or more other such documents, such combination being obvious to a person skilled in the art
"&" document member of the same patent family

Date of the actual completion of the international search	Date of mailing of the international search report
15 Jul 2012 (15.07.2012)	24 JUL 2012
Name and mailing address of the ISA/US Mail Stop PCT, Attn: ISA/US, Commissioner for Patents P.O. Box 1450, Alexandria, Virginia 22313-1450 Facsimile No. 571-273-3201	Authorized officer: Lee W. Young PCT Helpdesk: 571-272-4300 PCT OSP: 571-272-7774

Form PCT/ISA/210 (second sheet) (July 2009)